CHAPTER-4

RESULTS AND DISCUSSION

CHAPTER 4

RESULTS AND DISCUSSIONS

4.1: Concentrations of O_3 and its precursors over mid-Brahmaputra valley

Continuous measurements of ambient O_3 and its precursors along with meteorological parameters were monitored, and for this study the concentration data of the period 2013-2017 were taken. The years were divided into four definite seasons as per Indian meteorological department. The seasons were, winter (January and February); pre-monsoon (March to May); monsoon (June to September) and post-monsoon (October to December).

The concentrations of O_3, O_3max, NOx, OX, NO, and NO_2 for the years 2013-14, 2014-15, 2015-16 and 2016-2017 has been plotted in Fig4. 2. The maximum concentrations of O_3, O_3 *max* and NOx were found to be 19 ppb, 43 ppb and 7 ppb respectively during the year 2013-2014; 17 ppb, 41ppb and 7 ppb respectively during the year 2014-2015; 15 ppb, 85 ppb and 10 ppb respectively for the year 2015-2016 and 23.1 ppb, 79.7 ppb and 19.2 ppb during 2016-17 respectively. The minimum O_3, O_3max and NOx were found to be 1ppb, 1ppb and 2ppb respectively during the year 2013-2014; 1ppb, 11ppb and1ppb during the year 2014-2015; 1 ppb, 2 ppb and 1ppb respectively during the year 2015-16 and 1 ppb, 3.8ppb and 2 ppb respectively for the year 2016-2017.

The calculated OX values were found to be between 174 ppb and 2 ppb in 2013-2014; between 93 ppb and 2ppb in 2014-2015; between 85.4 ppb and 0.9ppb in 2015-2016 and between 134.7 ppb and 1.3 ppb in 2016-2017. NO and NO_2 concentrations are also plotted. For the year 2013-14 a maximum of 26.6 ppb and 33.6 ppb and a minimum of 0.4 ppb and 0.4 ppb were found for NO and NO_2 respectively, while for the year 2014-15 a maximum of 19.4 and 42.3 ppb and a minimum of 0.11 and 0.1 ppb were found for NO and NO_2 respectively. For the year 2015-16 a maximum of 24.2 and 45.3 ppb and a minimum of 0.4 and 0.1 were found for NO and NO_2 respectively while for the year 2016-17 a maximum of 50.8 and 102.8 ppb and a minimum of 1.3 and 0.4 ppb were found for NO and NO_2 respectively.

The median concentrations of the species were found to be 17, 19.8,5,2, 3 and 21 ppb during the2013-2014; 15, 18.2, 6, 3, 3 and 18 ppb during the year 2014-2015; 12, 17.7, 10, 5, 3 and 14ppb during the year 2015-2016 and 19, 37.8, 7.6, 6.7, 10.3 and 31.8 ppb during the year 2016-2017 for O_3, O_3 max, NOx, NO, NO_2 and OX respectively. The concentration modes (not shown

in the plot) were found to be 12, 15, 3, 3, 3 and 11; 8, 11, 4, 3, 4 and 7; 8, 12, 7, 5, 2 and 21; 15, 25, 6.2, 10.5 and 18 for O_3, O_3 max, NOx, NO, NO_2 and OX respectively for the four consecutive years. The modes of O_3 during the four years suggest that the ozone levels experienced over the present rural site were low. It is understood that the concentrations of O_3 typically depend on the absolute and relative concentrations of its precursors and the intensity of solar radiation and temperature [1-6].

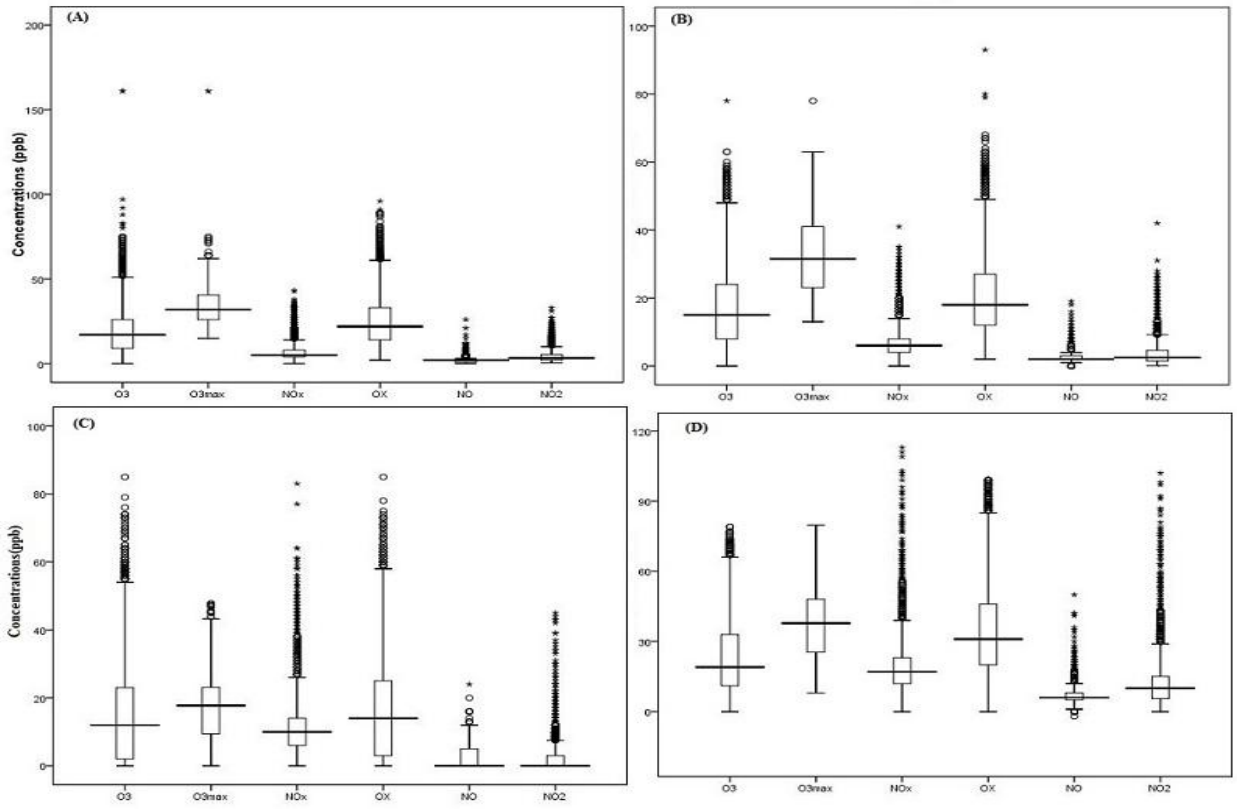

Fig .4.2. Concentrations: Box plot for the year (A) 2013-2014. (B) 2014-2015 (C) 2015-2016 and (D) 2016-2017 (the central solid lines inside the box represent median values of the respective species; the whiskers are maximum (95th percentile) and minimum values excluding the outliers).

The monthly daylight average concentrations of O_3, NOx, NO_2 and NO (to understand the concentration pattern, a representative two year period was taken) i.e during the year 2013-2015 have been given in Table 4.1.The daylight concentrations of O_3 were high during pre-monsoon season and low during monsoon. Sarangi et al. (2014) reported average monthly ozone concentrations of a remote high-altitude location of central Himalayas (Nainital, India) [7]. When the monthly average O_3 concentrations of the present study was compared with the reported average concentrations of Sarangi et al. [7], it appeared that the ozone levels over Nainital were much on the higher side that the present study. This difference observed between two studies may be understood with regard to the nearness of Nainital to one of the most polluted (Indo-Gangetic Plain) IGP region of India. The monthly daylight average concentrations of O_3 (Table 4.1) display explicitly that the high O_3 concentrations are seen in March-April (pre-monsoon), which agreed with the results reported by Sarangi et al. [7] from a remote location of Central Himalayas.

Table 4.1: Monthly daylight average concentrations (ppb) of O_3, NOx, NO_2 and NO during May 2013-May2015.

	O_3		**NO_2**		**NO**		**NOx**	
Month	Avg.±Std	Counts(days)	Avg. ±Std	Counts(days)	Avg. ±Std	Counts(days)	Avg. ±Std	Counts(days)
Jan	25±14	806(62)	5.1±3.0	806(62)	3±1.5	806(62)	8±3	806(62)
Feb	28±13	728(56)	5.6±2.7	728(56)	2.8±1	728(56)	8±3	728(56)
Mar	33±15	806(62)	4.5±2.7	806(62)	2.6±1.2	806(62)	7±3	806(62)
April	30±20	780(60)	3.1±3.9	780(60)	1.8±1.6	780(60)	7±2	780(60)
May	25±12	806(62)	2.9±1.3	806(62)	2.9±1.5	806(62)	6±2	806(62)
June	24±10	780(60)	2.1±0.8	780(60)	1.9±0.5	780(60)	4±1	780(60)
July	16±6	806(62)	1.5±0.7	806(62)	1.9±0.6	806(62)	3±1	806(62)
Aug	17±6	806(62)	1.5±0.7	806(62)	2±0.7	806(62)	4±1	806(62)
Sep	17±8	780(60)	1.8±1	780(60)	2.2±0.7	780(60)	4±1	780(60)
Oct	20±9	806(62)	2±1.4	806(62)	2.1±0.7	806(62)	4±2	806(62)
Nov	21±10	780(60)	2.9±2	780(60)	2.7±1	780(60)	4±2	780(60)
Dec	21±11	806(62)	4.1±2.6	806(62)	2.6±1.3	806(62)	7±3	806(62)
Annual	23±13	9490(730)	3.1±2.3	9490(730)	2.6±1.2	9490(730)	6±3	9490(730)

4.2: Comparison of ambient ozone and NOx measured at Tezpur station with different locations in India and other International Cities.

Table (4.2.1) and (4.2.2) showed the annual average concentration of ozone and NOx respectively measured at Tezpur station, Assam, compared with different locations in India as well as the world. Maximum O_3 concentrations were found in places like Anantapur, Agra, Dhaka, Giza etc as compared to the study site and minimum concentrations were found in places like Meadowlands, Barcelona etc. Whereas the maximum concentration of NOx was found in an urban site of Meadowlands, New Jersey and minimum concentration was found in a tropical rural site of Gadanki, India. The variation in O_3 and NOx concentration was found due to difference in population density, traffic density, industrial activities, human interference, land use patterns and rainfall frequencies. Moreover from the table the maximum concentration of ozone was seen during Premonsoon season and minimum in monsoon season except for some countries which shows their minimum concentration during winter. And the maximum concentration of NOx was seen during winter season and minimum during monsoon season.

Bhuyan et al. (2014) reported a maximum O_3 concentration of 43 ppb from urban Dibrugarh in the upper Brahmaputra Valley that was comparable to the present study values [8]. Tezpur experienced higher maximum concentrations of O_3 compared to several regions of the Indian mainland, e.g., uplands of Udaipur (28 ppb; [9]), city area of Ahmedabad (30 ppb; [10]), Coastal Tranquebar (37 ppb; [11]), and semi-urban areas of Jodhpur (22 ppb; [12]). There are several reports of higher maximum concentrations of O_3 compared to the present study form the mainland India (e.g., urban areas of Pune; 55 ppb; [13]), urban commercial areas of Agra (72 ppb; [14]), semi-arid rural continental location of Anantapur (72 ppb; [15]), and urban high-altitude area of Ooty (62 ppb; [16]) There were reports where the O_3 values were comparable to those in Tezpur. These locations include a rural mountain valley of Kannur (44 ppb; [17]), abusyurban industrial area of Lahore (41 ppb; [18]). Sarangi et al. (2014) reported average monthly O_3 concentrations in a remote high-altitude location of central Himalayas (Nainital, India) where concentrations were in the upper range of values observed in the mid Brahmaputra Valley [7]. The proximity of Nainital to one of the most polluted regions of India, the Indo-Gangetic Plain (IGP) could have resulted in higher O_3 values in the hills. In another

study from the Nepalese Himalayas, a maximum O_3 concentration of 60 ppb was reported that could have been an outcome of the valley effect. In neighboring Bangladesh, Sikder et al. (2013) reported a high maximum O_3 concentration of 97 ppb in Dhaka [19]. Therefore, it appears that the maximum ozone concentrations varied in different locations likely related to the land uses. Although the station at Tezpur is a rural location, the maximum O_3 values were on higher compared to other similar locations of Indian subcontinent. A maximum concentration of 172 ppb during the winter season and a minimum of 18 ppb during monsoon season were reported by Sikder et al (2013) in an urban location of Dhaka, Bangladesh [19]. Whereas, in another study a maximum of 1.85 ppb during April and a minimum of 0.19 ppb during August was reported by Udayasoorian et al.(2013) in an urban high altitude location of Ooty [16].

Table 4.2.1: Comparative table of the concentration of O_3 with other locations of India as well as from other reported studies elsewhere in the World.

Location	Land use	Max O_3	Min O_3	Reference
Tezpur, India (2013-2014)	Rural	43 ppb*	1 ppb	Present Study
Tezpur, India (2014-2015)	Rural	41 ppb *	1 ppb	Present Study
Anantapur, India	Semi-arid Rural, continental region	70.2 ± 6.9 ppbv (Summer)	20.0 ± 4.7 ppbv (Monsoon)	15
Kannur, India	Rural, valley of mountains	44 ppbv (Winter)	18.5 ppbv (Monsoon)	17
Udaipur, India	Urban, hill range	28 ppbv(Premonsoon)	19 ppbv (Monsoon)	9
Dibrugarh, India	Urban, upper Brahmaputra basin	42.9±10.3 ppb(March)	17.3±7.0 ppb (July)	8
Ahmedabad, India	Urban, Industrial area	30±3 ppbv(November)	12±2 ppbv(Aug)	10
Ooty, India	Urban, High Altitude western ghats	62 ppb (March)	17 ppb (Aug)	16
Jodhpur, Rajasthan	Urban, Semi arid desert	21.9 ppb (Premonsoon)	12.6 ppb (Monsoon)	12
Agra, India	Urban, Semi arid commercial zone	72.3 ppb (November)	2.2 ppb (February)	14
Tranquebar, India	Urban, Coastal region	37 ppbv (May)	9 ppbv (October)	11

India			(October)	
Pune, India	Semi Urban, industrial site	54.6 ppbv (February)	12.2 ppbv (August)	13
Oki, Japan	Rural, small remote island	55 ppb(Spring)	29 ppb(Summer)	20
Istanbul, Turkey	Urban, Industrial area	32 ppb (Summer)	8 ppb (Winter)	21
Meadowlands, New Jersey	Urban, heavily industrialized	63 ppb (June)	0.2 ppb (November)	22
Namibia, Africa	Urban, High Altitude	30 ppb (October)	11 ppb (March)	23
Dhaka, Bangladesh	Urban, Highly traffic congested	97 ppb (Winter)	16 ppb (Monsoon)	19
Nepal	Urban, High Altitude	60.9 ppbv (Premonsoon)	38.9 ppbv (Monsoon)	24
Lahore, Pakistan	Urban, Busiest town, Industrial area	41.36 ppb (June)	5.27 ppb (January)	18
Barcelona, Spain	Urban, Highly populated	24.51 ppb (June)	4.15 ppb (December)	25
Giza, Cairo	Urban, Industrial site	143 ppb (July)	50 ppb (January)	26
Marikana, South Africa	Urban, township	50.02 ppb (October)	21.07 ppb (April)	27
Mohal-Kullu, India	Semi-rural	74.6 ± 23.2 ppb (Summer)	16.0 ± 5.6 ppb (Monsoon)	28
Telengana, India	Sub-urban	35.54 ± 7.16 ppbv(Winter)	12.70 ± 3.55ppbv (Monsoon)	29

*95th percentile concentration

Table 4.2.2: Comparative table of the concentration of NOx with other locations of India as well as elsewhere in the World.

Location	Areas	Max NOx	Min NOx	Reference
Tezpur, India (2013-2014)	Rural	43 ppb (Winter)	2 ppb(Monsoon)	Present study
Tezpur, India (2014-2015)	Rural	41 ppb(Winter)	1 ppb(Monsoon)	Present study
Anantapur, India	Semi-arid Rural, continental region	12.8 ± 0.8 ppbv(Winter)	3.7 ± 0.5 ppbv (Monsoon)	15
Kannur, India	Rural, valley of mountains	2.9 ±0.8 ppbv (Summer)	2.3 ± 0.4 ppbv (Monsoon)	17
Udaipur, India	Urban, hill range	18.5 ppbv (February)	7.2 ppbv (July)	9
Dibrugarh, India	Urban, upper Brahmaputra basin	82±33.2 ppb (December)	11±13.6 ppb (April)	8
Ooty, India	Urban, High Altitude western ghats	1.85 ppb (April)	0.19 ppb (August)	16
Pune, India	Semi Urban, industrial site	20.7 ppbv (December)	2.8 ppbv (July)	13
Gadanki, India	Tropical, rural site	19 ppb (March)	0.5 ppb (January)	30
Meadowlands, New Jersey	Urban, heavily industrialized	109.9 ppb (January)	4.3 ppb (April)	22
Dhaka, Bangladesh	Urban, Highly traffic congested	172 ppb (Winter)	18 ppb (Monsoon)	19
Jeddah, Saudi Arabia	Urban, Commercial and coastal site	24.95 ppb (Spring)	1.05 ppb (Autumn)	31

4.3: Characteristics of ambient O_3 and its selected precursors over mid-Brahmaputra valley

Surface O_3 and its precursors displayed temporal variations with regard to seasonal, diel, monthly and annual trends [9, 15, 32-35]. The average concentration of ambient O_3 and NOx, during the whole study period from 2013-2017 were 18 ppb and 11ppb respectively. The diel, seasonal, monthly and annual trends of ambient O_3, and NOx were described below in particular.

4.3.1: Ambient O_3

4.3.1.1: Diel and monthly variations

The diel and monthly variations of O_3 for the entire study period have been shown in Fig.4. 3. The days of the week generally showed O_3 trends with single hump (maximum ozone) during the mid-day in all the four years. The photochemical activities of the precursor gases in presence of solar radiation lead to increase in solar radiation during daytime. However the concentrations remain low during night time due to lack of solar insolation, NOx titration and surface deposition [8]. Similar pattern of diurnal variations were reported earlier by many researchers [10, 20, 30, 36-39].This site being remote and rural, it has been explicit in NOT showing profound weekday-weekend variation in the trends of O_3 concentrations. This is unlike what is seen in the urban locations [32-33]. The O_3 distribution of the days of the week which however shows a mild rise in the concentrations mostly during midweek during the first three years but the rise in concentrations shifts towards weekends in the last year i.e. 2016-2017. The hourly variations of O_3 shows much clear 'bookish' hump around midday in all the four years [9, 15]. The monthly distribution of O_3 clearly shows a peak during the month of April (spring) maximum of O_3 concentrations at this remote site like several earlier researchers reported in all the years except in the year 2014-2015 which shows a slight increase in concentrations during the month of February [9,33-35]. Least concentrations were observed mainly from June to December in all the years. This may be due to the fact that ambient O_3 produced photochemically is affected by cloud cover and the washout of the concentration of the precursor gases by the monsoon rain and so the diurnal pattern observed during these months was rather flat [8]. The average monthly and annual concentrations of ambient O_3 in Tezpur during the study period are given in Tables 4.3.

Which shows the same results as mentioned earlier. The difference in concentrations were mainly observed due to photochemical activities, differences in concentrations of the precursor gases, meteorological parameters and the prevailing manmade activities like biomass burning etc. [11, 15, 30, 40].

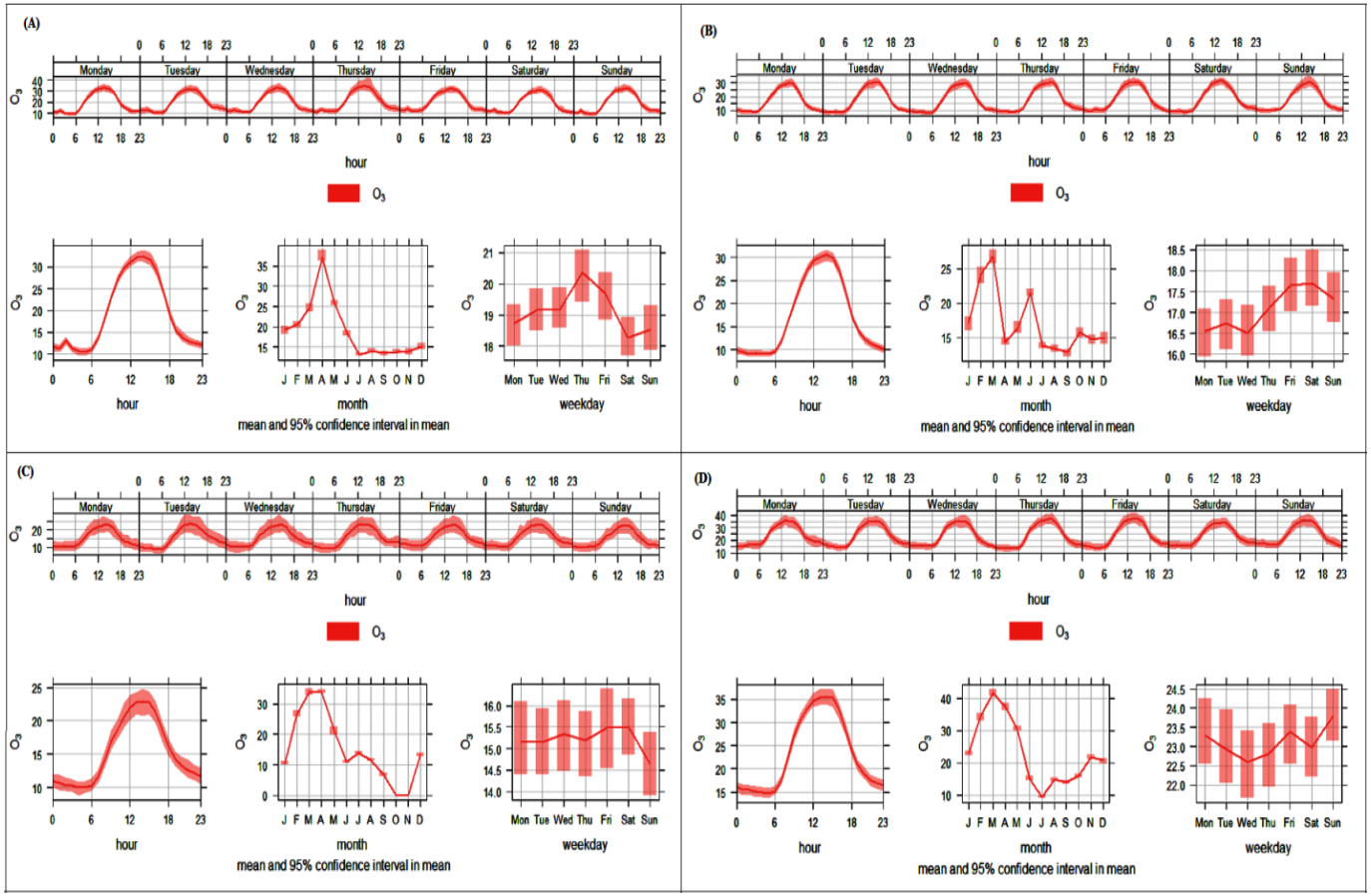

Fig.4.3. Diel and monthly Variations in the concentrations of O_3 (average conditions): (A) For the year 2013-2014 (B) 2014-2015 (C) 2015-2016 (D) 2016-2017.

Table 4.3: Average monthly concentrations of O_3 (ppb) for each year (2013-17) at Tezpur

Year	May	June	July	Aug	Sep	Oct	Nov	Dec	Jan	Feb	Mar	Apr	Annual
2013-2014	30±10	18±9.23	13±5.17	14±6.59	13±9	14±9.21	14±10.25	15±10.97	19±12.27	21±10.15	25±15.41	37±18.5	19±13.03
2014-2015	16±11.7	22±9.93	14±6.83	13±6.59	13±8.50	16±10.38	15±10.54	15±11.9	17±14.3	24±14.8	27±14	14±7.24	17±11.7
2015-2016	21±14.8	11±4.99	14±6.06	12±7.19	7±8.63	No data	No data	13±9.32	11±8.19	27±13.4	34±15.7	34±9.8	15±14.5
2016-2017	30.4±12.8	15.1±9.23	9.4±4.9	14.8±7.09	13.9±9.54	15.9±8.98	21.7±10.5	20.7±11.08	22.9±12.5	34.4±15.5	41.7±14.6	37.4±15.6	23.1±15.1

4.3.1.2: Seasonal variations

The seasonal distribution of O_3 during the study period is shown in Fig.4.4 which shows a clear variation. The graph clearly shows pre-monsoon (Spring) maximum of O_3 concentrations in all the three years except in the year 2014-2015 where maximum O_3 concentration was seen during winter season at this remote site like several earlier researchers reported [9, 33-35]. The mid-day maximum ozone concentrations of various seasons were different with the pre-monsoon season (springtime) showing the maximum mid-day O_3 compared to the other seasons, and the monsoon season showing the minimum mid day O_3. The rise in concentration of ambient O_3 during premonsoon season was mainly due to photochemical reactions and vehicular emissions [8, 15]. Also it may be noted that north-east India experienced active biomass burning from November to April that peaks in the premonsoon season which leads to maximum O_3 concentrations [42-43]. The lowest concentration during monsoon season is mainly due to heavy rainfall in the study site.

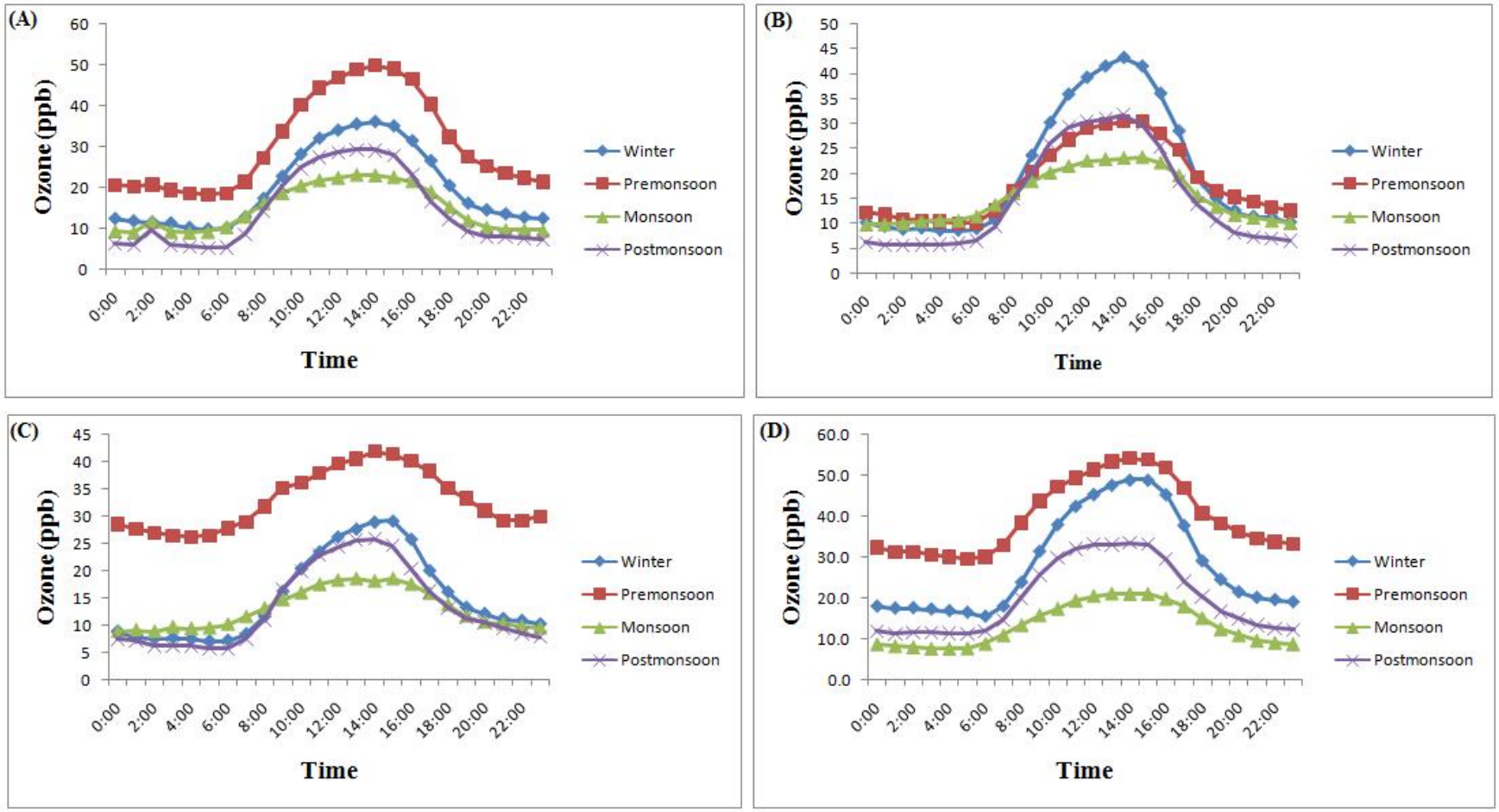

Fig.4.4. Seasonal variations in the diel concentration changes of ozone through the day during theYear (A) 2013-2014; (B) 2014-2015; (C) 2015-2016; (D) 2016-2017.

The calendar plots of ozone for the study period have been shown in Fig. 4.5. The spring maximum of O_3 is clearly shown in these plots. In the calendar plot we can also see the wind directions, and the highest concentration of O_3 was experienced while the wind direction was easterly, which matched with the direction of the congested and busy highway. It may just 'coincidental' that Li et al. (2017) too reported maximum ozone against easterly winds [44].

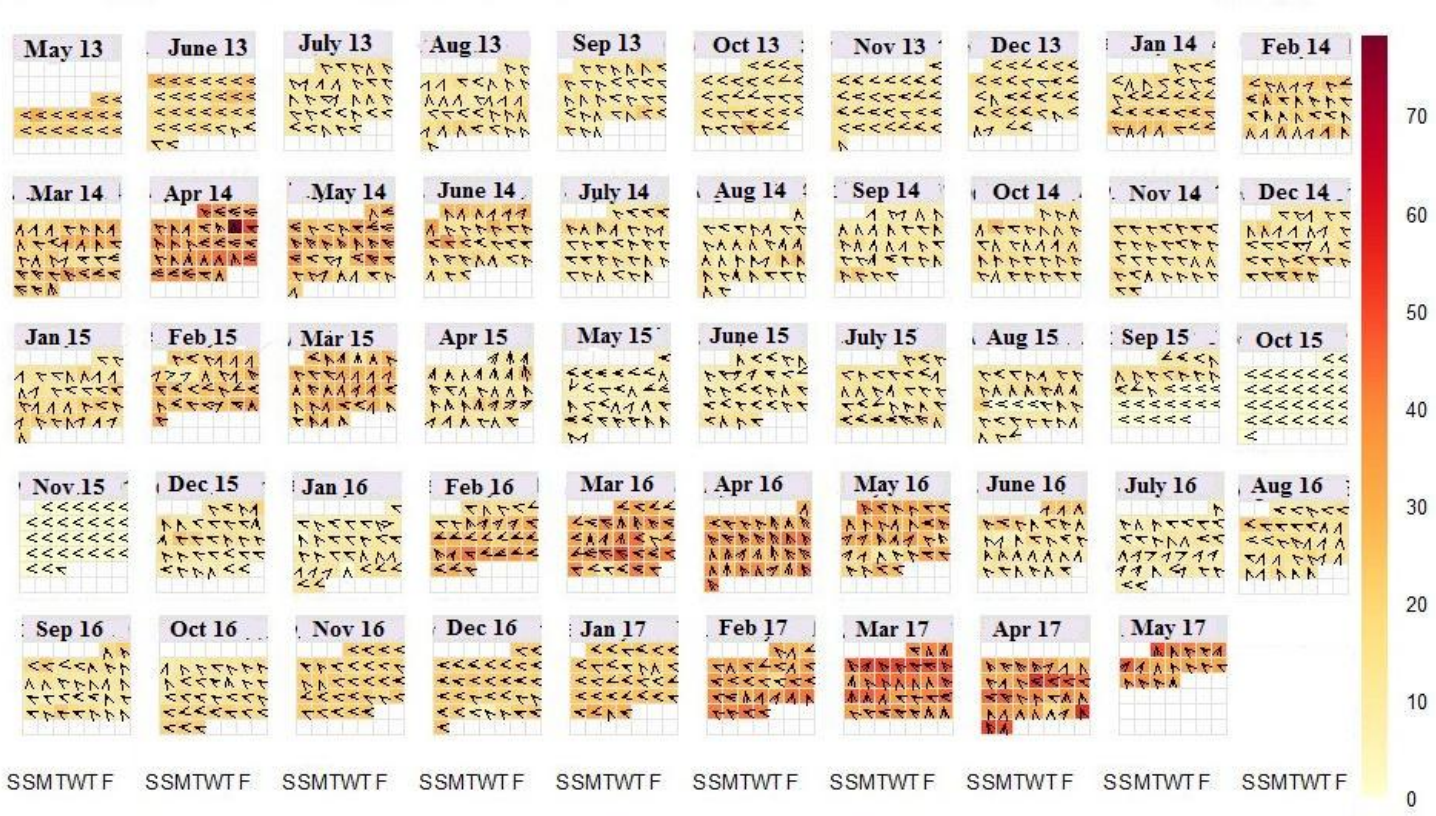

Fig.4.5. Calendar plot of the averaged data's of $O_3$with annotations showing wind angle scaled to wind speed i.e. the longer the arrow, the higher the wind speed during the study period.

4.3.2: Oxides of Nitrogen (NOx)

4.3.2.1: Diel and monthly variations

The diel and monthly variations of NOx for the entire study period have been shown in Fig. 4.6. The diel variation of maximum concentration of NOx exhibited a slight morning and a prominent evening peak i.e. at around 6 P.M. in all the four years. Similar studies were also reported by many researchers in earlier studies [17, 45]. The higher concentration of NOx during early morning hours and night time is basically due to local ambient wind pattern, chemical reactions, boundary layer processes and manmade emissions [30]. Moreover during night time the boundary layer remains at a lower height till early morning due to which the pollutants gets confined in the layer thereby increasing NOx concentration during night, but during daytime the concentrations of NOx being a precursors gets converted to ambient O_3 thereby increasing its concentration, hence low level of NOx is seen during daytime [10, 17]. The rise in concentrations of NOx was generally seen around midweek i.e Wednesday and Thursday during the entire study period. The monthly distribution of NOx clearly shows a peak during the month of January and February in all the three years except in the last year the peak was seen during March month. The average monthly and annual concentrations of NOx in Tezpur during the study period are given in Tables 4.2. Which shows the same results as mentioned earlier. The rise in concentration of NOx is mainly due to anthropogenic and natural activities like vehicular emissions, industrial discharge, exhaust fumes and lightning etc [17, 46]. The study site being a rural area is mainly a NOx sensitive regime with low concentration of NOx and high VOC [47] where the concentration of NOx is generally low. The daily cycle of NO level and its conversion to NO_2 has a pronounced impact on the daily cycle of ambient O_3 [48]. The peak during morning hours was mainly due to the emission-dilution balance of O_3 and NOx and also due to the photochemical activities. Also during morning hours the vehicular traffic is dense which contributes to the increased peak during the morning hours. But during noon time due to increased solar radiation the photochemical activities increases which produce ambient O_3 by the photolysis of NO_2 thereby decreasing NOx concentrations [15].

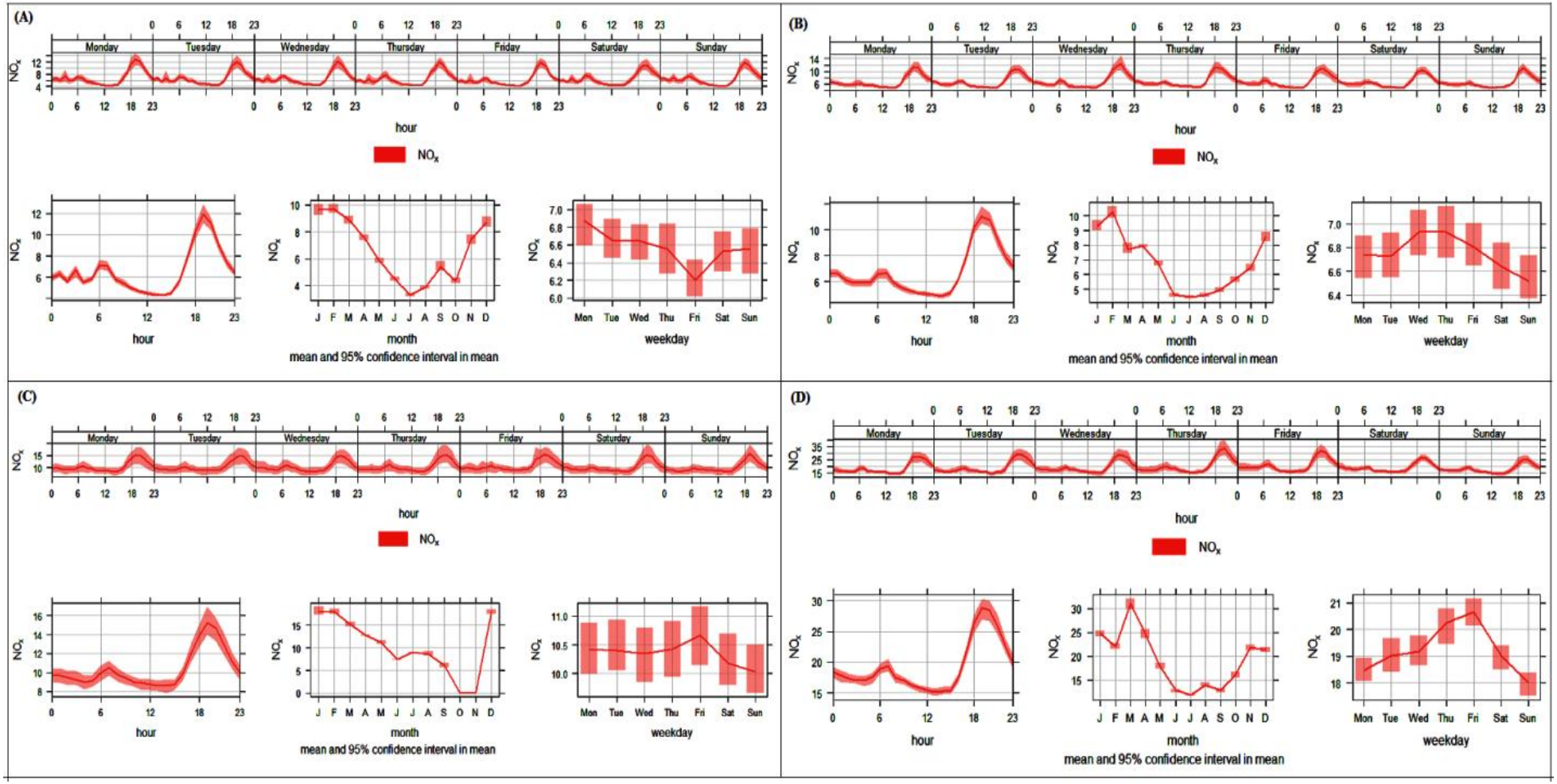

Fig.4.6. Diel and monthly Variations in the concentrations of NOx (average conditions): (A) For the year 2013-2014 (B) 2014-2015 (C) 2015-2016 (D) 2016-2017.

Table 4.4: Average monthly concentrations of NOx (ppb) for each year (2013-17) at Tezpur

Year	May	June	July	Aug	Sep	Oct	Nov	Dec	Jan	Feb	Mar	Apr	Annual
2013-2014	6±3	4±2	3±1	4±2	5±5	4±3	7±5	9±5	10±5	10±5	9±4	8±3	7±4.4
2014-2015	7±2.19	5±1.72	4±1.78	5±1.82	5±2.23	6±2.94	6±3.20	9±4.46	9±5.23	10±5.24	8±4.14	8±1.66	7±3.84
2015-2016	11±5.93	7±1.71	9±1.90	9±6.97	6±6.76	0±0	1±3.51	18±7.39	18±10.5	18±7.08	15±6.08	13±2.76	10±8.40
2016-2017	17.9±9.18	12.8±5.11	11.9±3.22	14±5.10	12.8±5.37	16.1±8.94	21.8±8.31	21.3±8.33	24.7±8.54	22.1±8.35	30.9±15.5	24.7±12.6	19.2±10.54

4.3.2.2: Seasonal Variations

The seasonal distributions of NOx during the study period have been given in Fig.4.7 showing a clear variation. The graph of the first two years clearly shows winter maximum whereas for the next two years maximum concentration was seen during postmonsoon season at this remote site. Least concentration of NOx concentration was seen during monsoon season in all the four years. Winter maximum of NOx concentration was reported in many earlier studies [9, 15, 17, 22, 45, 49-51]. The variations noted here is mainly due to poor dependency on NOx on climatic conditions. Also increased anthropogenic activities like burning of fossil fuels, emissions from industries, biomass burning etc. However, the manmade activities contribute more to NOx build up during winter season than the meteorological parameters [45]. Moreover, the seasonal variabilities of solar radiation, prevailing air mass type, changing wind pattern, seasonal changes in long range transport, boundary layer height, photochemistry also contributes to the seasonal variations of NOx [9]. Winter maximum of NOx is mainly due to the fact that during this season the emitted pollutants from different manmade and natural sources were trapped in the boundary layer because of temperature inversions [15].

Minimum concentration of NOx concentrations during monsoon season was seen due to the increased rainfall activities and formation of intense cloud cover which lead to the washout of the pollutants leading to NOx formation.

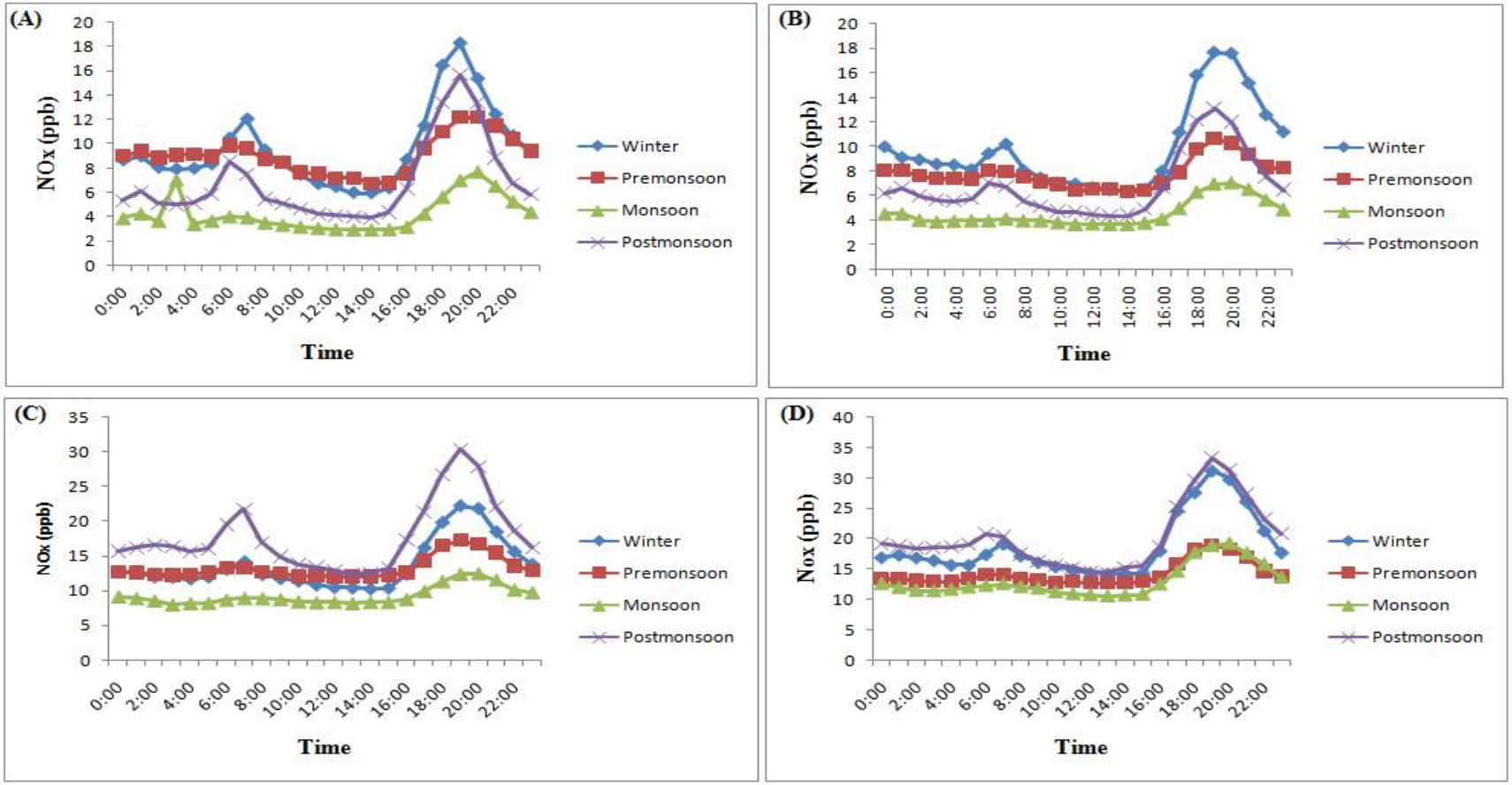

Fig.4.7. Seasonal variations in the diel concentration changes of NOx through the day during the Year (A) 2013-2014; (B) 2014-2015; (C) 2015-2016; (D) 2016-2017.

The calendar plot of NOx for the study period has been shown in Fig. 4.8. Higher concentrations of NOx were seen during the winter season which is mostly prominent in the year 2017. Highest concentrations were seen during March month. From the plot it is also evident that higher concentrations of NOx are associated with high windspeed from the easterly direction showing the same trend as O_3 concentrations.

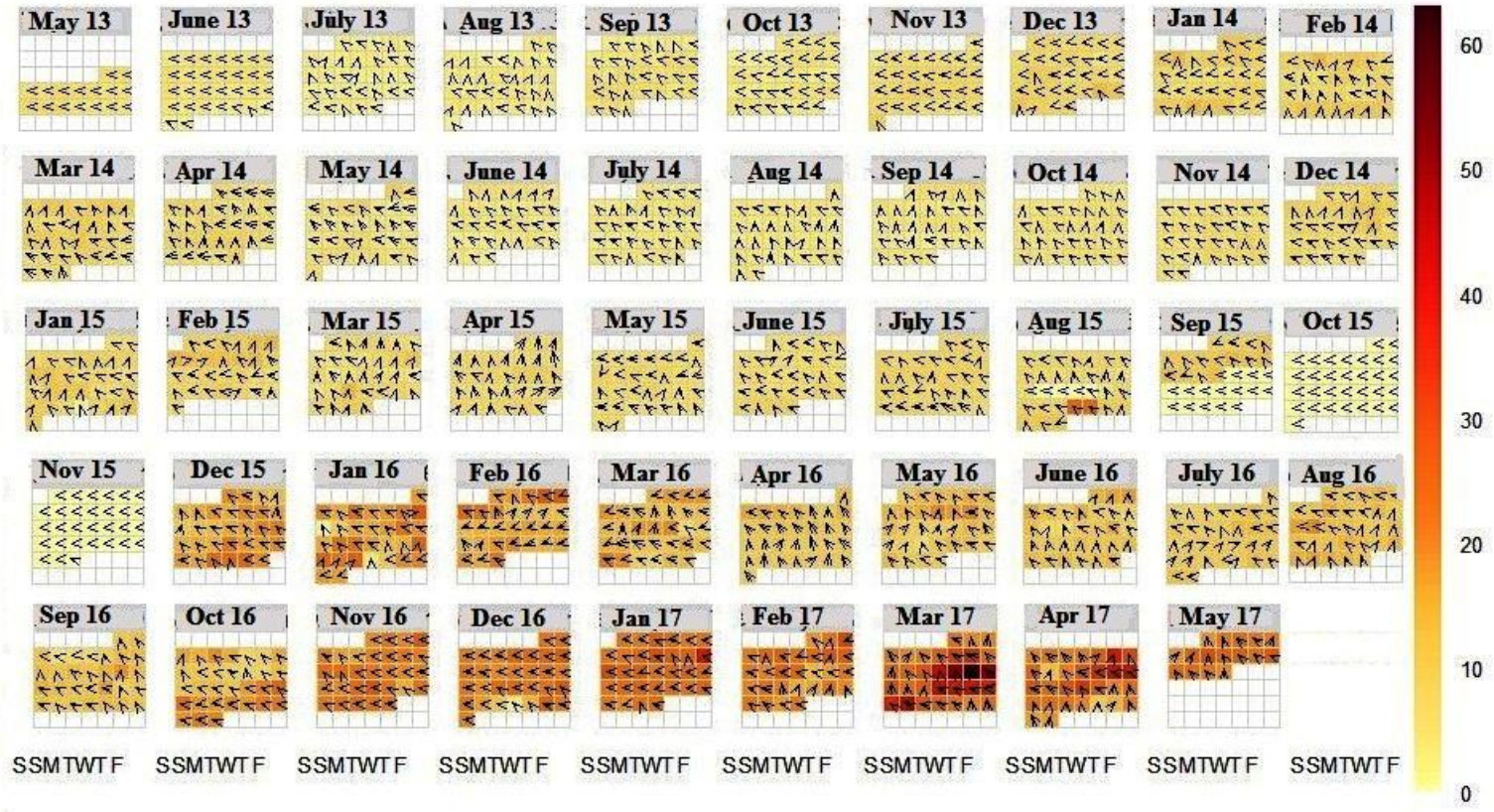

Fig.4.8. Calendar plot of the averaged data's of NOx with annotations showing windangle scaled to wind speed i.e. the longer the arrow, the higher the wind speed during the study period.

4.4: Diurnal and Seasonal variations of OX

The oxidation capacity of the atmosphere is indicated by the level of OX [52]. The daily profile of OX was found to be sharply increasing during the morning hours to the mid-day which is given in Fig.4.9.A.Gradual decrease in the concentration of OX wasobserved after sunset which has a similar trend like that of ozone. The reactive species – $O_3$and NOx – are rapidly titrated to form the reservoir species (NOz) after the sunset. However, at night theheat generated by anthropogenic activities leads to instability and vertical mixing in the ambient atmosphere leading to build up of nocturnal O_3 concentration as a result of dilution of major titration component of O_3 [53].

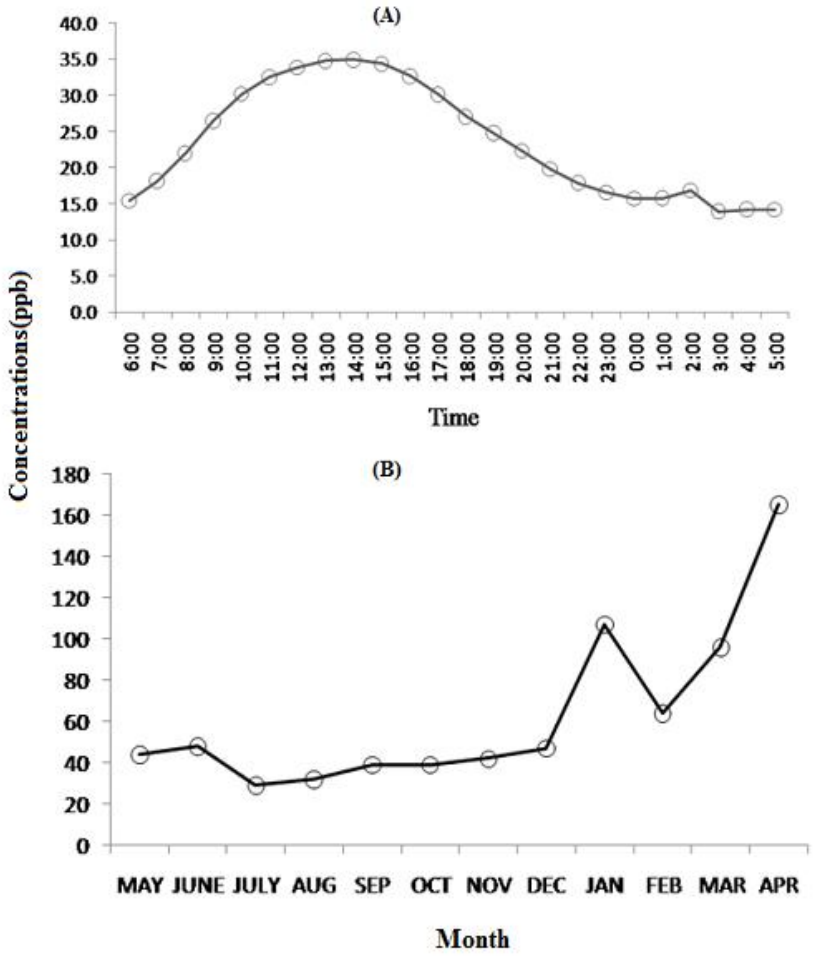

Fig.4.9. (A) Daily profile of OX during 2013(May) to 2014(May); (B) Monthly variation of OX during 2013(May) to 2014(April). (A representative data set of two years is taken for understanding the pattern of OX).

The monthly variation of OX is given in Fig.4.9.B. The maximum concentrations of OX were found during the pre-monsoon season mainly in the month of April. The increased photochemical activities in the presence of intense solar radiation lead to the increase in concentration during the premonsoon season. Similar behaviors were also reported by Ghude etal. (2008) which are based in a model study showing maximum ozone concentrations during the summer season in Delhi as a result of favorable meteorological conditions such as high solar insolation, clear skies, and low relative humidity [54].

4.5: Relationship of O_3 with NO, NO_2 and NOx.

The daylight hourly-average concentrations of O_3, NO and NO_2 against NOx of the study site have been plotted in Fig. 4.10. The chemical activity of a rural receptor site might be explained by the Polynomial fit curves for NO, NO_2, and O_3. In an earlier study, Clapp and Jenkin (2001) showed how the concentrations of NO, NO_2, and O_3 is depended on NOx (NOx in logarithmic scale) out of rural and urban locations together in a study from the UK [3]. Such relations of the species have also previously been explained by Tiwari et al. (2015) in Delhi which is one of the most polluted cities in the world. The comparison between the polynomial fit curves of the present study and the ones presented by Tiwari et el. (2015) made the behavioral shifts of the chemistry between less-polluted-remote-sites and heavily polluted-city-sites explicitly clear. It seemed that the polynomial fit curves for NO, NO_2, and O_3 against NOx of the remote rural location (Tezpur) were found NOT to follow the pattern of a highly polluted city (Delhi) as reported by Tiwari et al. (2015) [55].

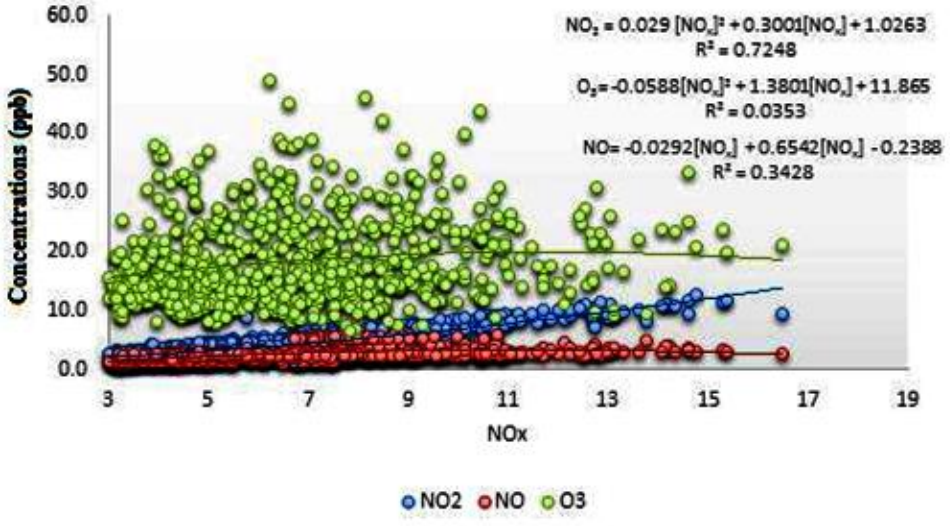

Fig.4.10. Daylight hourly-average concentrations of O_3, NO and NO_2 against NOx at remote site (Tezpur) during the study period.

The variation of O_3 concentration with NO_2/NO ratio have been given in fig.4.11. A logarithmic fit curve was used to describe the relationship. Similar study was also reported by Han et al. (2011) [32]. The figure exhibited a very strong correlation between O_3 and NO_2/NO ratio which implied that O_3 concentrations increases with increase in NO_2/NO ratio. O_3 concentrations tend to increase slowly with lower values of NO_2/NO ratio and gradually reaches a stable period which explains the photostationary state of O_3. From the figure it was evident that the concentrations of O_3 increases at low levels of NO_2/NO ratio which implies that at moderate concentrations of O_3 the reactions involved in its production is dominant. This data is then used to forecast the daytime O_3 concentration by fitting it in a polynomial function of *Ln* [NO_2]/[NO]:

$$[O_3] = 3.669 \times Ln\,[NO_2]/\,[NO] + 16.32 \qquad \text{[Eq. 5]}$$

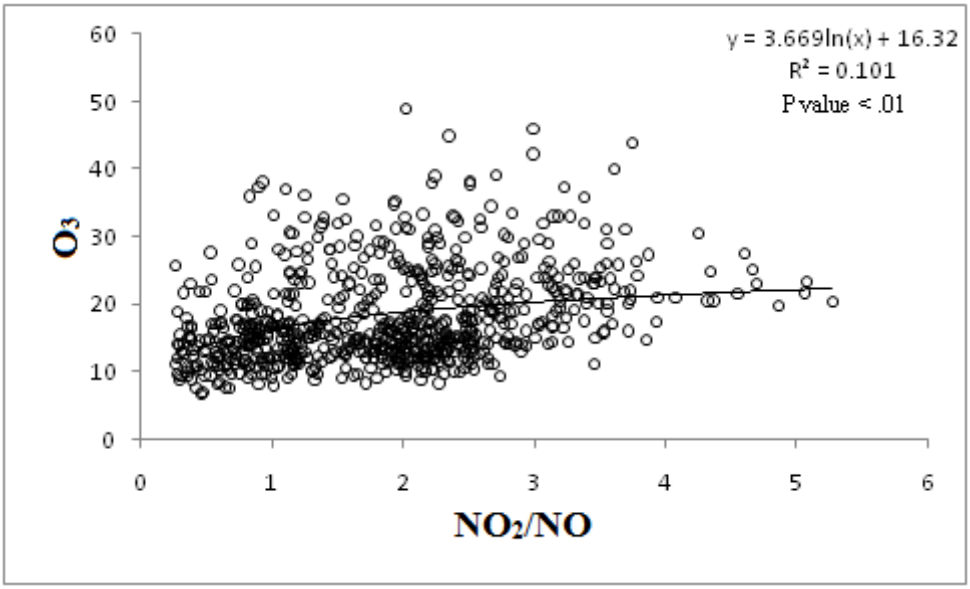

Fig.4.11. Variation of O_3 concentration with the NO_2 /NO.

4.6: O_3-NO and O_3-NO_2 relationships during daytime and nighttime

The variation of $O_3$with NO and NO_2 for daytime and Nighttime have been given in Fig 4.12(A) and 12(B) respectively. From the graphs it was evident that the concentration of O_3 decreases with increase of NO. The maximum concentration of O_3 and NO during daytime was found to be 75 ppb and 19.4 ppb respectively and during nighttime the concentrations were 63 ppb and 26.6 ppb respectively. From these values it was evident

that during daytime the concentration of O_3 is higher than the concentration of O_3 during nighttime while the concentration of NO is higher at nighttime than the concentrations during daytime. Also an inverse relation was seen during nighttime which indicates as NO increase during night O_3 concentration decreases.

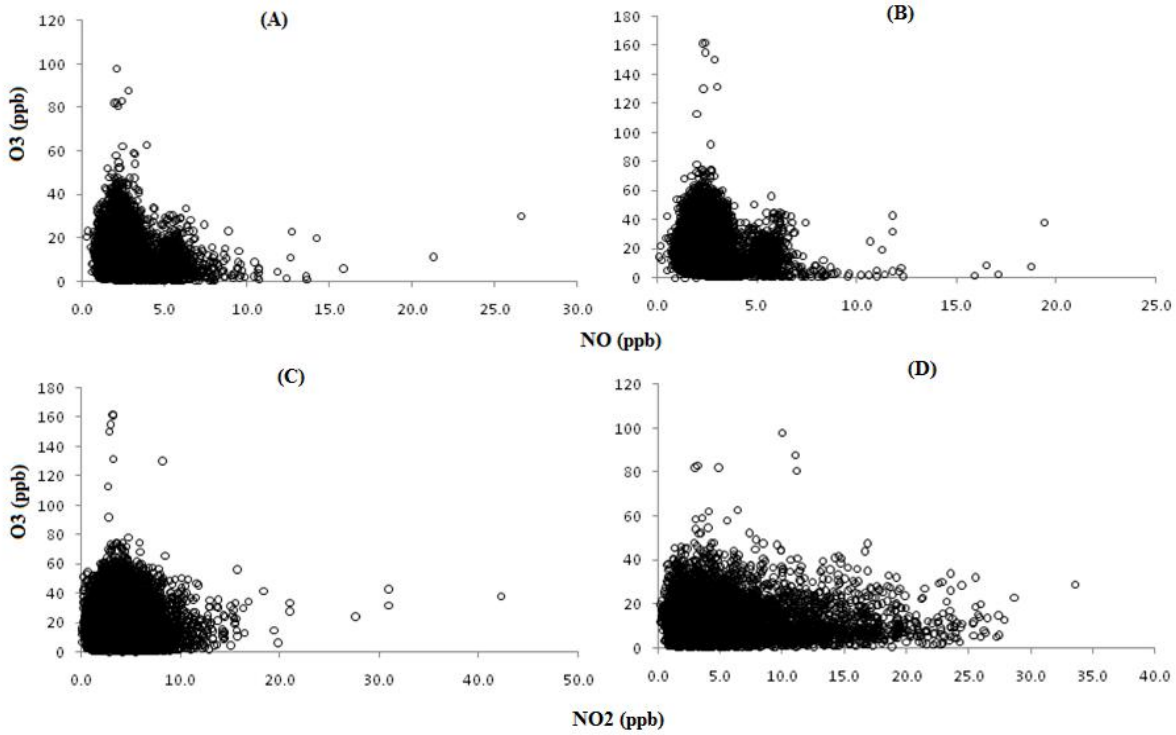

Fig 4.12. (A)Variation of mean values of O_3 with NO during (A) Daytime (B) Nighttime and Variation of mean values of O_3 with NO_2(C) during daytime (D) Nighttime.

The variation of O_3 and NO_2 for daytime and Nighttime have been given in Fig 4.12(C) and 4.12(D) respectively. From the plots it was evident that the concentration of O_3 increases with increase of NO_2 referring to the fact that NO_2 helps in build of O_3 in the ambient atmosphere. The maximum concentration of O_3 and NO_2 during daytime was found to be 75 ppb and 42.3 ppb respectively and during nighttime the concentrations were 63 ppb and 33.6 ppb respectively. From these values it was evident that higher the concentrations of NO_2 higher are the concentration of O_3 as during day time in the presence of sunlight NO and NO_2 are formed together but are killed differentially to form O_3, whereas during night time mostly destruction of NO and NO_2 takes place. In a similar study Han et al.2011 in Tianjin, China observed that the mean concentration of O_3 is highest during daytime as compared to night whereas the mean concentration of NO is highest during night as compared to daytime [32].

4.7.1: Relationship among NOx, NO_2 and NO during daytime

The relationships of NOx with NO_2 and NO for daytime have been given in Fig 4.13(A) and 4.13(B) respectively. From the graphs it was inferred that a strong correlation was seen between NOx and NO_2 during Daytime as compared to NO. So it can be said that NO_2 contributes more to O_3 buildup than NO during daytime. Same results were also observed by Han et al., 2011 in a study in Tianjin, China. Moreover during daytime the photochemical activities are high and also in the presence of solar radiation the production of O_3 is more from NO_2 then NO. Moreover, as NO is highly reactive therefore NO_2 has longer lifetime than NO [32].

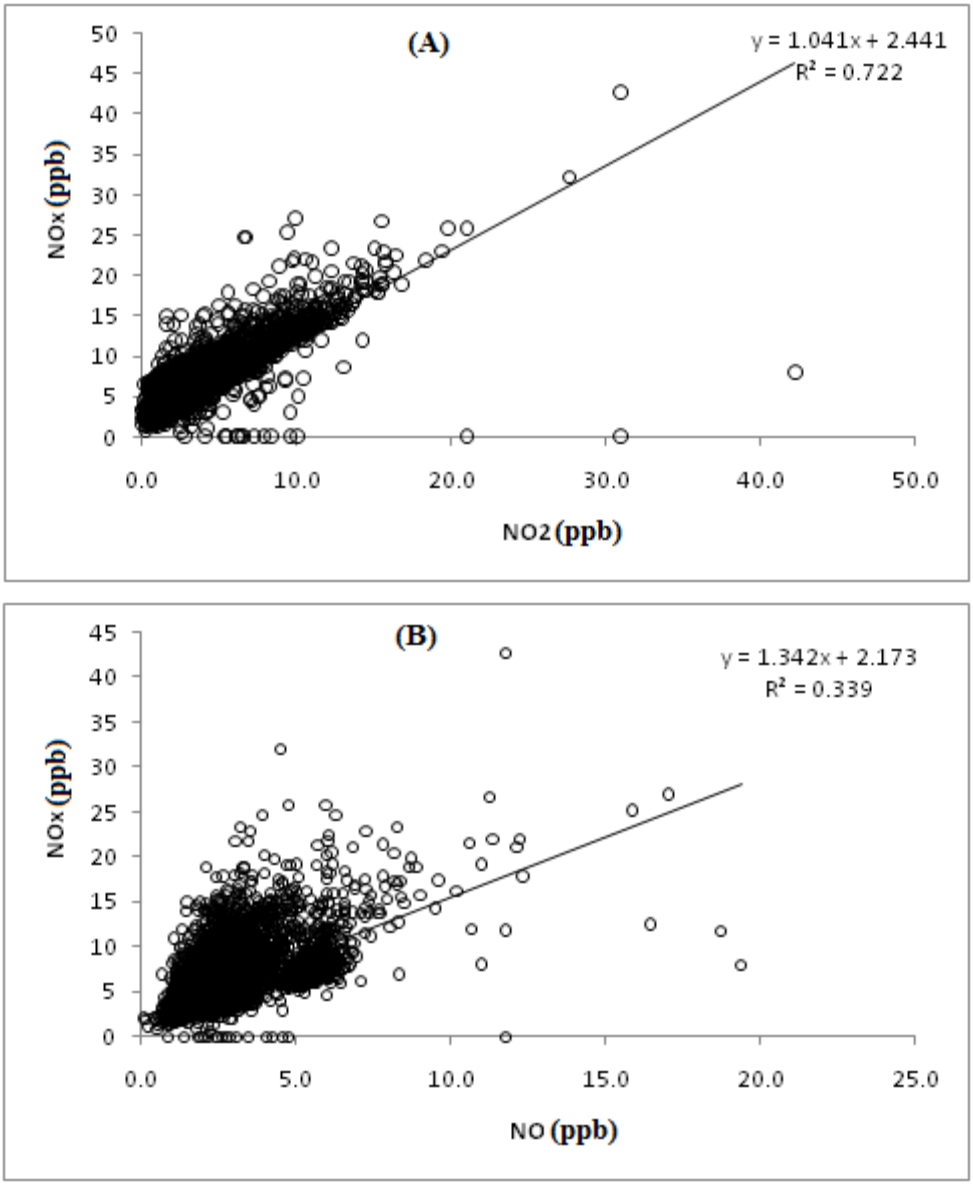

Fig.4.13: Variation of mean values of NOx with (A) NO_2; (B) NO during Daytime.

4.7.2: Relationship among NOx, NO_2 and NO during Nighttime

The relationships of NOx with NO_2 and NO for nighttime have been given in Fig 4.14(A) and 14(B) respectively. A very strong correlation of NOx and NO was observed during nighttime as compared to day. During night the emission of NO is more than that of NO_2 due to more traffic congestion in night hours. Han et al., 2011 reported a similar behaviour in Tianjin, China. Moreover, in the absence of sunlight the nighttime chemistry is different than that of day and so a different behaviour of the pollutants is observed during night [32].

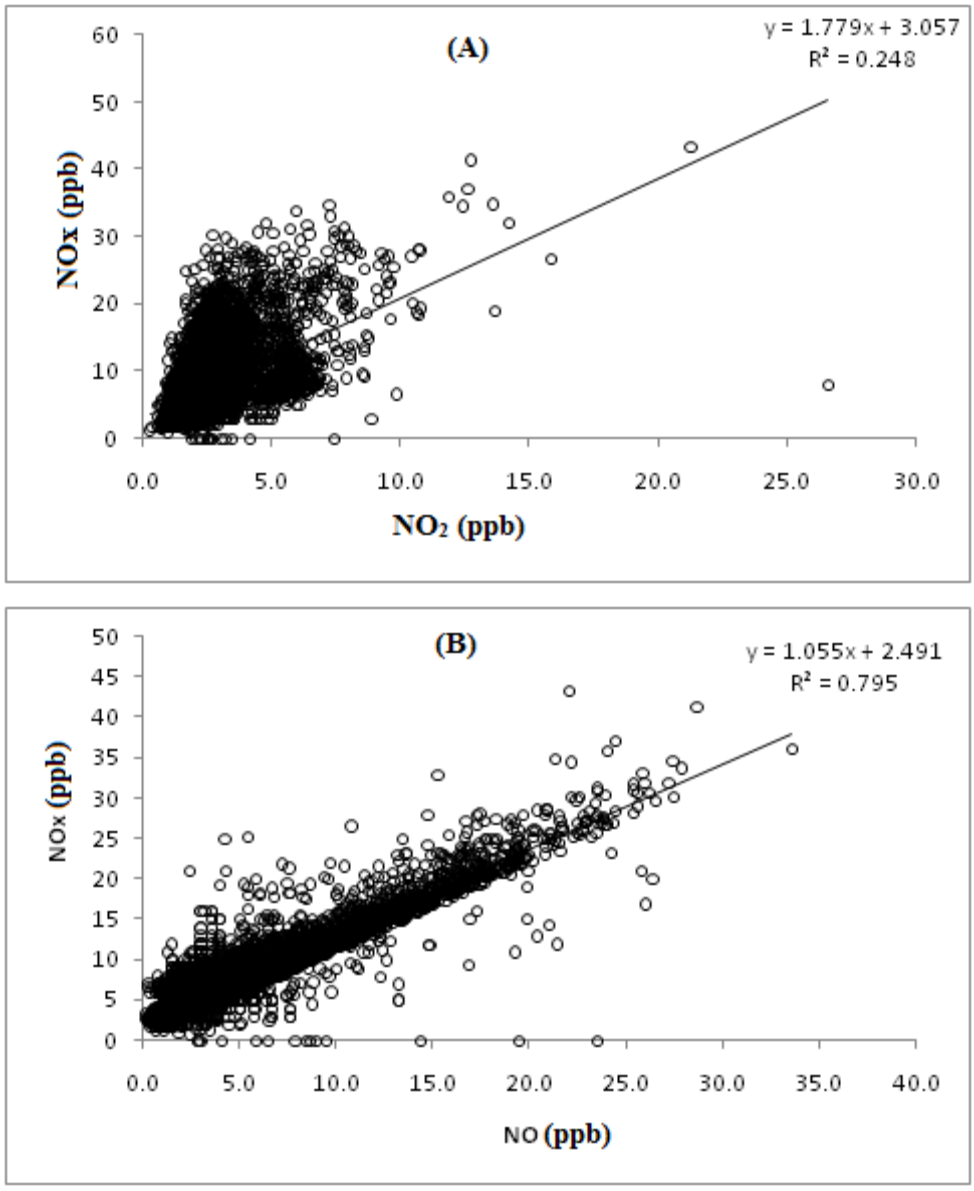

Fig.4.14: Variation of mean values of NOx with (A) NO_2; (B) NO during Nighttime.

4.7.3: Relationship of OX and NO_2 during Daytime and Nighttime

The relationship of OX and NO_2 for daytime and Nighttime have been given in Fig 4.15(A) and (B) respectively. From the graphs it was evident that OX and NO_2 have a linear relationship which inferred that as NO_2 concentration increases OX concentration also increases. Moreover, it is known that OX in a particular site has an NO_2 dependent and NO_2 independent contribution. The dependent condition refers to the local emissions and the independent contribution refers to the regional emissions. From the graphs it was seen that the NO_2 dependent contribution which is the local contribution is lower during nighttime than that of daytime however the regional contribution is similar during both day and night time.

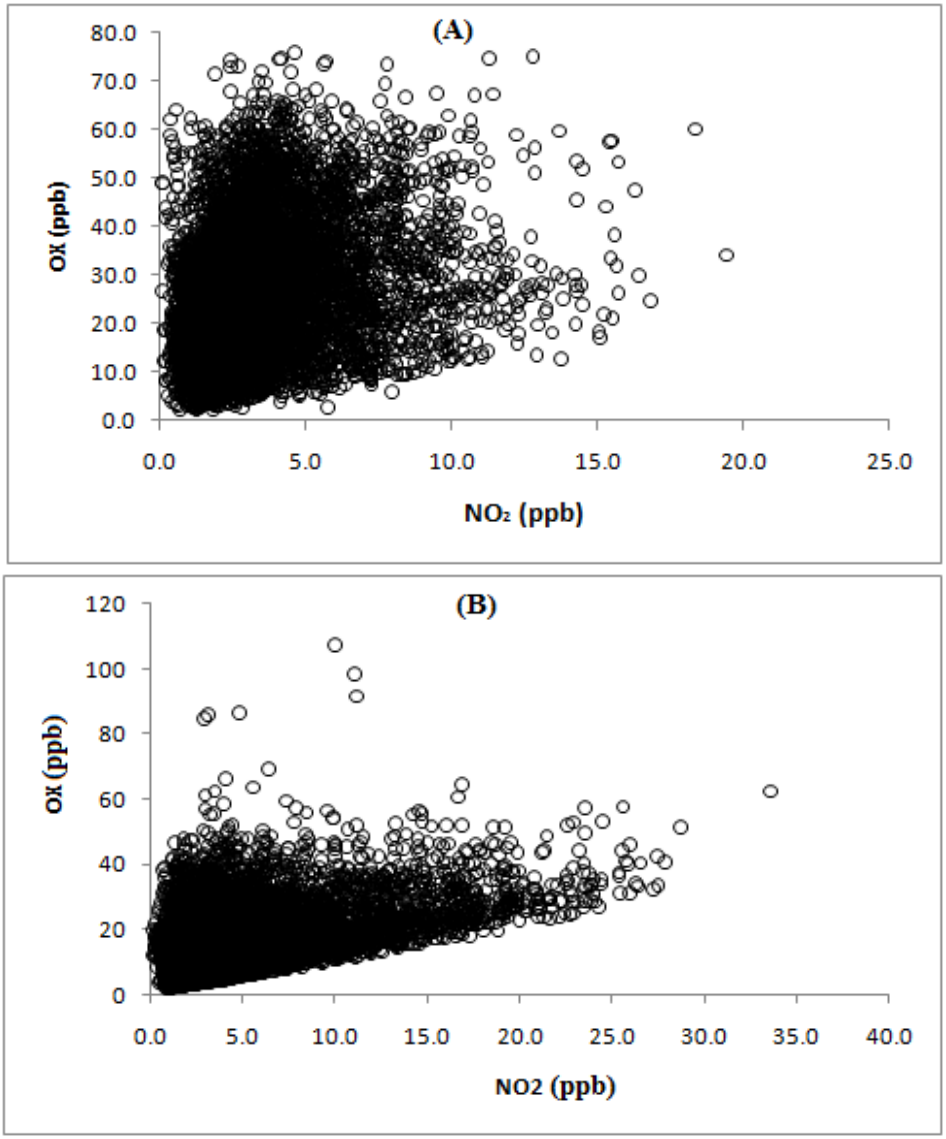

Fig.4.15: Variation of mean values of OX with NO_2 during (A) daytime; (B) Nighttime.

4.8: Ambient O_3 during special days

Trends of ambient O_3 and its precursors were observed during special events as compared to the normal days. The special events considered for this study are Diwali and Solar eclipse as there are very less record of the trends observed in case of ambient O_3 in rural site of India during Diwali and Solar eclipse.

4.8.1: Trends of O_3 during Diwali festival

Ambient O_3 trends during the Diwali festival for the representative year (A) 2013 (B) 2014 (C) 2016 and (D) 2017 have been given in Fig 4.16 respectively. During the year 2014 and 2016 the effect of Diwali crackers on O_3 concentration during night time was found to be more prominent. The maximum concentration of O_3 during the year 2013, 2014, 2016 and 2017 were 27 ppb; 35 ppb; 38.5 ppb; 39.8 ppb respectively. Many earlier studies reported that burning of fireworks during Diwali festival or during other festivals contributes to the increase of O_3 concentration in the ambient atmosphere [56-58].

Moreover the effect of fireworks on Diwali night was more prominently seen in the year 2014. However the after effect of Diwali festival on O_3 concentration was noticed during the year 2017 where highest ambient O_3 concentration was seen during one week after the Diwali festival. The variations and the increase in concentration of ambient O_3 concentrations during Diwali festival was mostly due to transport of O_3 and its related atmospheric conditions, increased vehicular traffic, emission of O_3 precursors form burning of fireworks etc [59]. The concentration of O_3 trends to increase many folds due to burning of fire crackers.

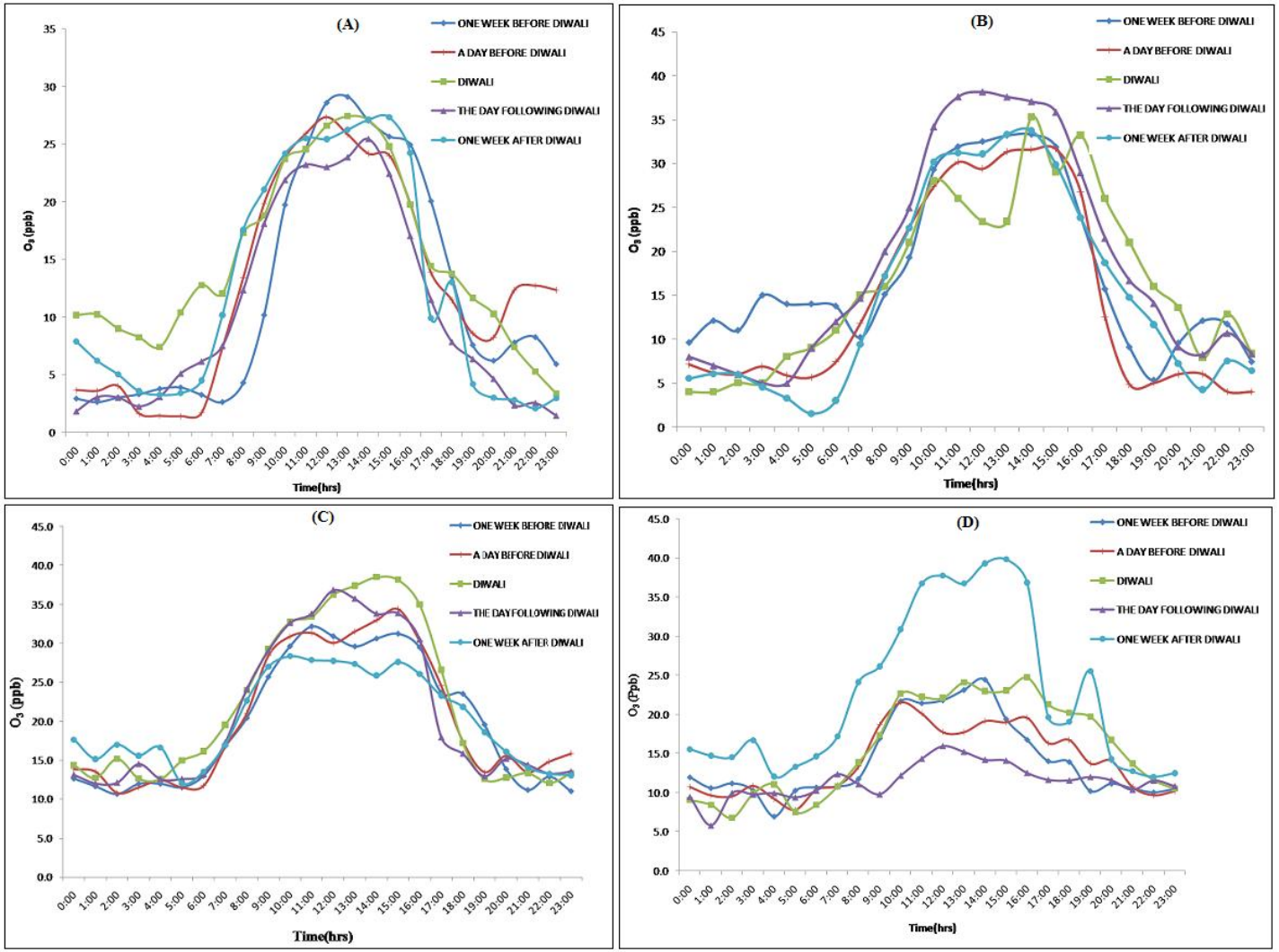

Fig.4.16. Trends of ambient O_3 during the days of Diwali festivals for the years (A) 2013 (B) 2014 (C) 2016 and (D) 2017.

4.8.2: Trends of NO_2 during Diwali festival

Ambient NO_2 trends during the Diwali festival for the year (A) 2013 (B) 2014 (C) 2016 and (D) 2017 have been given in Fig 4.17 respectively. From the plots it was evident that maximum concentration of NO_2 was generally observed during night hours especially in the 20^{th} hour.The maximum concentration of NO_2 during the year 2013, 2014, 2016 and 2017 were 15.8 ppb; 12.1 ppb; 36.7 ppb; 10 ppb respectively. This supports the fact that during the festival, the emissions from crackers tends to increase the concentration of NO_2 in the ambient atmosphere and thereby increasing the concentration of ambient O_3. Moreover maximum NO_2 concentration was observed during the year 2016 showing the same trend as that of ambient O_3 during the festival of Diwali. According to a study in Kannur, South India the photo-dissociation of NO_2 takes place due to the flash of fire crackers during night hours thereby increasing the concentration of O_3. Moreover the concentration of NO_2 and O_3 increased many folds during the festival [58]. Increased concentrations of NO_2 along with other pollutants were also found in many major cities of India during Diwali festival due to emission of huge amount of pollutants from burning of fire crackers [60].

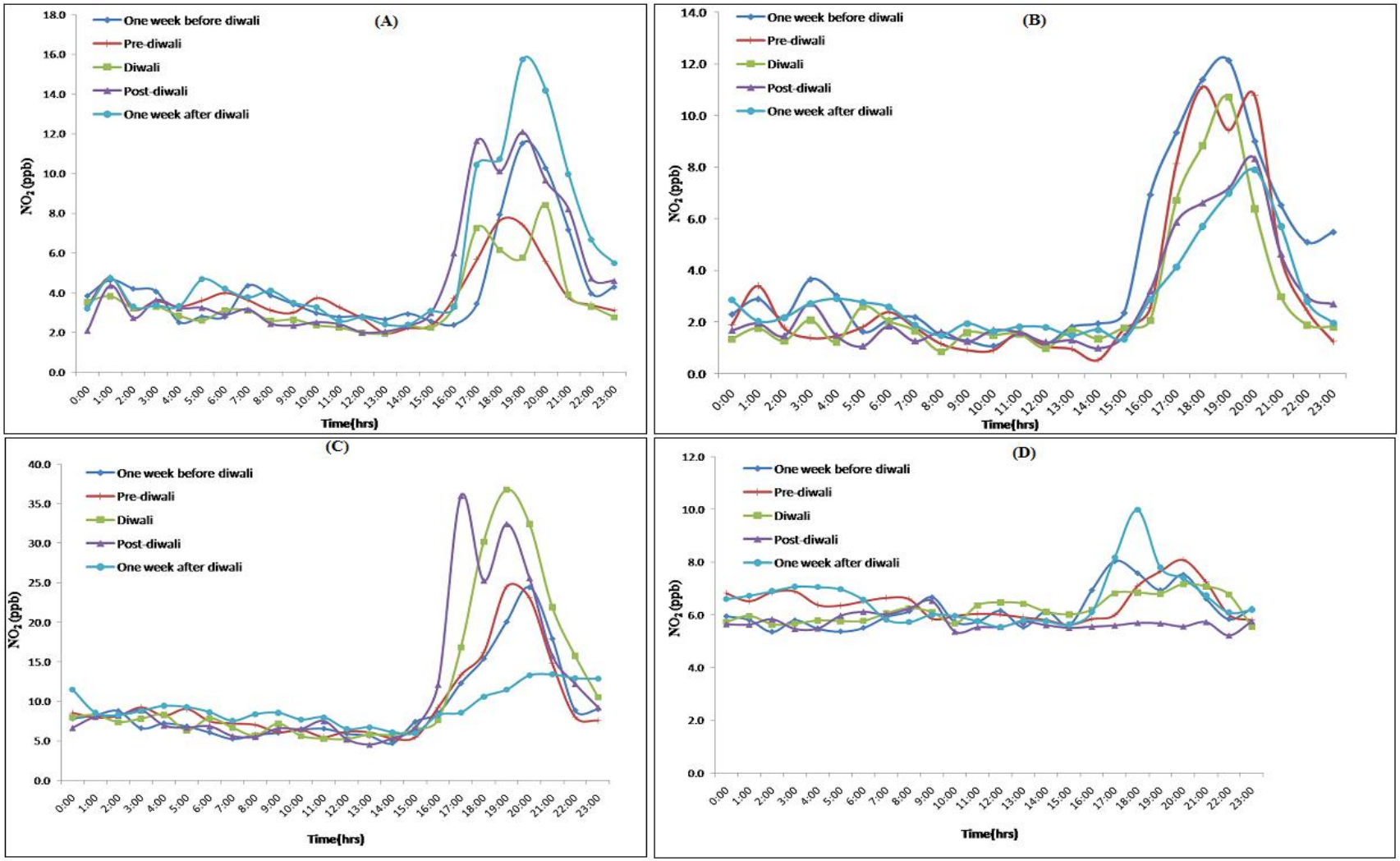

Fig.4.17. Trends of NO_2 during the Diwali festival for the year (A) 2013 (B) 2014 (C) 2016 and (D) 2017.

4.8.3: Relationship of ambient O_3 with NO_2 during Diwali festival

The relationships between O_3 and NO_2 during Diwali and Non-Diwali nights in the year (A) 2013 (B) 2014 (C) 2016 and (D) 2017 have been given in Fig 4.18. During the year 2013 O_3 and NO_2 shows a strong relationship with r^2= 0.123 than the non-Diwali nights showing a poor relation. Same trend was also observed during the following years. The year 2014 has shown the strongest relation than the other years during the Diwali night with an r^2 value of 0.5. It was observed NO_2 undergoes photo-dissociation to form ambient O_3 and so the higher the concentration of NO_2 the higher is the concentration of O_3. Moreover the burning of crackers during Diwali night contributes to the increase in concentration of ambient O_3. and NO_2. The bursting of crackers leads to increase in concentration of NO_2 which ultimately increases the concentration of O_3. Moreover smaller p value was observed during Diwali period as compared to the normal days which interprets that a very strong relationship between O_3 and NO_2 was observed during Diwali period as compared to the normal days. Finlayson-Pitts and Pitts in 1997 proposed that the NO_2 present in the ambient atmosphere undergoes photolysis in the presence of the blaze of firecrackers to form O_3 due to bursting of fire crackers. Similarly, in a study in Jamshedpur, India strong positive relations were reported between O_3 and NO_2 [62].

(A)

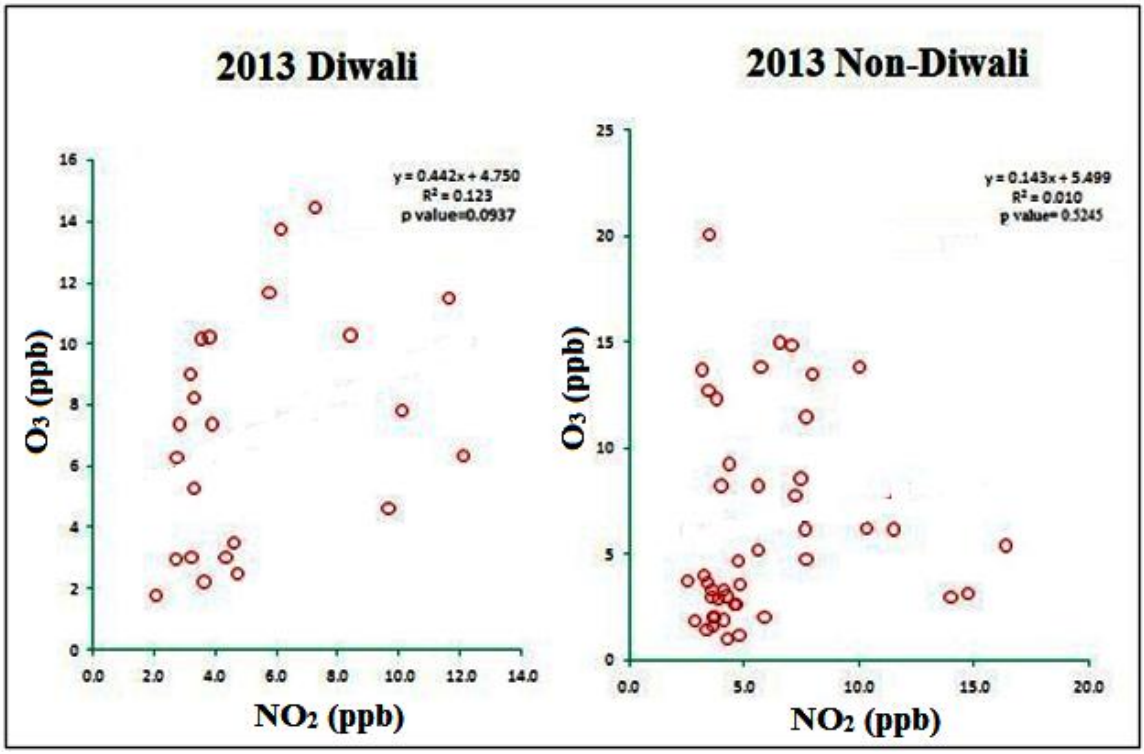

(B)

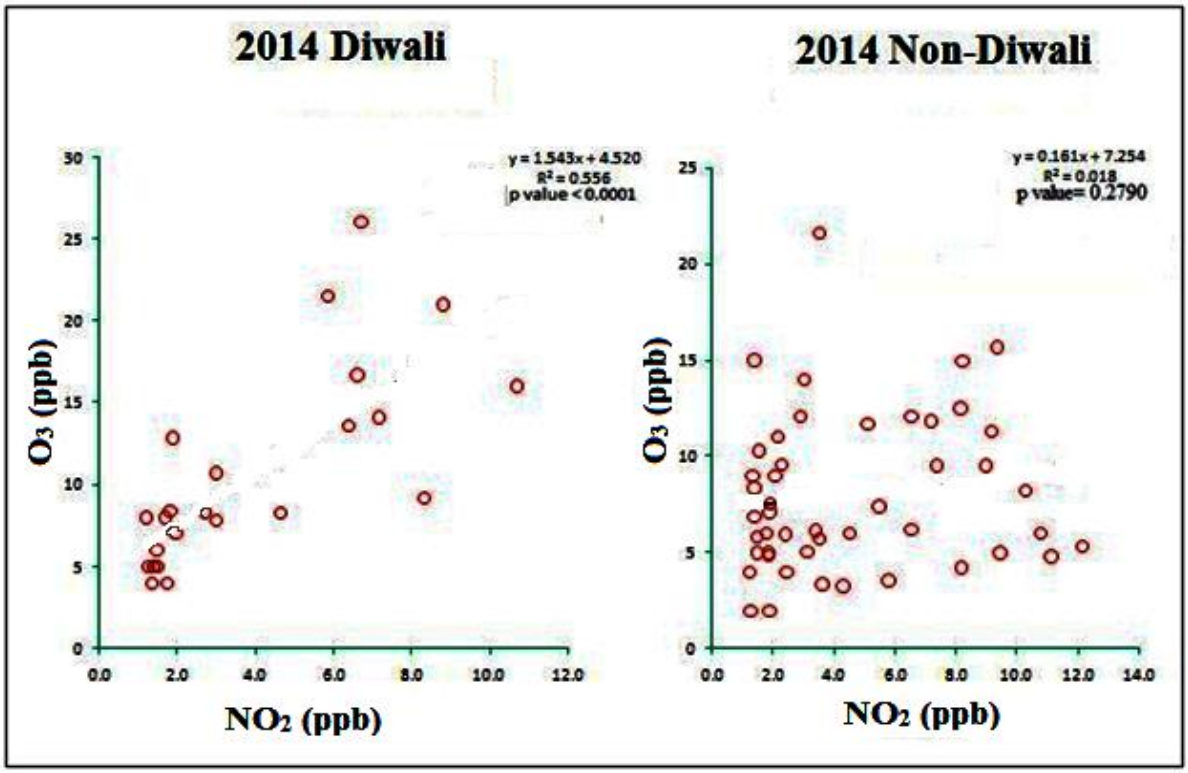
2014 Diwali
y = 1.543x + 4.520
R² = 0.556
p value < 0.0001
O3 (ppb)
NO2 (ppb)
2014 Non-Diwali
y = 0.161x + 7.254
R² = 0.018
p value= 0.2790
O3 (ppb)
NO2 (ppb)

(C)

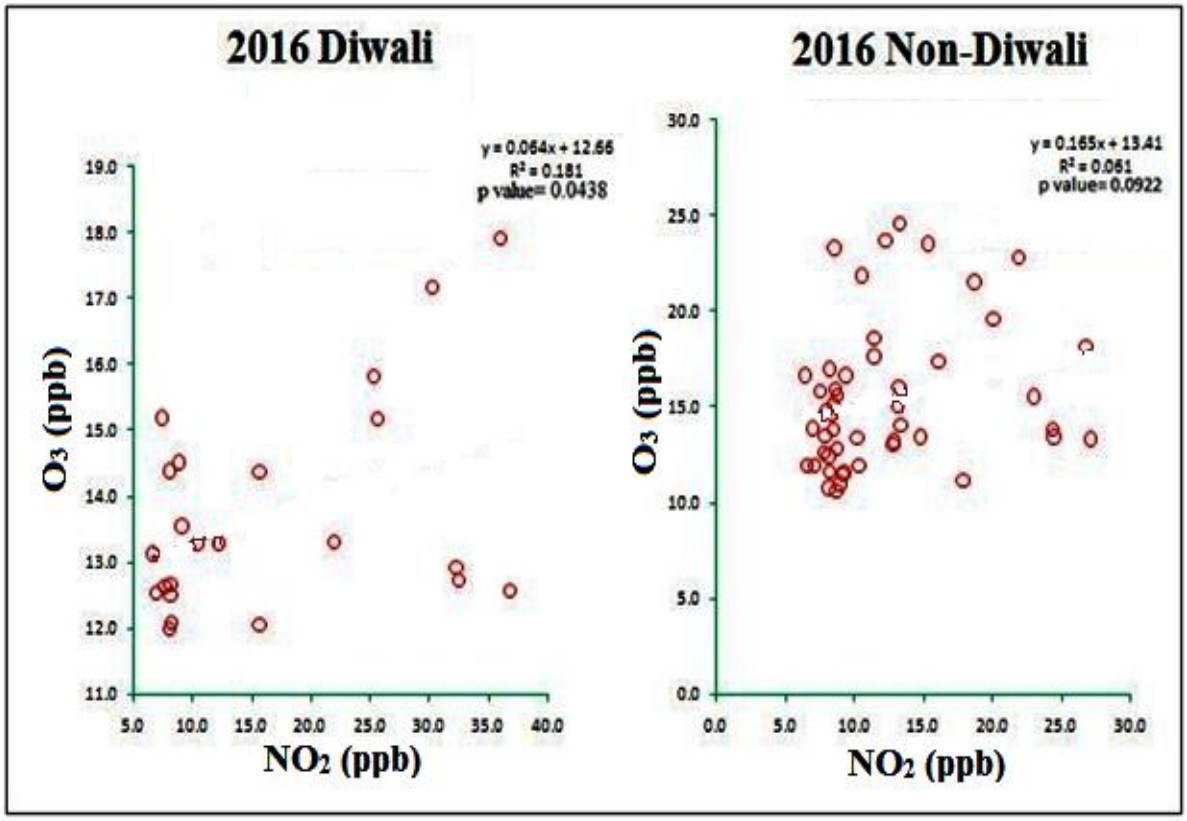
2016 Diwali
y = 0.064x + 12.66
R² = 0.181
p value= 0.0438
O3 (ppb)
NO2 (ppb)
2016 Non-Diwali
y = 0.165x + 13.41
R² = 0.061
p value= 0.0922
O3 (ppb)
NO2 (ppb)

(D)

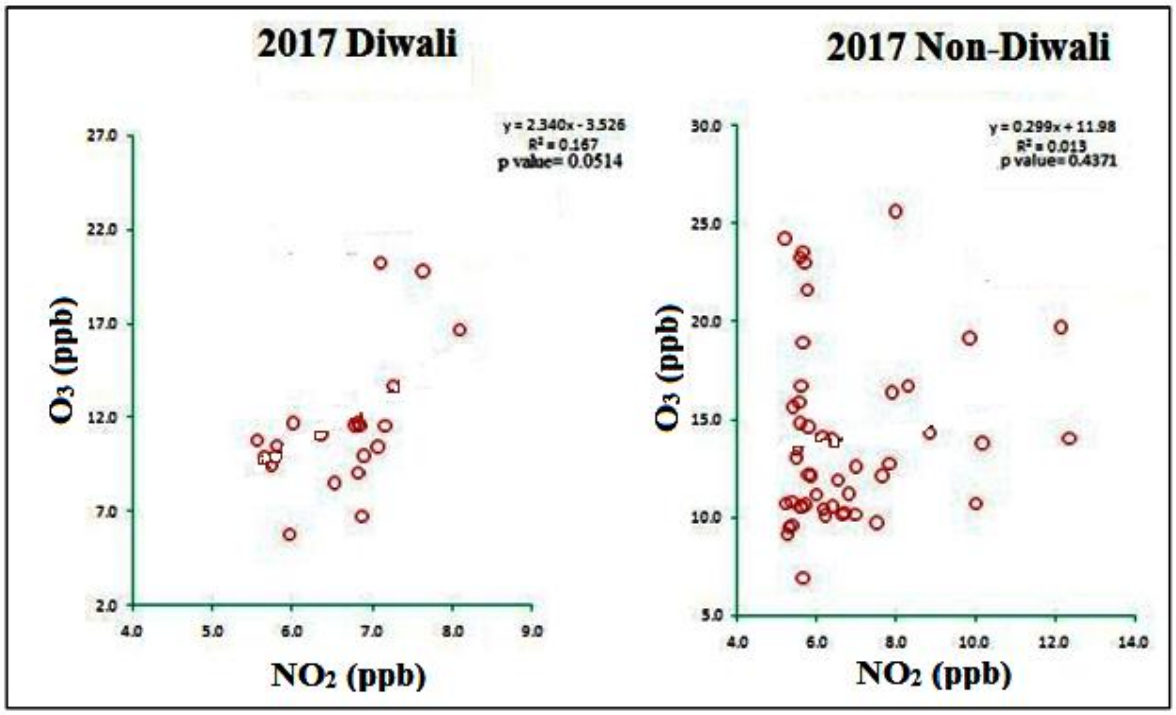

Fig.4.18. Relationship of ambient O_3 with NO_2 during Diwali festival in the year (A) 2013 (B) 2014 (C) 2016 (D) 2017.

4.8.4: Concentrations of O_3, NOx, NO, NO_2 and metrological parameters during solar eclipse days.

The concentrations of ambient O_3 during the year 2014 and 2015 during solar eclipse day and normal days are shown in Fig 4.19(A) and 19(B) respectively. During the first year the concentrations of O_3 were found to be decreasing during eclipse hours as compared to the normal days. The solar eclipse during 2014 started at 9:22 am and its maximum obscuration was observed at 11:34 am and ended at 1:44 pm. During this period it was observed that the concentrations of ambient O_3 were low during the eclipse hours as compared to the normal days. Generally, it was observed that Surface O_3 tends to rise during the morning hours and reach its maximum peak during noon [9, 64]. However, during 2015, eclipse hours contrast results were observed. The average mixing ratios of ambient O_3 and NOx were listed in Table 4.5. The concentration of O_3 during maximum obscuration for the year 2014 was 36 ppb during eclipse day whereas; during normal days the concentration was 52 ppb for the same hour. However for the next year the concentration was only slight different from the normal day's i.e during eclipse days it was

51 ppb at maximum obscuration level and 52 ppb during normal days at the same hour. During the next year, the solar eclipse started at 1:10 pm, maximum solar obscuration was at 3:15 pm and ended at 5:20 pm. Moreover 2015 eclipse also coincided with March equinox which is why the results were slight different from the previous eclipse, as the effect of eclipse might be masked by the effect of March Equinox. During the year 2015 only a slight change in O_3 concentrations was observed. The changes observed during eclipse hours were generally due to low photochemical activities during eclipse hours leading to low concentrations of surface O_3.

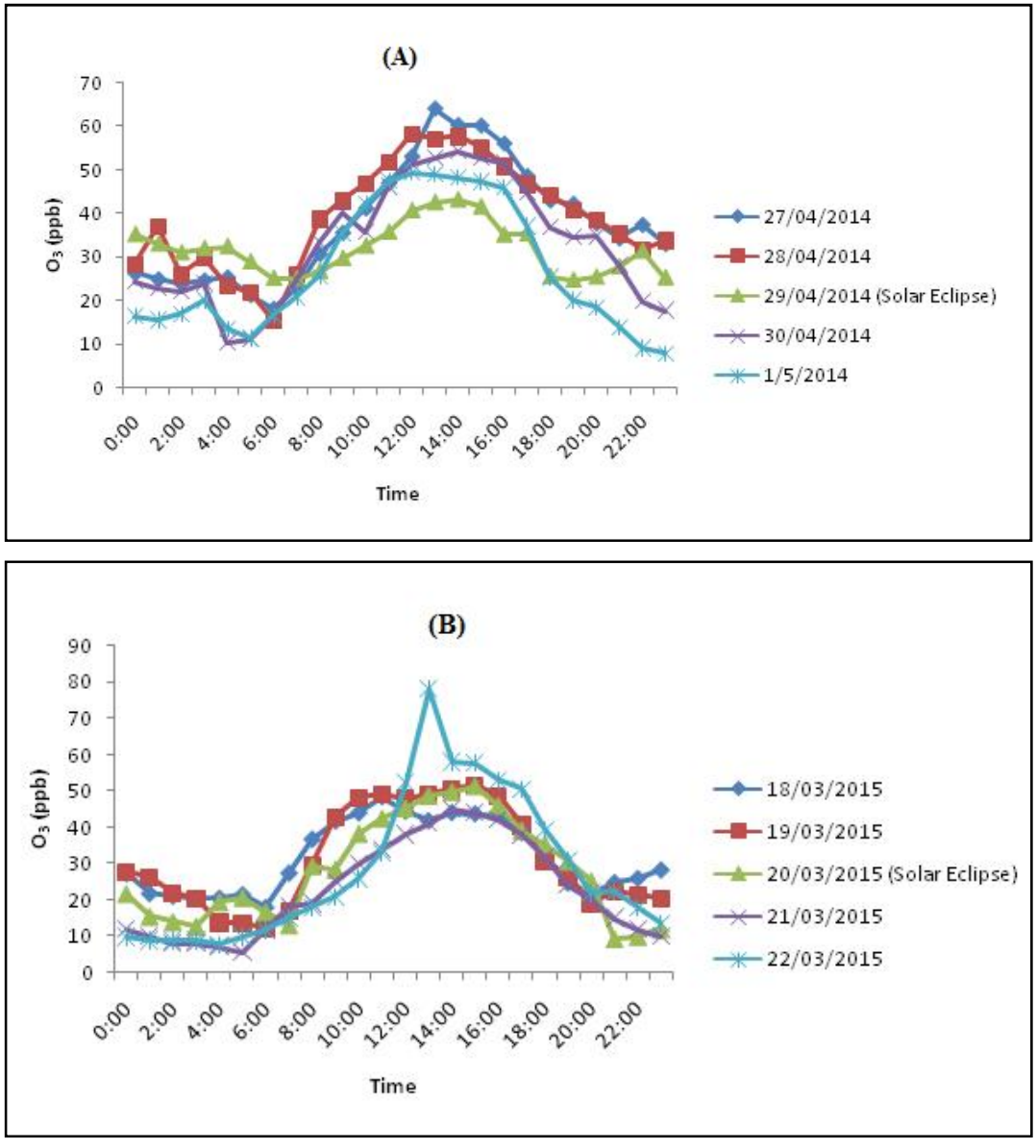

Fig. 4.19. Variations in ambient ozone observed during solar eclipse day and normal days for the year (A) 2014 and (B) 2015.

Table 4.5: Ambient O_3 and NOx (ppb) observed during one day before eclipse and on eclipse day for the year (A) 2014 and (B) 2015.

(A)

Time (Hrs)	O_3 in normal day (ppb)	O_3 in Eclipse day(ppb)	NOx in normal day(ppb)	NOx in Eclipse day(ppb)
9:00	43	30	7	6
10:00	47	33	6	6
11:00	52	36	6	6
12:00	58	41	7	6
13:00	57	43	7	6
14:00	58	43	6	5

(B)

Time (Hrs)	O_3 in normal day (ppb)	O_3 in Eclipse day(ppb)	NOx in normal day(ppb)	NOx in Eclipse day(ppb)
13:00	49	48	3	2
14:00	51	50	3	3
15:00	52	51	2	3
16:00	49	46	5	7
17:00	41	39	11	8
18:00	31	35	17	10

The variations of NO_2, NO and NOx during normal days and solar eclipse days for the year 2014 and 2015 were shown in Fig 4.20(A), (B) and (C) respectively. For the year 2014 the concentrations of NO_2, NO and NOx did not show any significant changes during eclipse hours as compared to the normal days. However, the changes were observed during 2015 where the concentrations of NO_2 and NOx tend to rise during the eclipse hours and gradually decrease towards the end of the eclipse. However, the concentration of NO did not show any significant change in both the years. Generally, it was seen that the concentration of NO_2 and NOx decreased during daytime leading to formation of O_3 and increased only at night due to the photochemical reactions between O_3 and NOx and also the mixing process of both the horizontal and vertical convective layers [15-63]. The

reduction in the rate of photochemical reactions of NO_2 could, thus, lead to the increase in concentration of NOx and NO_2 during eclipse hours.

The changes observed in O_3, NOx, SR, AT and RH during Solar eclipse for the year 2014 and 2015 were listed in table 4.6(A) and (B) respectively. The changes observed in the case of ambient O_3 were pretty much different during 2014 as compared to the year 2015. However, slight change in NOx concentration was observed during solar eclipse in both the years. Moreover, prominent changes in case of meteorological parameters were observed during solar eclipse hours.

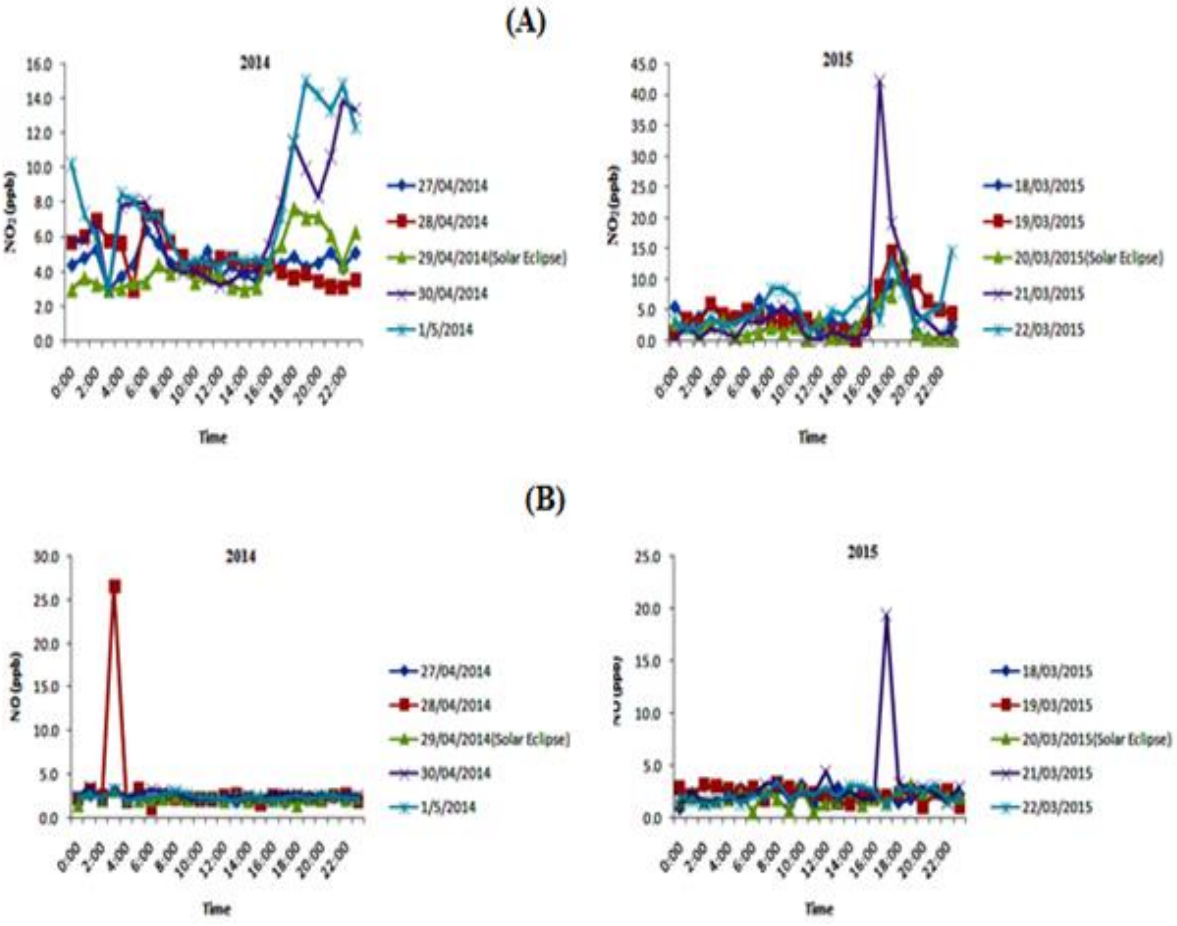

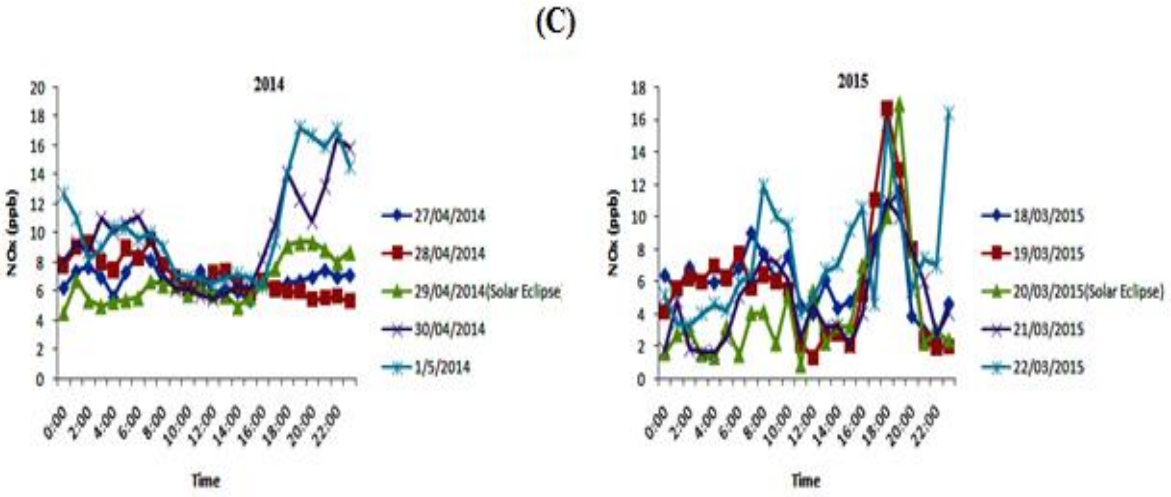

Fig 4.20. Variations in (A) NO_2, (B) NO and (C) NOx concentrations observed during solar eclipse day and normal days during the year 2014 and 2015.

Table 4.6: Changes observed in ambient O_3, NOx, SR, AT and RH during eclipse day during the year (A) 2014 and (B) 2015

(A)

Time (Hrs)	Change in O_3 (ppb)	Change in NOx(ppb)	Change in SR(W/m2)	Change in AT(°C)	Change in RH (%)
9:00	13	1	586	6.3	-15
10:00	14	0	425	5.4	-12
11:00	16	0	278	4.2	-9
12:00	18	1	232	3.7	-6
13:00	14	2	215	3.4	-4
14:00	15	1	196	3.1	-4

(B)

Time (Hrs)	Change in O_3 (ppb)	Change in NOx(ppb)	Change in SR(W/m2)	Change in AT(°C)	Change in RH (%)
13:00	1	1	77	0.4	-1.0
14:00	1	0	70	0.1	-3.8
15:00	0	1	66	0.5	-4.3
16:00	3	2	18	0.4	-2.7
17:00	2	3	0	0.4	-2.2
18:00	4	7	0	1.0	-3.0

Fig 4.21 (A)-(C) shows the variation of AT, RH and SR during solar eclipse days and normal days for both the years respectively. The ambient temperature (Fig 4.21.A) observed during solar eclipse is relatively low in both the years as compared to the normal days. However, the same couldn't be said in case on Relative humidity (Fig 4.21.B). It was observed that relative humidity tends to rise during solar eclipse hours as compared to the normal days. On the other hand, the intensity of solar radiation was also low during the eclipse period (Fig4.21.C) as compared to the normal days. These definite changes in the meteorological parameters during eclipse hours ultimately lead to the changes of photochemical behaviour in ambient O_3 thereby affecting the boundary layer processes [64].

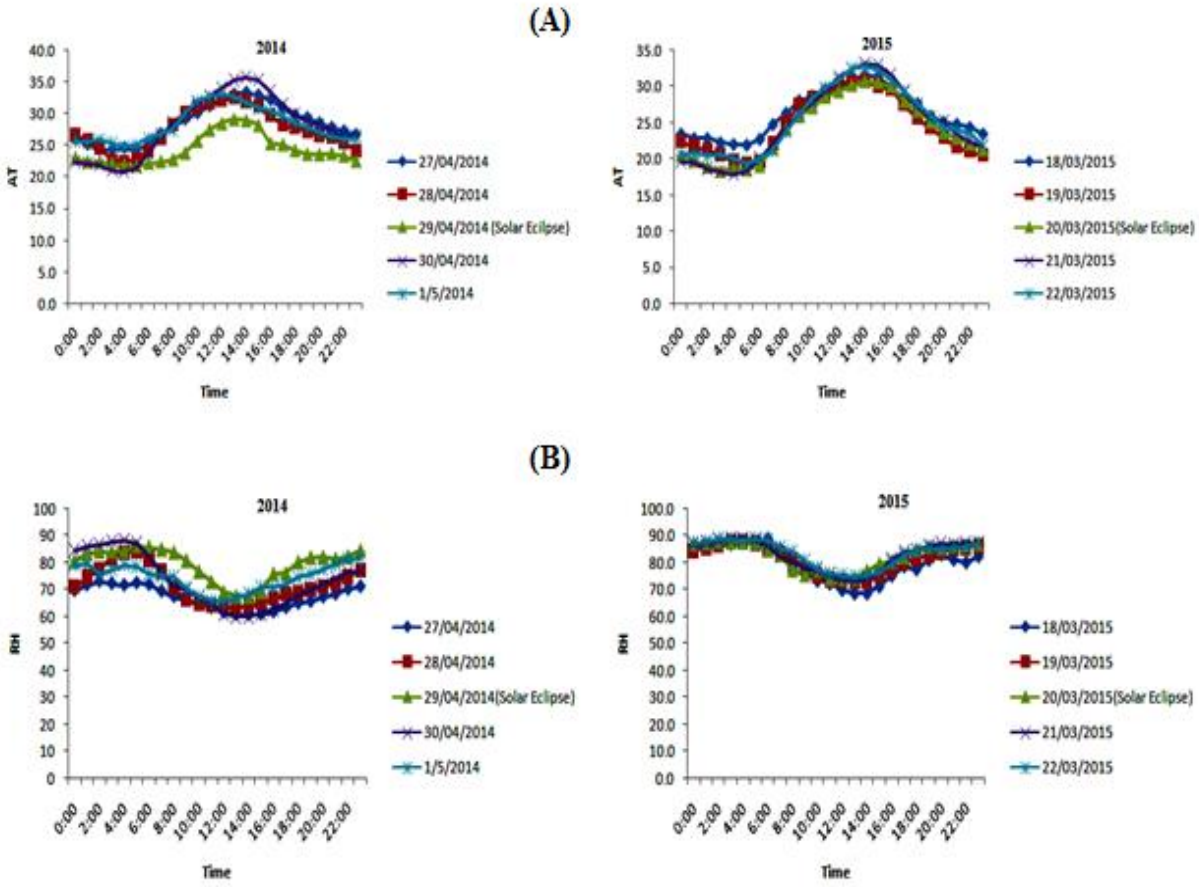

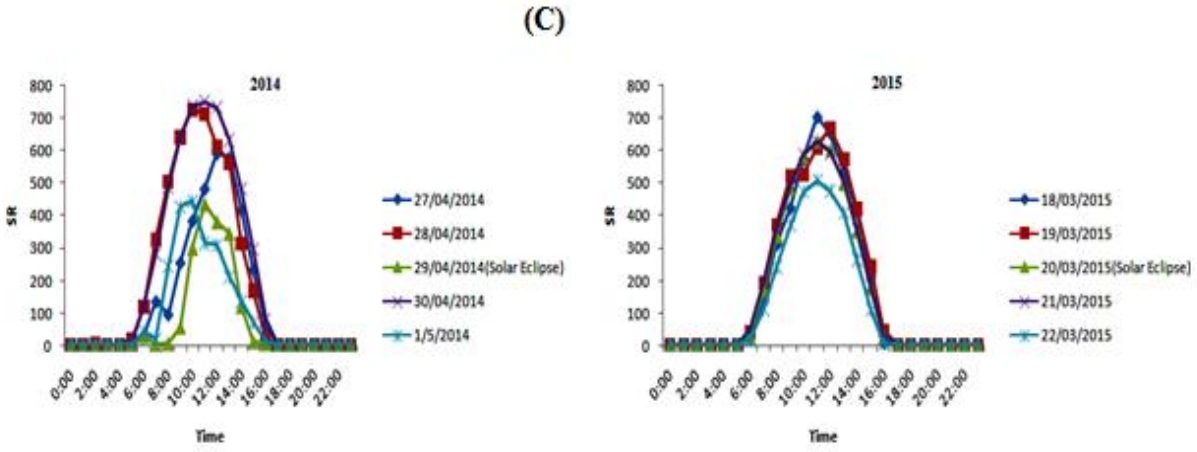

Fig. 4.21. Variations in (A) AT, (B) RH and (C) SR observed during solar eclipse day and normal days during the year 2014 and 2015.

4.8.5: Relationship of ambient O_3 with NOx and Solar radiation (SR) during eclipse days

The correlation of surface O_3 with NOx and SR for the year 2014 and 2015 were shown in Fig. 4.22(A) and (B) respectively. A positive correlation was seen between O_3 and SR during eclipse period for both the years. However more prominent correlation was seen in the year 2015 (r^2=0.3) than the previous year (r^2=0.2). This may be due to the fact that during eclipse hours the intensity of solar radiation decreases which ultimately leads to lower photochemical activities resulting in decrease in concentration of surface O_3.

But, contrasting results were observed in Fig 4.22(B), which showed an inverse relationship of ambient O_3 with NOx. During eclipse hours, it was observed that as the concentration of NOx increased, the concentration of O_3 decreased thereby leading to an inverse relationship between them. However, the correlation (r^2=0.3) seen in the year 2014 which is more prominent than seen in the next year (r^2=0.002). The correlations seen during eclipse hours were might be the result of scattered solar radiation during eclipse hours resulting in low production of O_3 by photolysis of NO_2 [64].

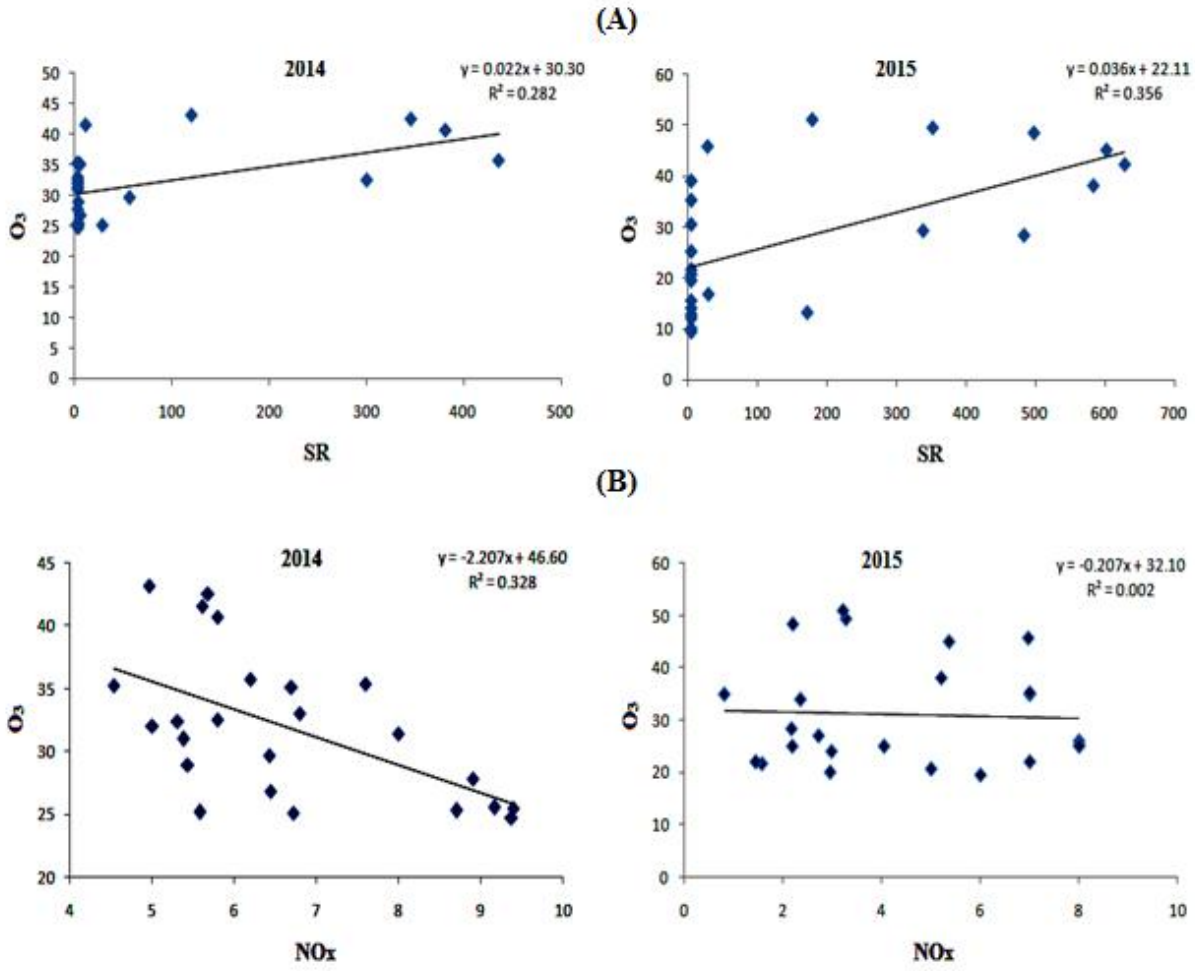

Fig. 4. 22. Scatter plot showing relationship between (A) O_3 and Solar radiation (SR) (B) O_3 and NOx on the solar eclipse day.

4.9: Dependency of O_3 on meteorology

Accumulation of ambient O_3 in the atmosphere is greatly influenced by the meteorological processes resulting in different seasonal and diurnal variations [65]. The different meteorological parameters like wind speed, wind direction, temperature, relative humidity and rainfall plays an important role in changing the different temporal variations of O_3 and its precursors. So a detailed study of the different meteorological parameters at the study site is discussed below:

4.9.1: Temperature and its relation with O_3

The monthly average temperature of Tezpur during the study period 2013-2017 are presented in the Table 4.7.1 .The study sites experienced similar range of temperature

during the whole period of the study. The average monthly ambient temperature at Tezpur during the period 2013-17 ranged from 18 to 30^{o}C. The minimum temperature recorded was 11^{o}C in January 2014 and 2017 while the maximum temperature recorded was39^{o}C in August 2016.

Table 4.7.1: Monthly average, minimum and maximum temperature of Tezpur during the study period 2013-2017

Year	May	June	July	Aug	Sep	Oct	Nov	Dec	Jan	Feb	Mar	Apr	Annual
2013-2014	26(21-36)	29(24-37)	29(25-38)	29(25-38)	29(24-37)	26(20-34)	22(15-30)	19(12-30)	19(11-29)	20(13-30)	24(17-33)	27(19-37)	25(11-38)
2014-2015	26(20-36)	28(24-36)	29(24-36)	28(23-36)	27(22-34)	26(19-35)	23(17-32)	19(12-29)	20(12-29)	20(12-29)	25(17-34)	24(19-35)	25(5-36)
2015-2016	26(21-36)	27(23-35)	29(24-35)	28(24-35)	28(24-35)	No data	No data	19(12-28)	18(12-27)	21(15-31)	24(18-33)	24(19-33)	19(11-36)
2016-2017	26(21-35)	29(24-36)	28(24-36)	30(23-39)	28(24-34)	27(21-36)	23(16-32)	20(14-28)	19(11-28)	21(15-31)	22(16-32)	24(19-33)	25(12-39)

Fig. 4.23 shows the dependency of O_3 with maximum temperature. Here a positive dependency of O_3 on temperature (max) (R_2 = 0.15) is seen. As observed by Ordonez et al. (2005) and Camalier et al. (2007) [66-67] temperature and solar radiation are important factors of O_3 formation. Ambient O_3 shows a strong correlation with ambient temperature even in hot climatic conditions [68-73].

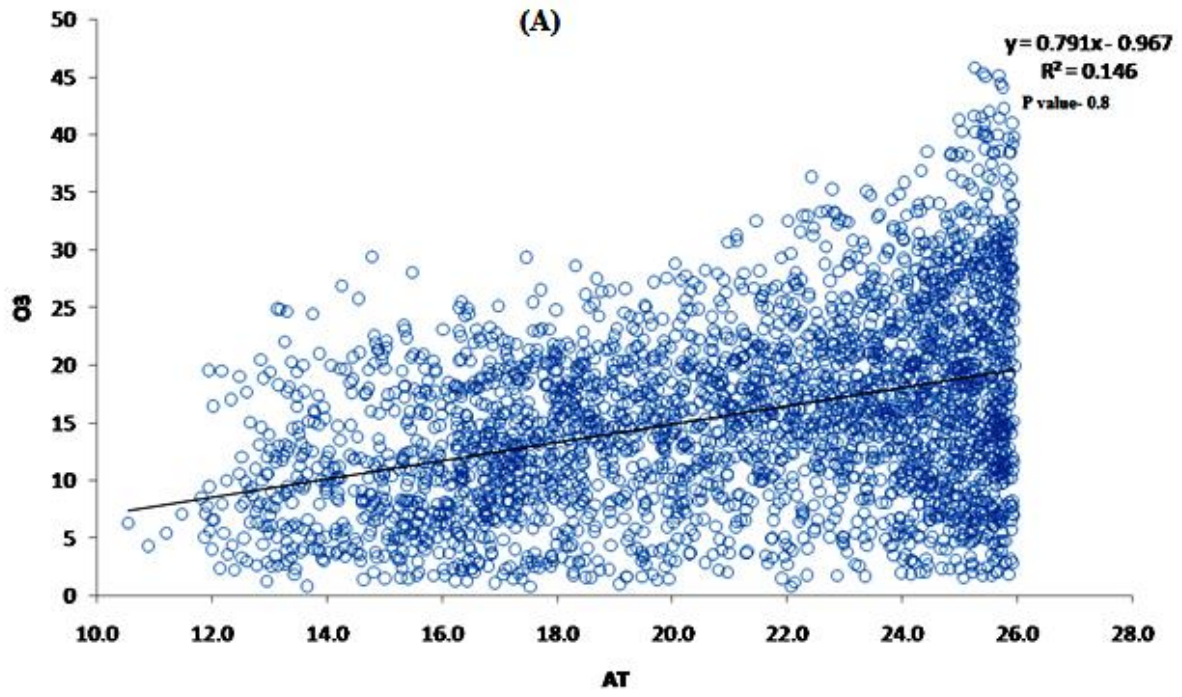

Fig. 4.23. Variation of O_3 with maximum temperature

4.9.2: Relative humidity and its relation with O_3

The monthly average relative humidity of Tezpur during the study period 2013-2017 is presented in the Table 4.7.2. The study sites experienced similar range of relative humidity during the whole period of the study. The monthly average relative humidity during the whole study period varied between 71 and 86%. The maximum humidity was during June 2016 and 2017 (92%) and the minimum was during April 2014 (55%).

Table 4.7.2: Monthly average, minimum and maximum relative humidity of Tezpur during the study period 2013-2017

Year	May	June	July	Aug	Sep	Oct	Nov	Dec	Jan	Feb	Mar	Apr	Annual
2013-2014	82(64-90)	81(61-90)	83(67-90)	82(66-90)	82(65-90)	82(65-90)	79(61-90)	80(62-90)	79(60-90)	78(58-90)	75(58-90)	71(55-89)	80(55-90)
2014-2015	82(64-90)	83(65-90)	83(69-90)	84(68-90)	84(69-90)	80(64-90)	80(63-90	80(60-90)	80(60-90)	78(58-90)	77(59-90)	80(60-90)	81(59-90)
2015-2016	82(64-90)	85(70-90)	82(65-90)	85(69-90)	85(68-91)	No data	No data	81(60-90)	82(64-90)	79(58-90)	77(57-90)	82(66-90)	63(57-91)
2016-2017	82(64-90)	83(66-92)	85(68-90)	82(65-90)	85(70-91)	83(66-91)	79(63-90)	79(63-90)	78(59-90)	77(56-90)	79(59-90)	82(60-91)	80(57-92)

Fig.4.24 shows an inverse relationship of O_3 with relative humidity (RH) (R^2 =0.2). High relative humidity helps removal of O_3 [74] and on the other hand, high temperature facilitates O_3 formation provided other meteorological conditions are favorable [75].

Increased water vapor may increase ozone loss by the reaction sequence:

$$O_3 + hv \rightarrow O_2 + O(^1D) \quad (4.1)$$

$$O(^1D) + H_2O \rightarrow 2^{\bullet}OH \quad (4.2)$$

$$^{\bullet}OH + O_3 \rightarrow HOO^{\bullet} + O_2 \quad (4.3)$$

$$HOO^{\bullet} + O_3 \rightarrow {}^{\bullet}OH + 2O_2 \quad (4.4)$$

The excited oxygen atom O (^1D) of Eq.(4.1) may compete with reaction the N_2 or O_2, stabilizing O (^1D) to the ground-state atom O (^3P), which eventually reacts with O_2 to return ozone. But, the •OH released from Eq 6 proceed with removing O_3 through Eq (4.3 and 4.4) [76]. Under polluted conditions, however, this effect is more complicated, because the •OH radicals produced by (Eq 4.2) would react with VOCs and CO to produce more ozone, while also competing to converting NO_2 to HNO_3.

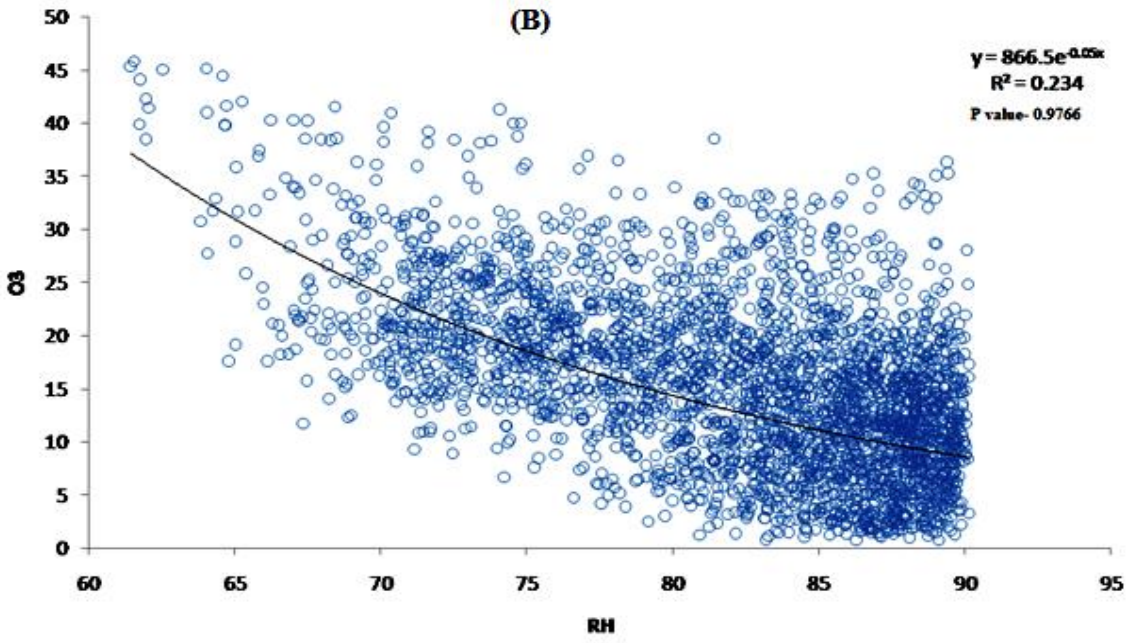

Fig. 4.24. Variation of O_3 with Relative humidity.

4.10: O_3-NOx photostationary state

The O_3– NO_x relationship can be explained by the following reactions after Leighton (1961) [77]:

$$NO_2 + h\nu(< 424\ nm) \xrightarrow{J_1} NO + O^{\bullet} \quad (4.5)$$

$$O^{\bullet} + O_2 + M \xrightarrow{k_2} O_3 + M \quad (4.6)$$

$$O_3 + NO + h\nu \xrightarrow{k_3} NO_2 + O^{\bullet} \quad (4.7)$$

Daytime O_3, NO_2, and NO equilibrate on a timescale of a few minutes [3] to reach a 'dynamic' equilibrium called the 'photostationary state' (*PS*), wherein $d[O_3]/dt = 0$ [78]. If J_1 is the rate of the photodissociation of NO_2 including the light intensity (Eq. 4.5) and k_3 is the rate coefficient of the formation of NO_2 (Eq. 4.7) then the *PS* can be explained by the ratio $J_1/k_3 = [O_3][NO]/[NO_2]$, which will govern the concentrations of O_3, NO_2, and NO during the day. J_1 is a function of solar intensity so it includes diel variability whereas k_3 is a function of temperature. The k_3 varies with temperature as given by [78]:

$$k_3\ (ppm^{-1}min^{-1}) = 3.23x10^3 \exp[-1430/T] \quad (4.8)$$

However, the accumulation of O_3 in the lower atmosphere is more complicated and reactions that convert NO to NO_2 with no-or-less destruction of O_3 is required for O_3 to accumulate. O_3 reacts with olefins to form Criegee intermediates that can decomposer to produce $^{\bullet}OH$ and peroxy radicals. The $^{\bullet}OH$ radicals oxidize other VOCs and CO to form additional oxidizing radicals like $HOO^{\bullet}$ and $ROO^{\bullet}$. These oxidants convert NO to NO_2 without the destruction of O_3 [Eq.4.7] as outlined in [Eq.4.9] to [Eq.4.14] [2, 79-80]:

$$RH + OH \rightarrow R + H_2O \quad (4.9)$$

$$R^{\bullet} + O_2 \rightarrow ROO^{\bullet} \quad (4.10)$$

$$ROO^{\bullet} + NO \rightarrow RO^{\bullet} + NO_2 \quad (4.11)$$

$$CO + {}^{\bullet}OH \rightarrow CO_2 + H \quad (4.12)$$

$$H^{\bullet} + O_2 \rightarrow HOO^{\bullet} \quad (4.13)$$

$$HOO^{\bullet} + NO \rightarrow {}^{\bullet}OH + NO_2 \quad (4.14)$$

There are external factors that can affect the *PS*including transport of O_3, the nature and concentrations of VOCs, alternate generation of peroxy radicals such as photolysis of short-chin carbonyls and local sources and transport of NO_x [81]. Due to these complexities, a "true" *PS* is rarely attained in the ground level atmosphere. Thus, the n*et* O_3 (measured O_3 concentration) and J_1/k_3 were plotted against time of day for the different seasons to ascertain how the temporal variation of O_3 behaved relative to J_1/k_3 (Fig. 4.25). The *net* O_3 and J_1/k_3attained a maximum during midday to the early afternoon hours and then both parameters declined as the day progressed.

During the pre-monsoon and monsoon seasons (Figs. 4.25a, b), the *net* O_3 and J_1/k_3attained their maxima and were about equal during midday to afternoon (1130 hr to 1530 hr local time). In this period, much of the NO_2has photolyzed to give $O_3$and the net O_3 was a function of NO_x. These two seasons are much warmer seasons compared to the post-monsoon and winter periods and the days are longer. Maximum sunshine and temperature occur during that time period (1130 hr to 1530hr). It was also interesting to see that the maxima were attained long after the sunrise, which is the high traffic period of the morning hours.

During post-monsoon and winter seasons (Fig. 4.25c, d), the *net* O_3 and J_1/k_3 peaked for a shorter duration at around 14:00 local time. During the post-monsoon *net* O_3 and J_1/k_3 were nearly equal at ~1400hr local time. However, during the winter, *net* O_3 and J_1/k_3 never became equal. During the peak hour, the levels of *net* O_3were much higher than the J_1/k_3 during the winter month.

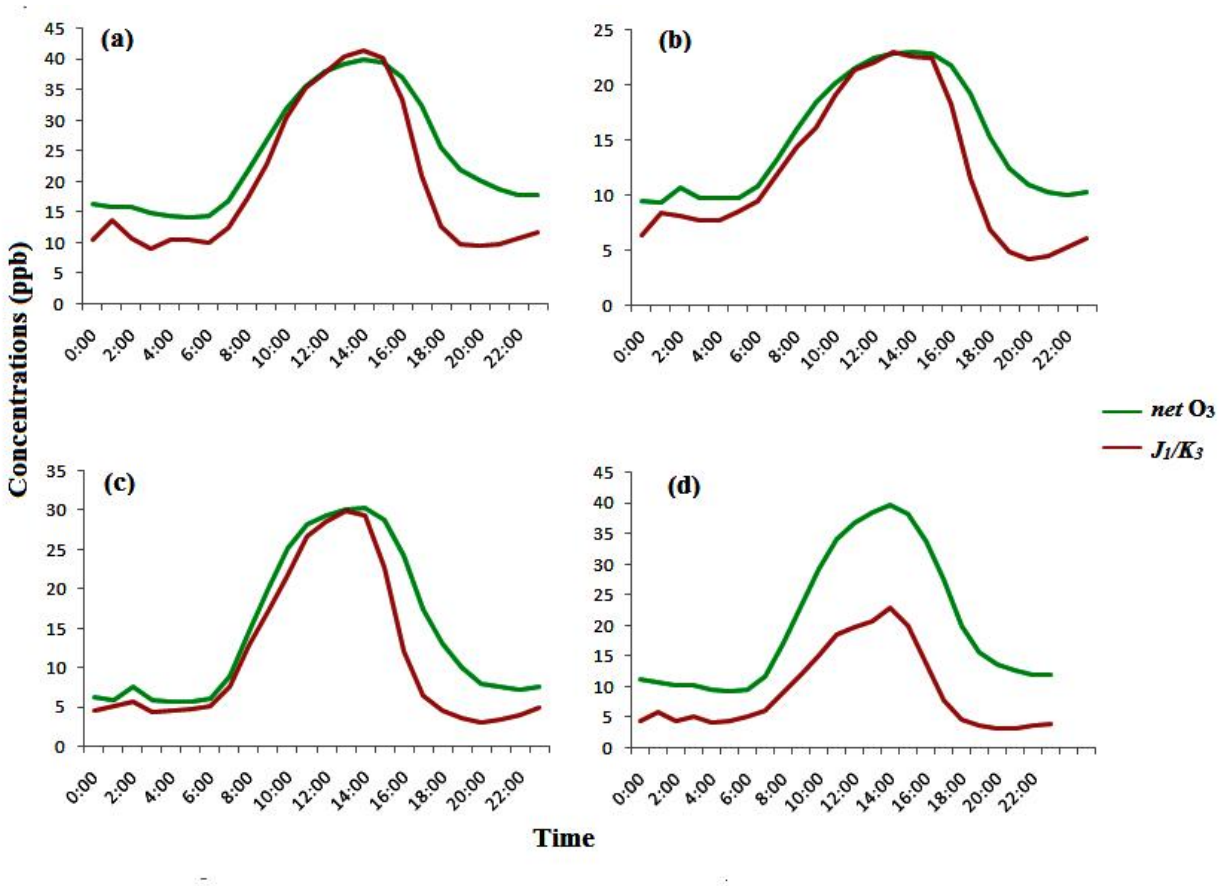

Fig.4.25: *net* O_3 (measured concentrations) and J_1/k_3 plotted against time of the day in different seasons: (a) Pre-monsoon; (b) Monsoon; and (c) Post-monsoon, (d) winter

During all seasons, the ratio (J_1/k_3) and *net* O_3 fell after the peak. The slopes of *net* O_3 and J_1/k_3 were not similar. The fall in the case of J_1/k_3 was much sharper than *net* O_3 and the levels of *net* O_3 remained higher than the ratio during the rest of the day. Also, *net* O_3 was found to be higher than J_1/k_3 during the period preceding the peak period. During the winter season, the *net* O_3 was always much higher than J_1/k_3. This discrepancy points at the factors that cause deviations of net O_3 from the *PS.* Those factors include transport of O_3 and the role of VOCs. The activity of VOC and involvement of OH is local [81] and OH generation and reactions of VOC degradation and production of O_3 in the process happens *in situ*. However, the VOCs and NO_xcould be from both local emission and long-range transport. The local sources of elevated levels of VOCs were biomass burning and biogenic emissions. The long-range transport of peroxy acyl nitrate (PAN) and other PAN homologues from the IGP can add NOx and radicals in the region during the winter, which are important drivers of O_3 production.

Though biomass burning is prevalent in the region [82], during the winter months there is escalation in the biomass burning which is a major source of VOCs in the atmosphere.A unique festive biomass burning, locally known as *meji* burning during mid-January each year is a major emitter of particulate matter and gases [83-84] that also have implications on the oxidative behavior of the regional atmosphere and O_3 buildup in the winter period.

Biomass burning emits loads of oxygenated hydrocarbons like aldehydes, ketones and alcohol which are important sources of free radicals linked with the reactivity of NOx and ozone formation. Acetone alone can provide a high production of HOx ($^{\bullet}OH$ and $HOO^{\bullet}$) radicalsthereby enhancing the production of O_3 [85]. The alcohols also further undergo oxidation giving rise more reactive aldehydes and radicals that would favorO_3 formation explained by the following reaction [85]:

$$CH_3OH + {}^{\bullet}OH + (O_2) \rightarrow CH_2O + HOO^{\bullet} + H_2O \qquad (4.15)$$

$$C_2H_5OH\ {}^{\bullet}OH + (O_2) \rightarrow CH_3CHO + HOO^{\bullet} + H_2O \qquad (4.16)$$

Another important source of VOC in the winter months is agriculture. The whole of the Brahmaputra Valley region is widely cultivatedwith crops from the Brassicaceae family that are known to emit volatile organics [86-87]. Rapeseed, cabbage, and radish are principal winter crops of the Brahmaputra Valley. There is a large area (0.276 million ha) under rapeseed cultivation [88]. Even the fallow lands are used for rapeseed since it is a hardy crop and does not need irrigation and excessive manuring. Similarly, large areas are under cabbage (33.24 thousand ha) and radish (21.17 thousand ha) [89]. The Brassicaceae family is known to emit large volumes of CH_3Br and other organics [86-97]. CH_3Br is a reactive gas and provides a source of radicals that covert NO to NO_2 and enhance the production of O_3 [90], shown in Eq. 4.17-4.19:

$$CH_3Br + {}^{\bullet}OH \rightarrow {}^{\bullet}CH_2Br + H_2O \qquad (4.17)$$

$$^{\bullet}CH_2Br + O_2 + M \rightarrow CH_2BrOO^{\bullet} + M \qquad (4.18)$$

$$CH_2BrOO^{\bullet} + NO \rightarrow CH_2BrO + NO_2 \qquad (4.19)$$

PAN is a source of NOx and organic radicals in the remote atmosphere. The thermochemical stability of PAN depends on the temperature and is quite stable at low temperature. At 7 ^{0}Cand NO_2/NO ratio of 2-20, the lifetime of PAN (τ_{PAN}) is ~19 to 120

Hrs., and at 27^0C, τ_{PAN} is ~0.75 hr. to 4.4 hr [91]. Other PANs have similar lifetimes.Therefore, at low temperatures, PAN can be transported long-range and pump in NOx and organic radicals to the remote regions.Analysis of the airmass back trajectories reaching the site during winter suggests that 28% of the trajectories travelled from the IGP region of India. The IGP is one of the most polluted regions of India from where aided by the low temperatures, there was likely transport to the study area of PAN. As the trajectories reached the site where the temperature is 10^0Cto 24^0C in the winter, the PAN decomposed to NOx and organic radicals (Eq. 4.20)

$$CH_3C(O)OONO_2 + M \rightarrow CH_3C(O)OO^{\bullet} + NO_2 + M \qquad (4.20)$$

The ventilation coefficients (VC) calculated for winter month (January) as mixedlayer height (MLH)x windspeed (WS), illustrated in Fig.4.26 showed that the maximum VC was experienced at ~9:00am in the morning and that is then there was steep rise in the winter period concentration of *net*O_3.

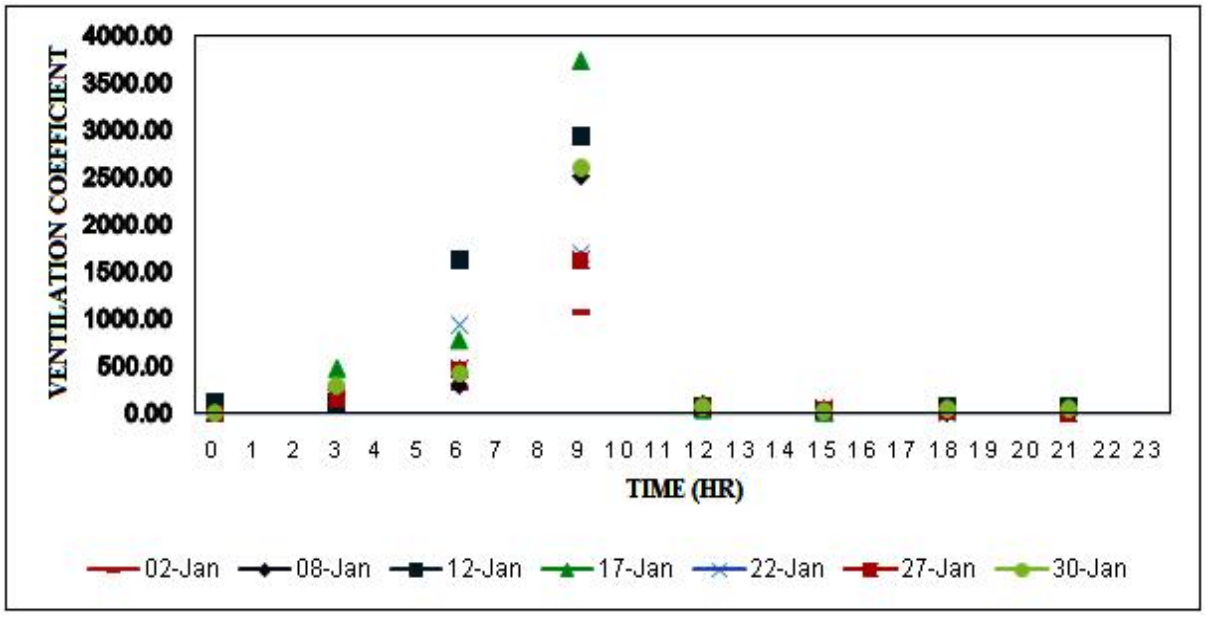

Fig. 4.26: Ventilation Coefficient (VC) during winter period (January 2014). VC was calculated as VC = MH x WS; MH was calculated by HYSPLIT

4.11: Effect of atmospheric transport on concentrations of ambient ozone

Transport of O_3 also has greater implication in the deviation of *PS* as seen in the period before and after the peak O_3 time of the day, wherein the O_3 concentrations were always higher than the ratio (J_1/k_3). The transport of O_3 to the station was examined by comparing (i) the polar plots of O_3 and NO_2 (for local transport) and (ii) the concentration weighted trajectories (CWT) of O_3 (for regional transport representing the precursors like PAN). The polar plots of NO_2 were considered because O_3 is ultimately produced (through all photochemical processes) from the photolysis of NO_2. If O_3 was to be produced only from the photolysis of NO_2, the polar plots of O_3 and NO_2 would look similar. The polar plots of O_3 and NO_2 are given in Fig. 4.27, in which the concentrations are plotted against windspeed and wind direction.

Through the seasons, high O_3 concentrations were found to accompany high windspeed, that suggeststransport of O_3 to the site (Fig 4.27. a-d). However, stagnant conditions would also allow locally emitted NO to titrate the O_3. Alternatively, higher concentrations of NO_2were observed under lower windspeeds (Fig. 4.27. e-h).Onlymoderate and low levels of NO_2 were associated with high windspeeds indicating that the NOx was locally emitted and dispersed under higher ventilation conditions. It is clear from the plots that higher O_3 and higher NO_2 were seen to be associated with winds from different directions. It was important to look at the winter polar plots (Fig. 4.27.d; h). As discussed in the previous section, in the winter season, O_3 did not show a diel pattern corresponding to J_1/k_3 *(PS),* and the O_3 concentration was much higher than J_1/k_3. The winter polar plot of O_3 shows that O_3 was higher when the windspeeds were high, a pattern that is different from the polar plot of NO_2. The wind directions with respect to high ozone and the direction with respect to high NO_2 were found to be different, which may be inferred as transport of O_3 to the site. During the winter and pre -monsoon seasons, the region receives airmass trajectories that originated and/or passed over the IGP [92-93], and bring high pollutant concentrations to the region [94-95].

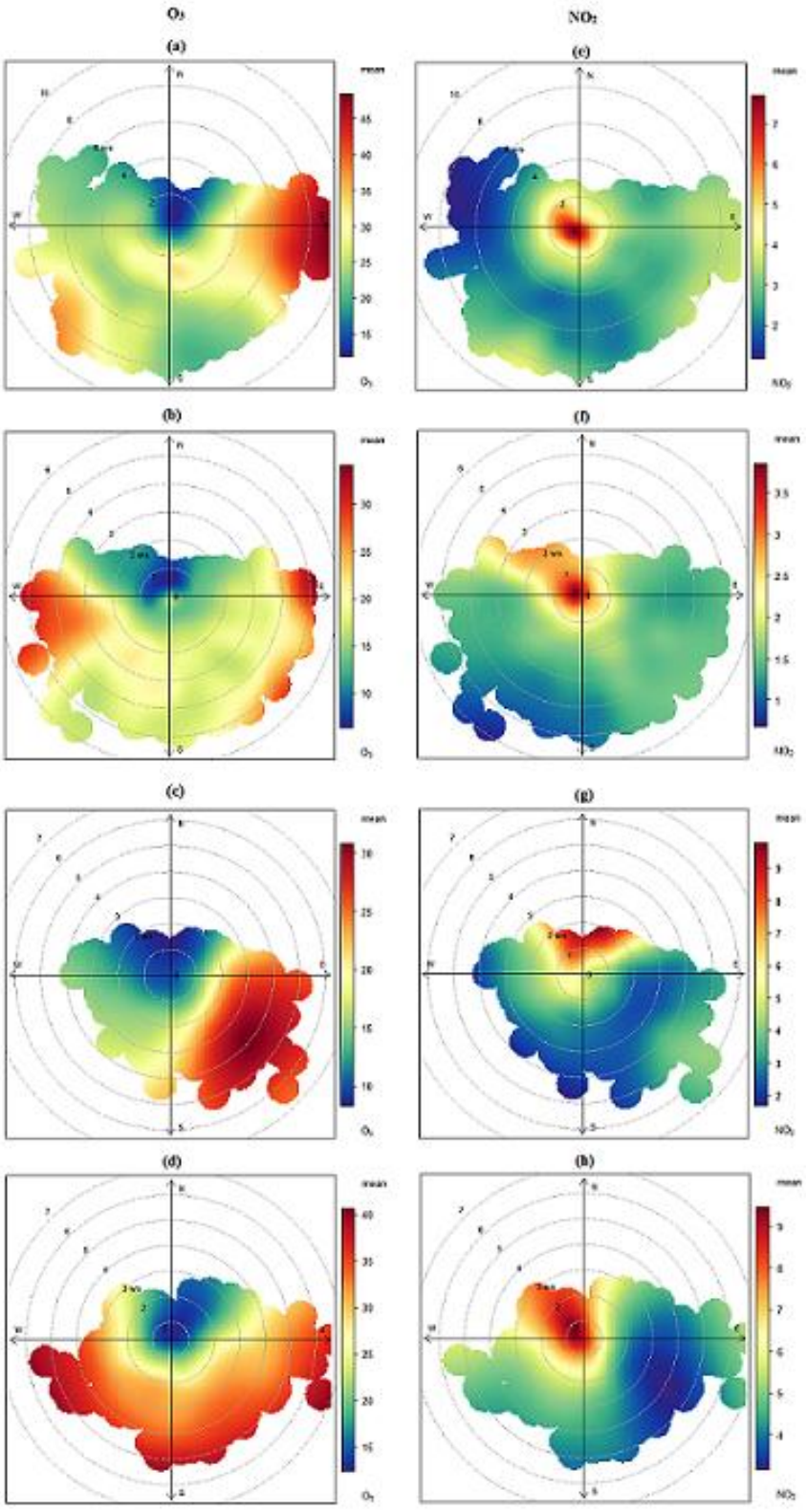

Fig.4.27: Polar plots of O_3 (a-d: Pre-monsoon, monsoon, post-monsoon, winter), and (b) NO_2 (e-h: pre-monsoon, monsoon, post-monsoon, winter): concentrations plotted against wind direction and windspeed during the study period.

The pollution rose for the year 2014-2017 have been shown in fig 4.28. The pollution roses were arranged separately for each one of the four seasons in order to show the seasonal trends of ambient O_3 concentrations. The effects of wind direction on ambient O_3 pollution can be well understood by the use of Pollution rose. Higher concentration of ambient O_3 concentration was dominant towards southeasterly direction in all the seasons. From the plots it is quite evident that the source of O_3 concentration is long range transport or regional transport which is usually seen in case of rural areas. The increase in concentrations might be due to anthropogenic activities like biomass burning, vehicular emissions, industrial exhaust etc. Higher concentrations of ambient O_3 were seen during premonsoon season. Hatzianastassiou et al, 2007 stated that increase ambient O_3 concentrations were seen during summer season due to increase rate of solar radiation. Calm conditions observed in the plots are 1.4%, 1.3%, 7.3%, and 17.3% for winter, premonsoon, monsoon and postmonsoon seasons respectively. Hence it is seen that lower the calm conditions higher the concentration of ground level O_3 concentrations, which is prominent during premonsoon [96].

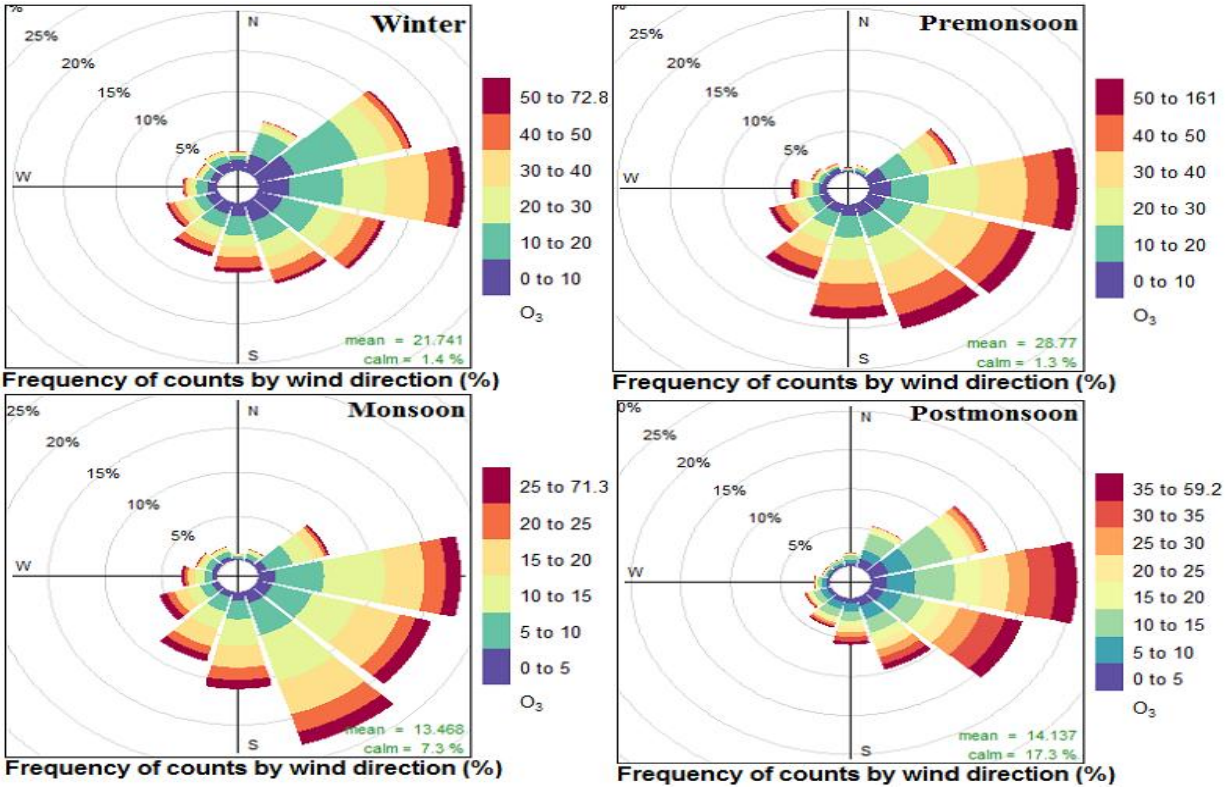

Fig.4.28. Pollution rose of O_3 for the year 2014-2017.

The Conditional Probability Function (CPF) and Conditional bivariate probability function (CBPF) roses for ambient O_3 at 75th percentile in Tezpur during the year 2014-2017 have been plotted in fig.4.29. Extreme ambient O_3 episodes at hourly interval can be studied by the calculation of CPF [97]. The CPF function is used to indicate the relation between definite wind direction and utmost O_3 episodes whereas the CBPF function is used to show the variation of O_3 concentration in relation to wind direction and wind speed. It also provides significant information on the type of identified sources. The CPF and CBPF results, plotted in the graph were according to the pollution roses shown in fig.4.28. this signifies extreme ambient O3 episodes under the influence of wind from south-easterly directions. However, during the year 2016, higher concentrations of ambient O_3 were also seen in the western region along with the eastern regions, which was an exception to the other years and only prominent in the CBPF plots. In addition to the source regions the CBPF plots also shows that higher concentration of ambient O_3 occurs at low wind speed conditions. Moreover, the plots clearly indicate higher concentration of ambient O_3 pollution from eastern direction during the whole study period. The extreme O_3 episodes observed in fig.4.28.Were might be due to the transportation of O_3 precursors from the highway and the city located towards the eastern side of the study area. So from this, the highways and the Tezpur city centre contribution to the photochemical air pollution were identified. Moreover, the Peroxy acyl nitrate and PAN homologous transportation from the Indo-Gangetic plain also contributes to the increase of NOx concentration leading to increase of ambient O_3 in the study site, which inturn acts as a source of regional contribution. Local festivities like Meji burning activities also contribute to the local sources of O_3 in this region [82]. Agricultural practices like cultivation of Brassicaceae crops in these regions also contributes to biogenic emissions leading to higher VOCs thereby contributing as a local source of O_3 [86-87].

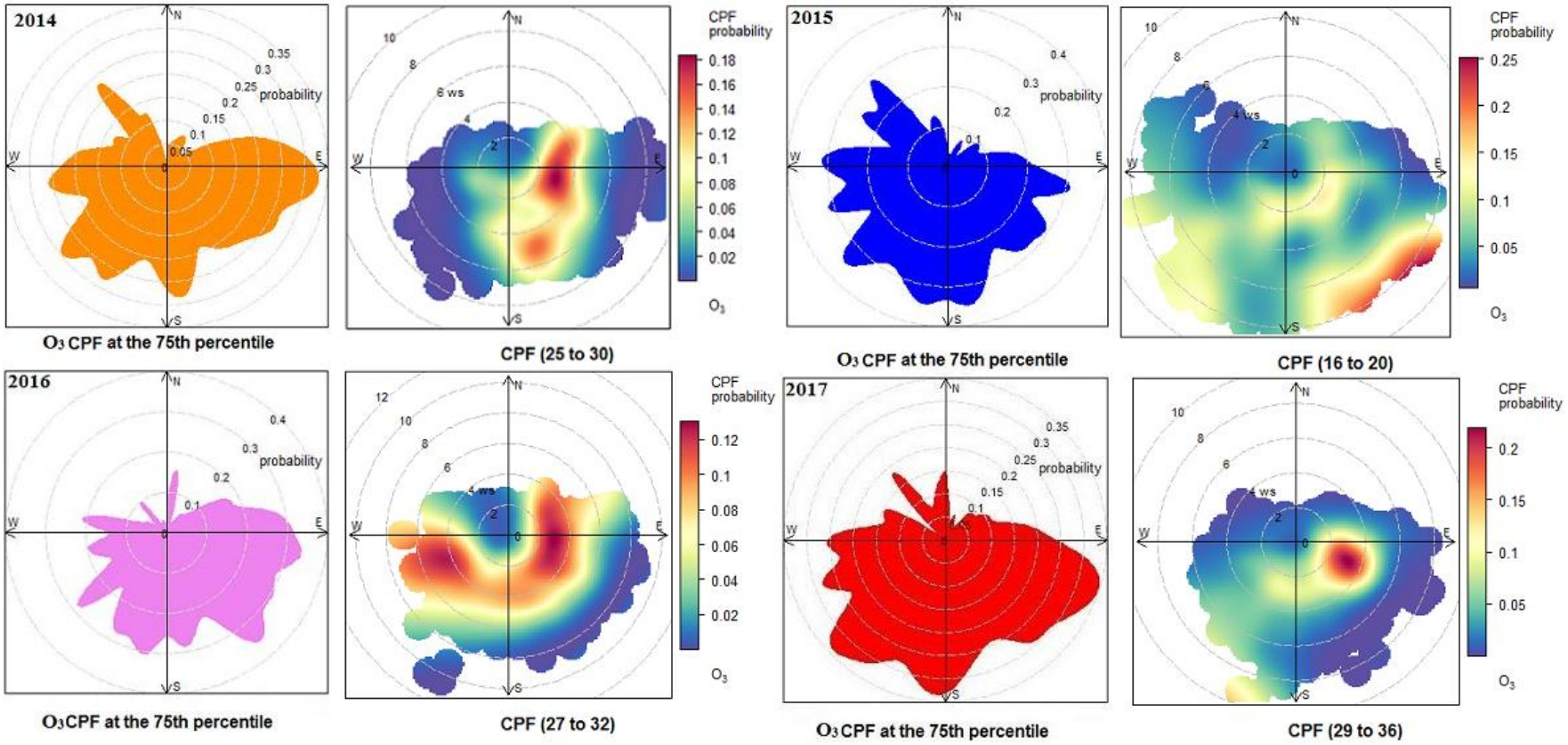

Fig 4.29.CPF and CBPF plots for O_3 in Tezpur during the year 2014-2017.

4.12: NO_x Dependent and NO_x Independent Contributions to OX

The daily average concentration of OX which is regressed on NOx is shown in Fig.4.30. From the graphit was evident that the slope of the graph divides the total concentration into NOx-Dependent and NOx-Independent contribution [3, 98]. NOx-dependent contribution attributes to the local emissions mainly due to biomass burningand vehicular exhaust, which was found to be ~20ppb. However, the regional contribution attributes to theNOx-independent contributionas the concentration of OX during this phase remains unaffected and wasfound to be ~18ppb. This signifies that the regional to local contribution was 1:1 over mid BrahmaputraValley. The rate of production of the total oxidant signifies that the trends of atmospheric oxidants levels largely depends on the ratio of VOCs / NOx [99]; as the rapid reduction of VOC reactivity would be very effective for decreasing the total oxidants.

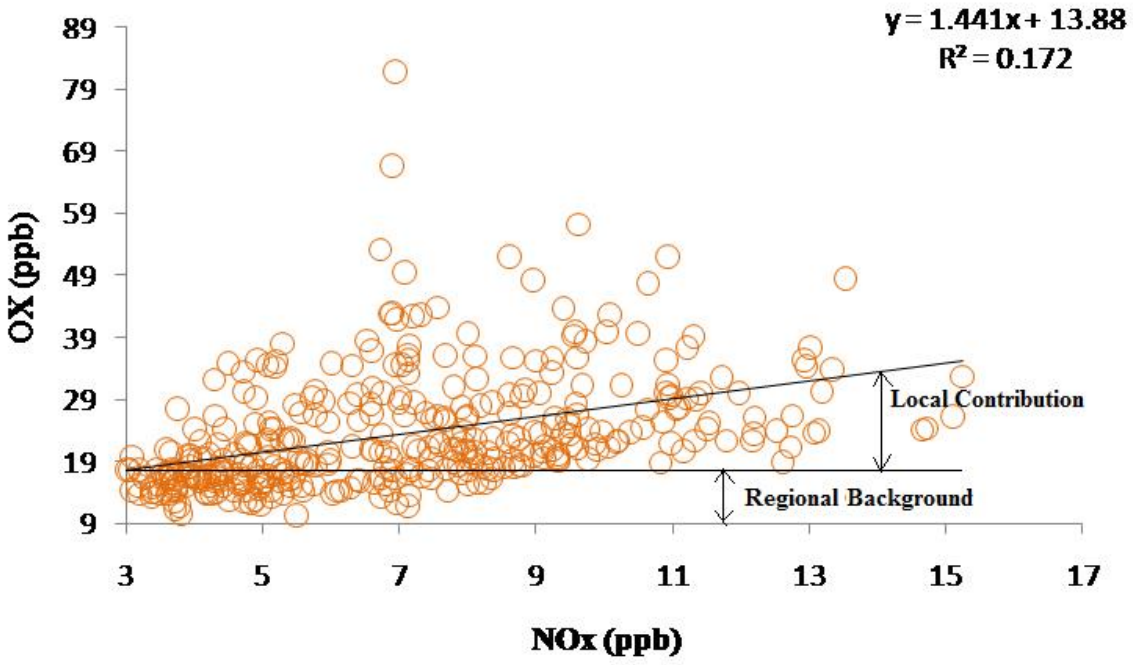

Fig.4.30. Daily Variation of Values of OX with respect to NO_x during the period of May 2013-2014. The regional to local contribution – 1:1.

4.13.1: Long range transport of ambient O_3

The weighted PSCF maps for the year 2014, 2015, 2016 and 2017 have been plotted in fig 4.32.(A) (B), (C) and (D) respectively and their clusters were plotted in fig 4.31.(A), (B),

(C) and (D) respectively. These maps were used to identify the possible source regions contributing to ambient O_3 levels in Tezpur. The PSCF maps were also plotted to study the impact of continental and marine air masses on ambient O_3 concentrations at Tezpur by calculating 3 days back trajectory during winter, premonsoon, monsoon and postmonsoon season for the year 2014-2017 using meteoinfo and trajstat software. During the year 2014 as plotted in fig 4.32(A), potential transboundary source regions of ambient O_3 during winter season were mainly from North-eastern part of India, the local surrounding areas of the study site and somewhat from Tajikistan, Kyrgyzstan and China. During premonsoon, the source regions were mainly from the Indo-Gangetic plain, the North-eastern region, the local areas and somewhat from Bay of Bengal. But during monsoon season the major source areas were Bay of Bengal, North-eastern region and the local surrounding areas. The airmass trajectories which are received from the IGP region bring higher concentrations of pollutants in these regions [94-95]. Post-monsoon season show a similar trend like that of winter as the potential source regions contributing to ambient O_3 levels at Tezpur were the Indo-Gangetic plain ,the North-eastern region, the local areas and some areas of China, Tajikistan and Kyrgyzstan. From the fig 4.32(A) and (B) it was seen that during 2014 and 2015 winter, premonsoon and monsoon season highest percentage of pollutants was transported from Bangladesh and Bay of Bengal region while during postmonsoon highest percentage of pollutants were seen from Nagaland area during 2014 and from Tibetan plateau during 2015. However in fig. 4.32(C), in the year 2016, it was depicted that during winter and postmonsoon season highest percentage of pollutants were carried from Tibetan plateau and during Premonsoon and Monsoon season highest pollutants were carried from Bangladesh region. During the year 2017 it was seen that (fig 4.32.D) highest percentage of pollutants were carried from Bangladesh region during all the three seasons except postmonsoon where highest percentage of pollutants were carried from Nagaland region.

The PSCF maps of all the seasons for the year 2015 as plotted in fig 4.32(B) shows a similar trend as seen during all the seasons of 2014. However same cannot be said incase of 2016 (fig 4.32.C). During this year the potential source region of ambient O_3 during winter season were similar to that of 2014 and 2015 winter but the premonsoon season shows a slight different trend. Some source areas during premonsoon include the western part of India along with the Indo-Gangetic plain, the North-eastern region, local areas and somewhat from Bay of Bengal. During monsoon a small portion from china were also

included as potential source region along with Bay of Bengal, North-eastern region and the local surrounding areas. The postmonsoon season also shows a similar trend like winter however including some parts of Iran as potential source areas of ambient O_3 at Tezpur. In fig 4.32(D), it was seen that the potential source regions in all the seasons were concentrated mainly over the Indo-Gangetic plain, some areas of China, the north-eastern region, a small portion from Bay of Bengal during premonsoon and monsoon season and the local surrounding areas. As mentioned in earlier studies, transportation process of high concentration of ambient O_3 is associated mostly with downward transport rather than transportation of manmade pollution in horizontal direction [100-103]. The trajectories from the western direction were mostly linked with downward transport episodes of ambient O_3 whereas the trajectories from eastern direction were mostly seen as a carrier of anthropogenic pollution and carry low concentrations of ambient O_3 [104]. The airmass trajectories that are received from the over polluted regions brings O_3 precursors like PAN with them, which contributes to higher concentration of O_3 in the study area.

(A)

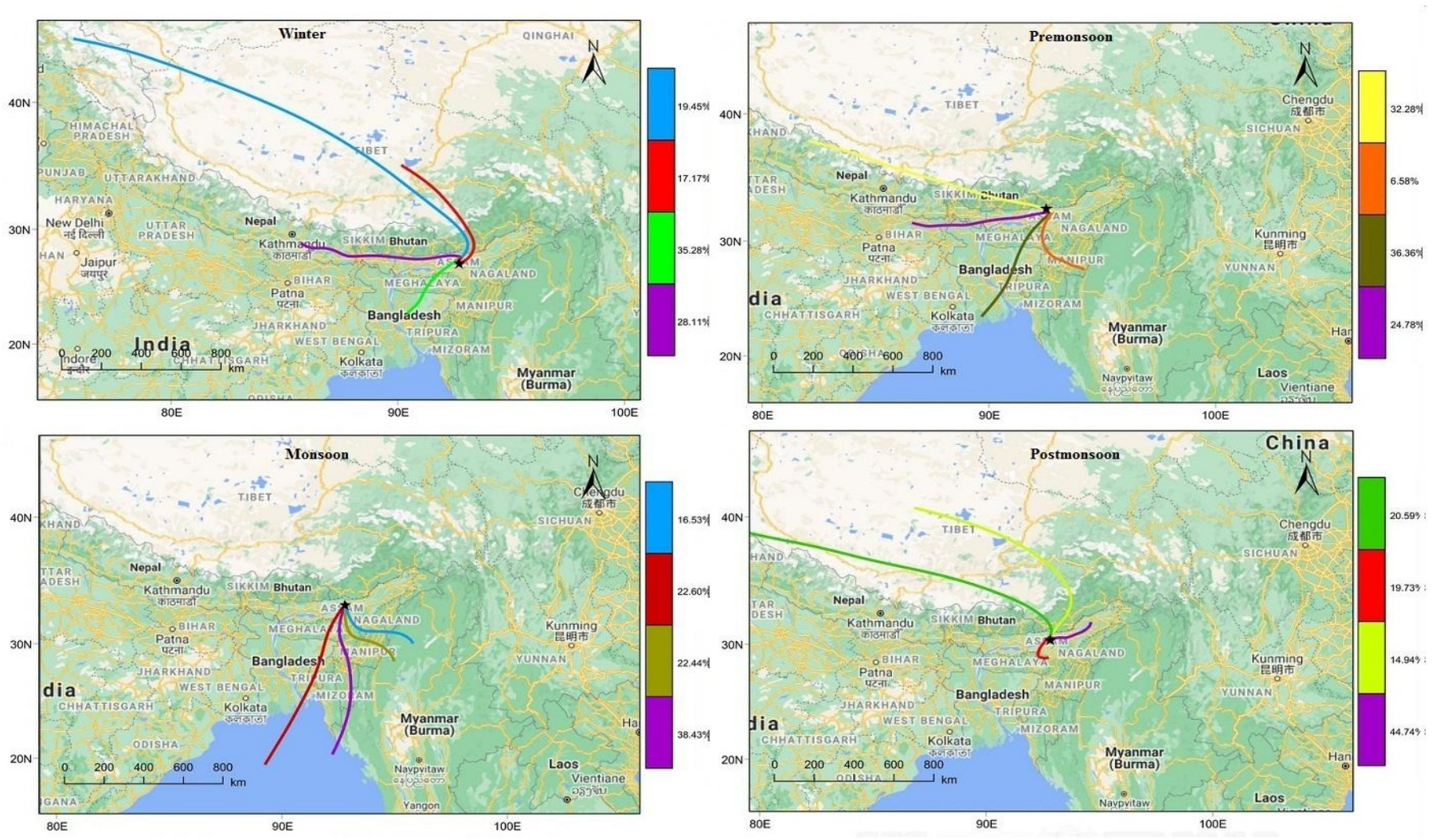

Fig. 4.31 (A). Trajectory clusters reaching the city of Tezpur during the year 2014 at 500 m AGL.

(B)

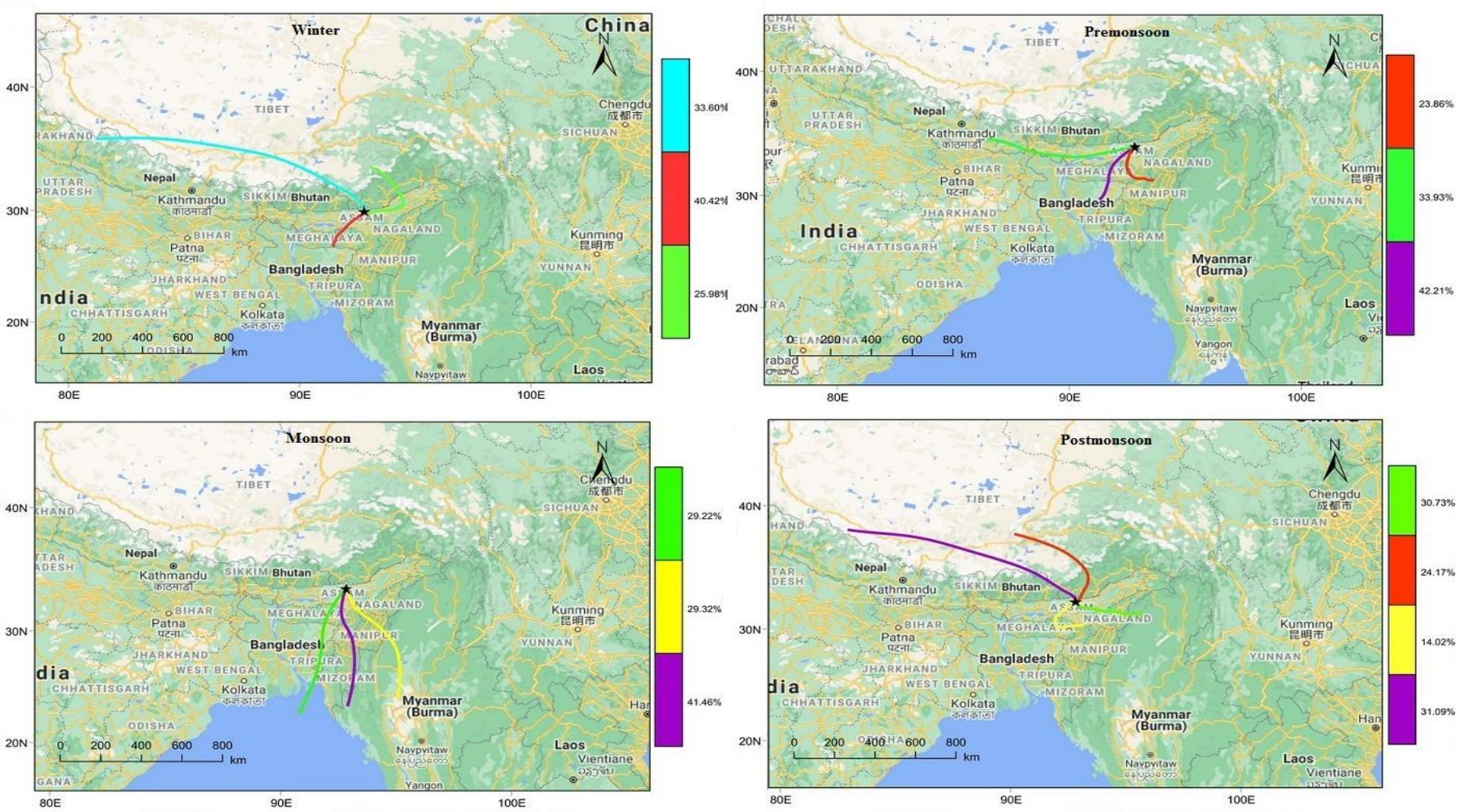

Fig.4.31 (B). Trajectory clusters reaching the city of Tezpur during the year 2015 at 500 m AGL.

(C)

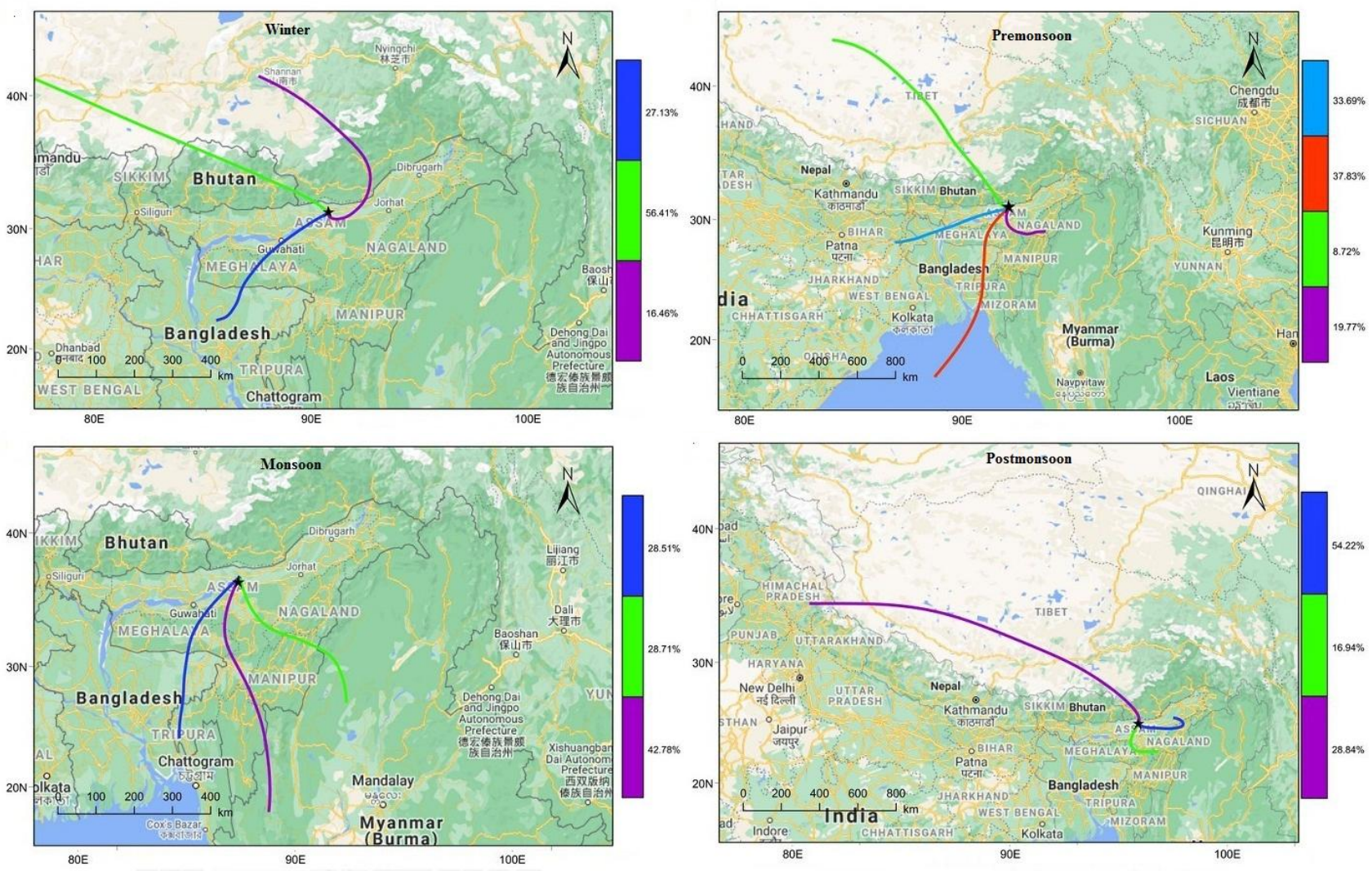

Fig. 4.31(C). Trajectory clusters reaching the city of Tezpur during the year 2016 at 500 m AGL**.**

(D)

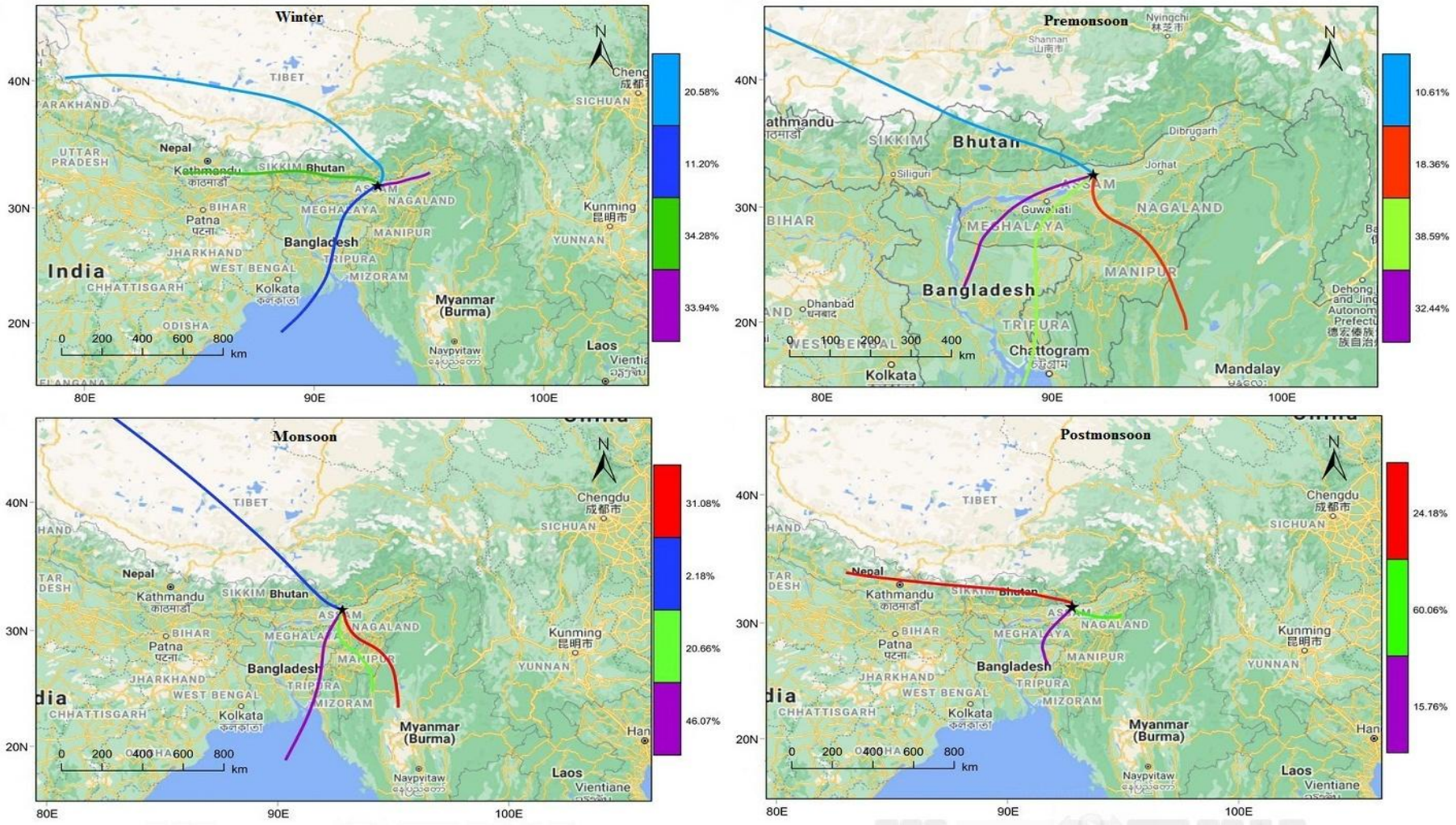

Fig. 4. 31(D). Trajectory clusters reaching the city of Tezpur during the year 2017 at 500 m AGL.

(A)

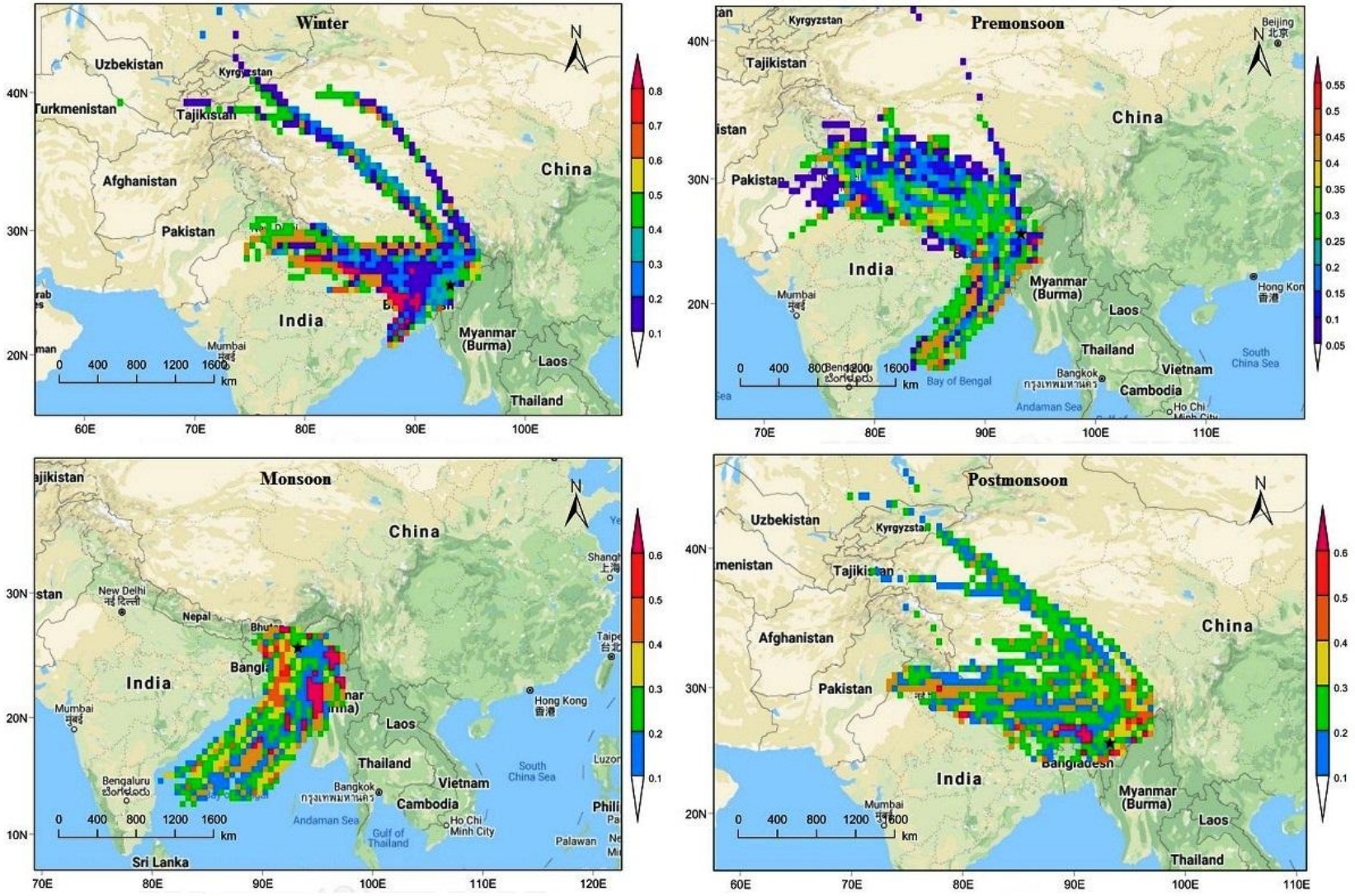

Fig 4.32(A). PSCF density maps of O_3 concentration for Tezpur during the year 2014. The position of the cities is marked with a black star.

(B)

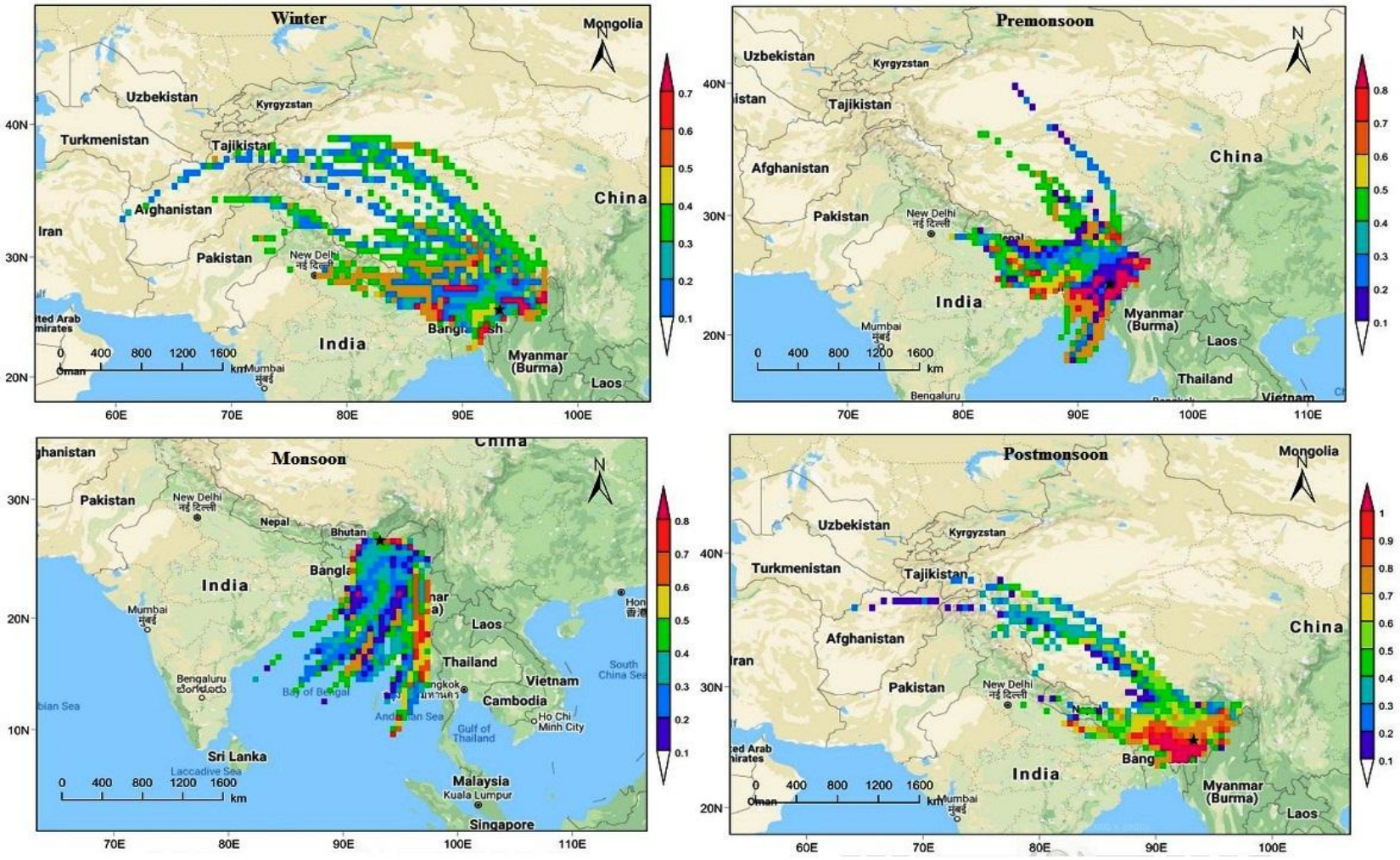

Fig 4.32(B). PSCF density maps of O_3 concentration for Tezpur during the year 2015. The position of the cities is marked with a black star.

(C)

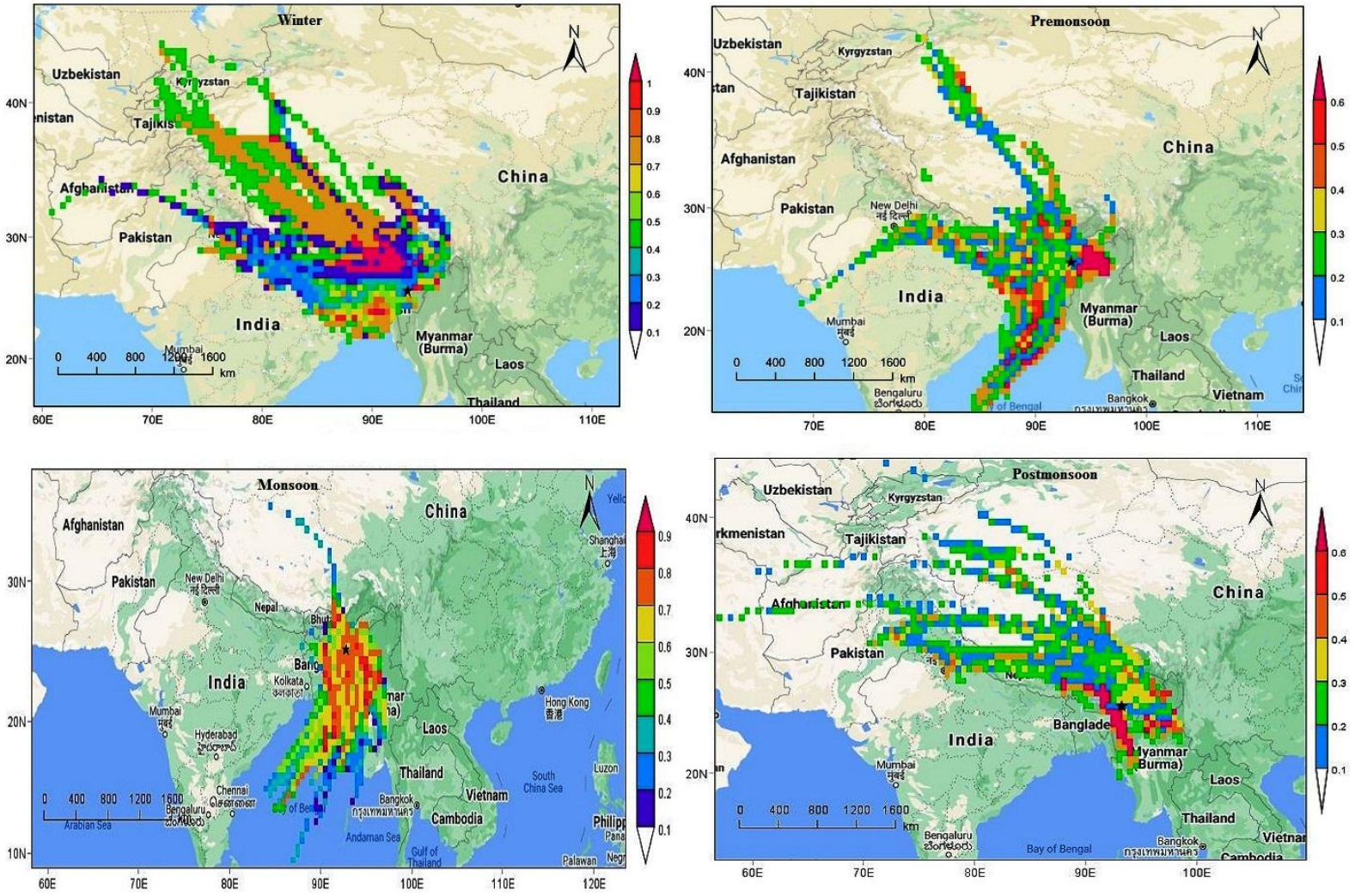

Fig 4.32(C). PSCF density maps of O_3 concentration for Tezpur during the year 2016. The position of the cities is marked with a black star.

(D)

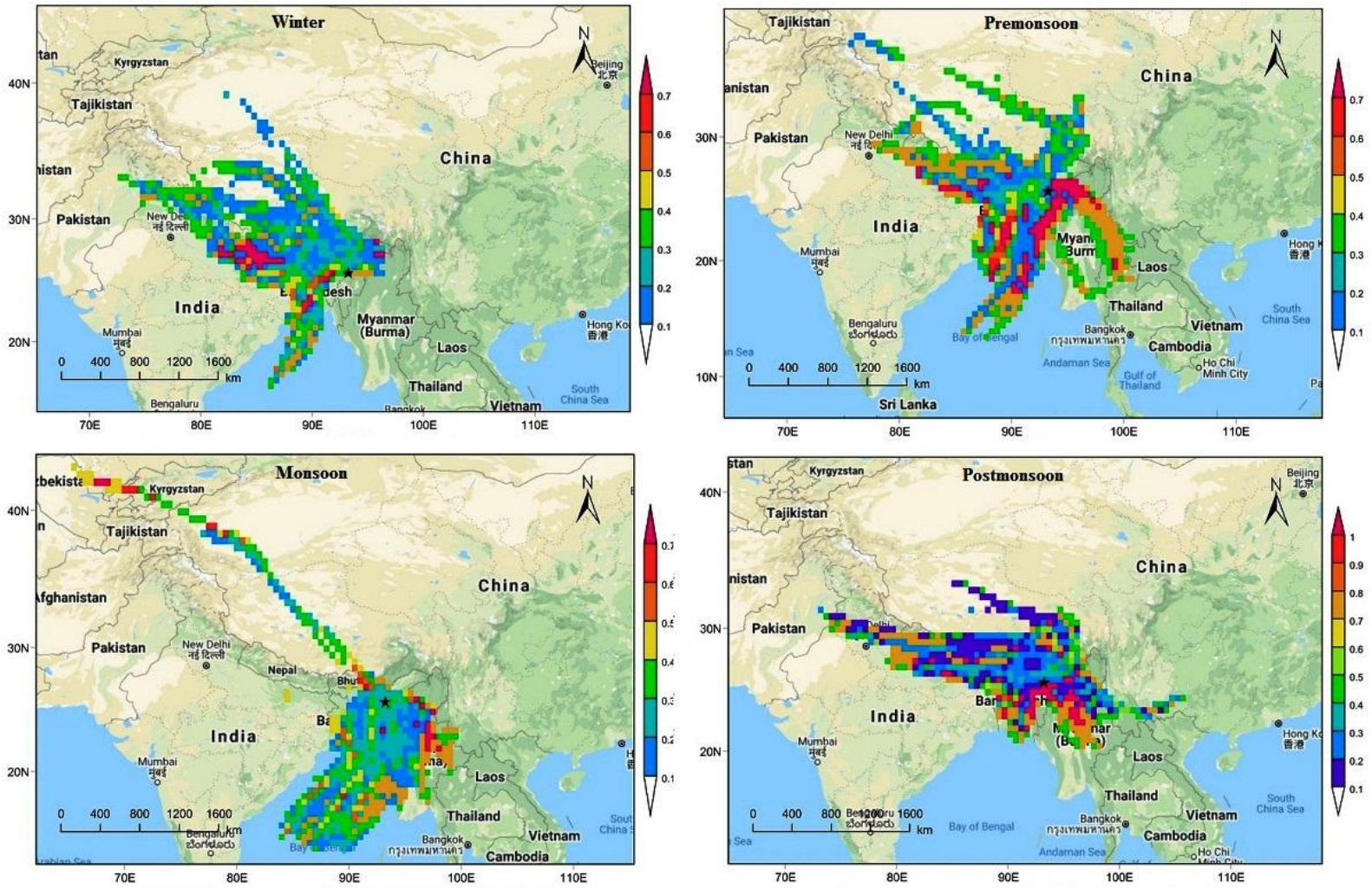

Fig 4.32(D). PSCF density maps of O_3 concentration for Tezpur during the year 2017. The position of the cities is marked with a black star.

4.13.2: Long range transport of NO_2

The trajectory clusters and the weighted PSCF maps of NO_2 for the year 2014, 2015, 2016 and 2017 have been plotted in fig4.33.(A) (B), (C) and (D) respectively and in fig 4.34.(A), (B), (C) and (D) respectively. The PSCF maps and their respective clusters were used to identify the origin of the pollution and from where the concentrations of NO_2 were transported to the study site. During the year 2014 as plotted in fig 4.34(A), potential transboundary source regions of NO_2 during winter season it was seen that higher percentage of NO_2 were transported from regions like Bangladesh and Bhutan. Moreover, areas like Pakistan, Afghanistan also contributed to be the regions from where NO_2 was transported to Tezpur. Similarly in the other three seasons also the same pattern was observed except during premonsoon and monsoon season marine areas like Bay of Bengal are involved in contributing as the source regions for NO_2 transportation. Moreover it was observed that the same trend was followed for the next three consecutive years. The cluster analyses helps to find the most feasible source of pollution including secondary emissions, sea spray, industrial and combustion sources [105]. NO_2 concentrations have a statisticallynotable effect in case of airmass trajectory analyses as recorded earlier [106]. In lower atmospheric regions NO_2 plumes can travel through characteristic paths for many days to other continents which originates from manmade pollution. Mostly NO_2 transportation was seen during the winter and postmonsoon seasons when the conditions of Meterological parameters and anthropogenic emissions were most advantageous [107].

(A)

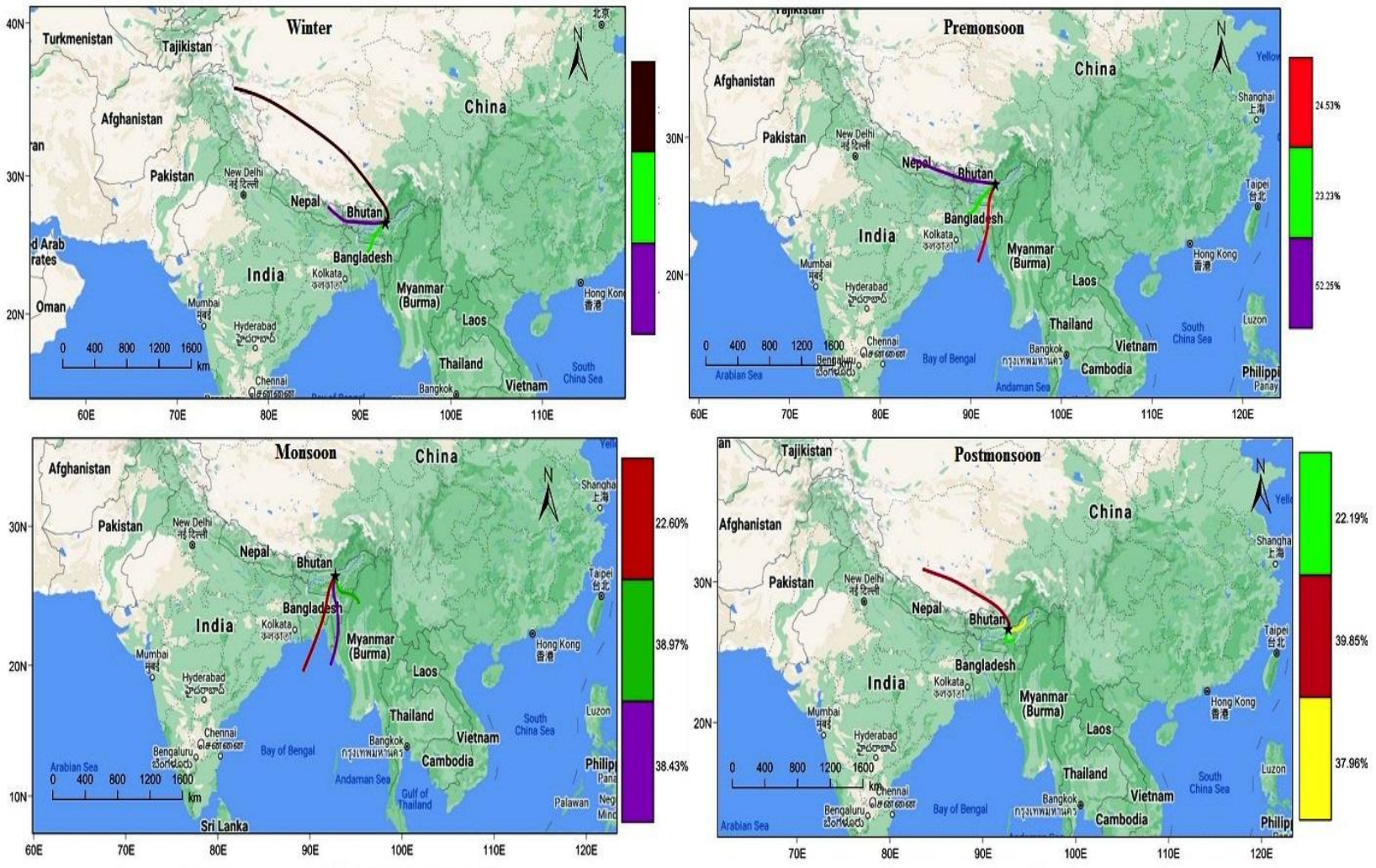

Fig 4.33 (A). Trajectory clusters of NO_2 reaching the city of Tezpur during the year 2014 at 500 m AGL.

(B)

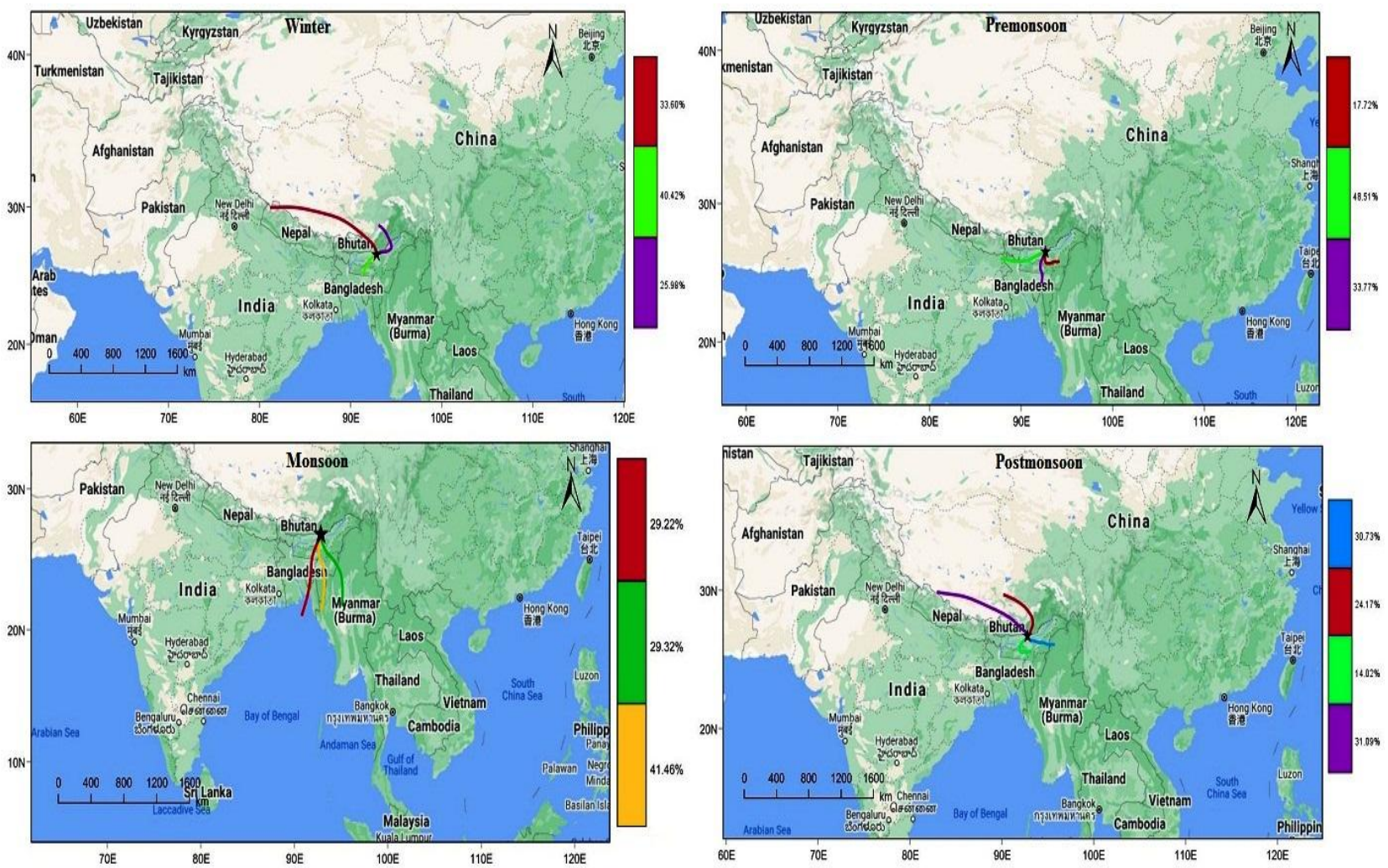

Fig 4.33(B). Trajectory clusters of NO_2 reaching the city of Tezpur during the year 2015 at 500 m AGL.

(C)

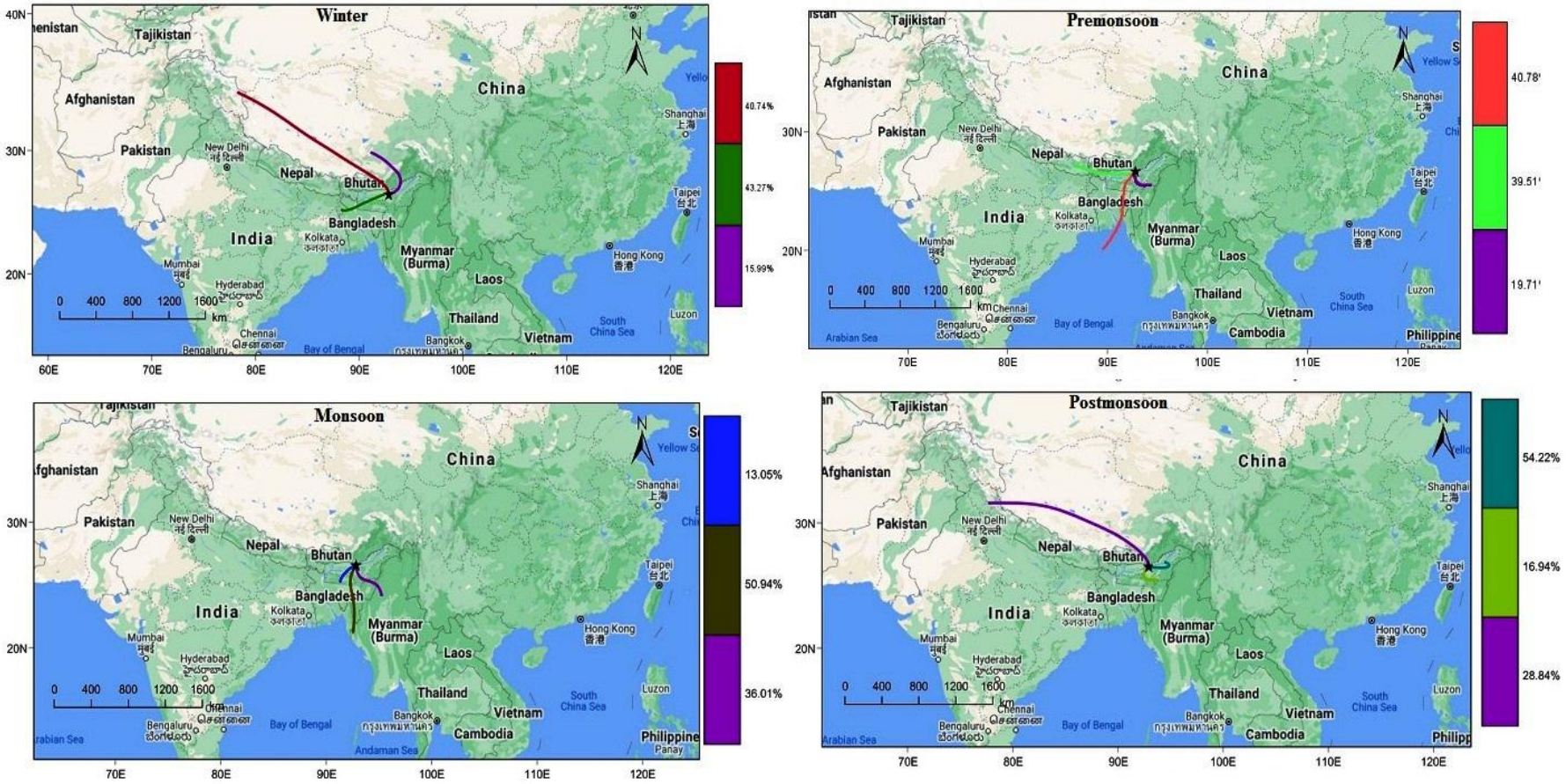

Fig 4.33 (C). Trajectory clusters of NO_2 reaching the city of Tezpur during the year 2016 at 500 m AGL.

(D)

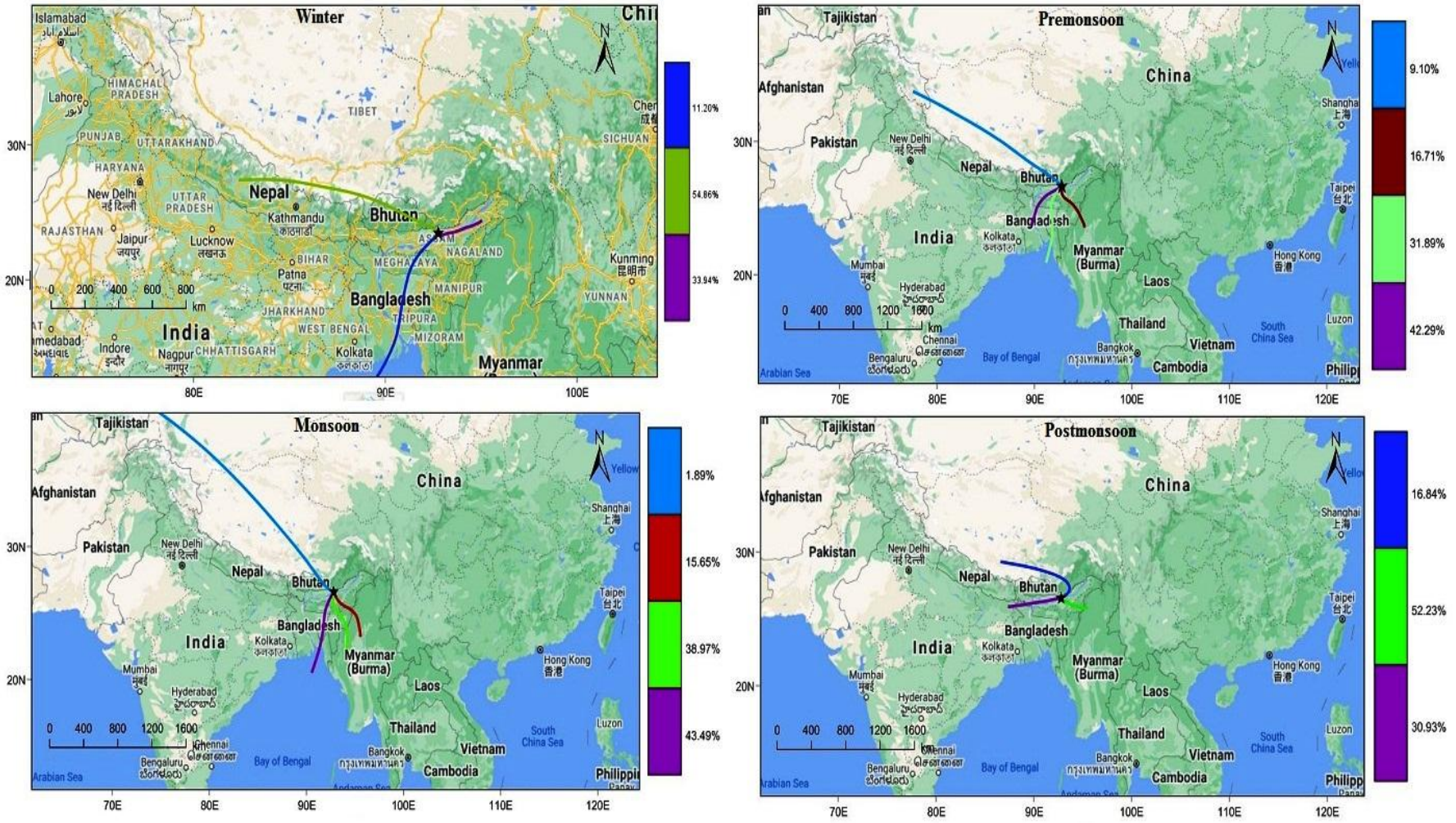

Fig 4.33 (D). Trajectory clusters of NO_2 reaching the city of Tezpur during the year 2017 at 500 m AGL.

(A)

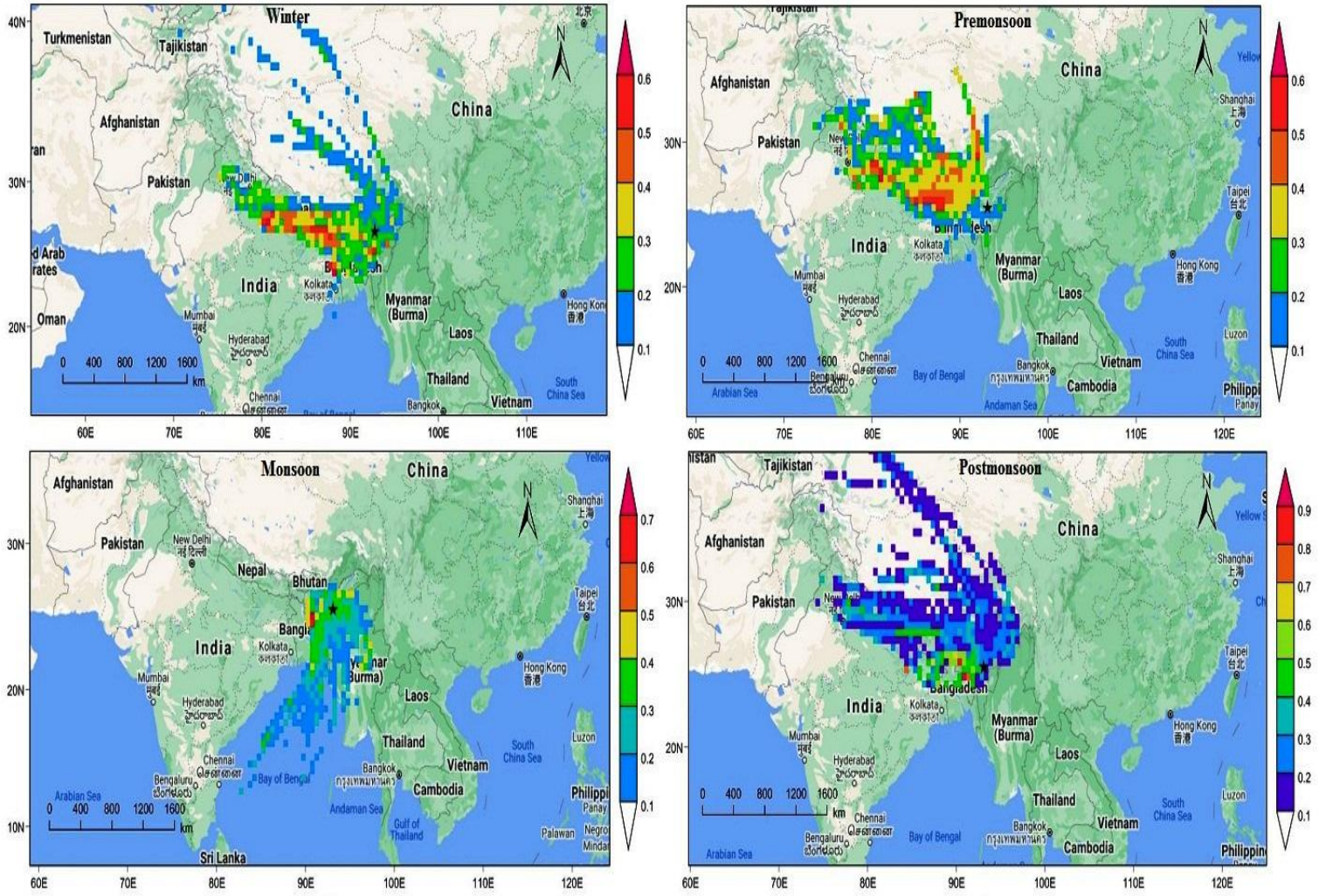

Fig 4.34(A). PSCF density maps of NO_2 concentration for Tezpur during the year 2014. The position of the cities is marked with a black star.

(B)

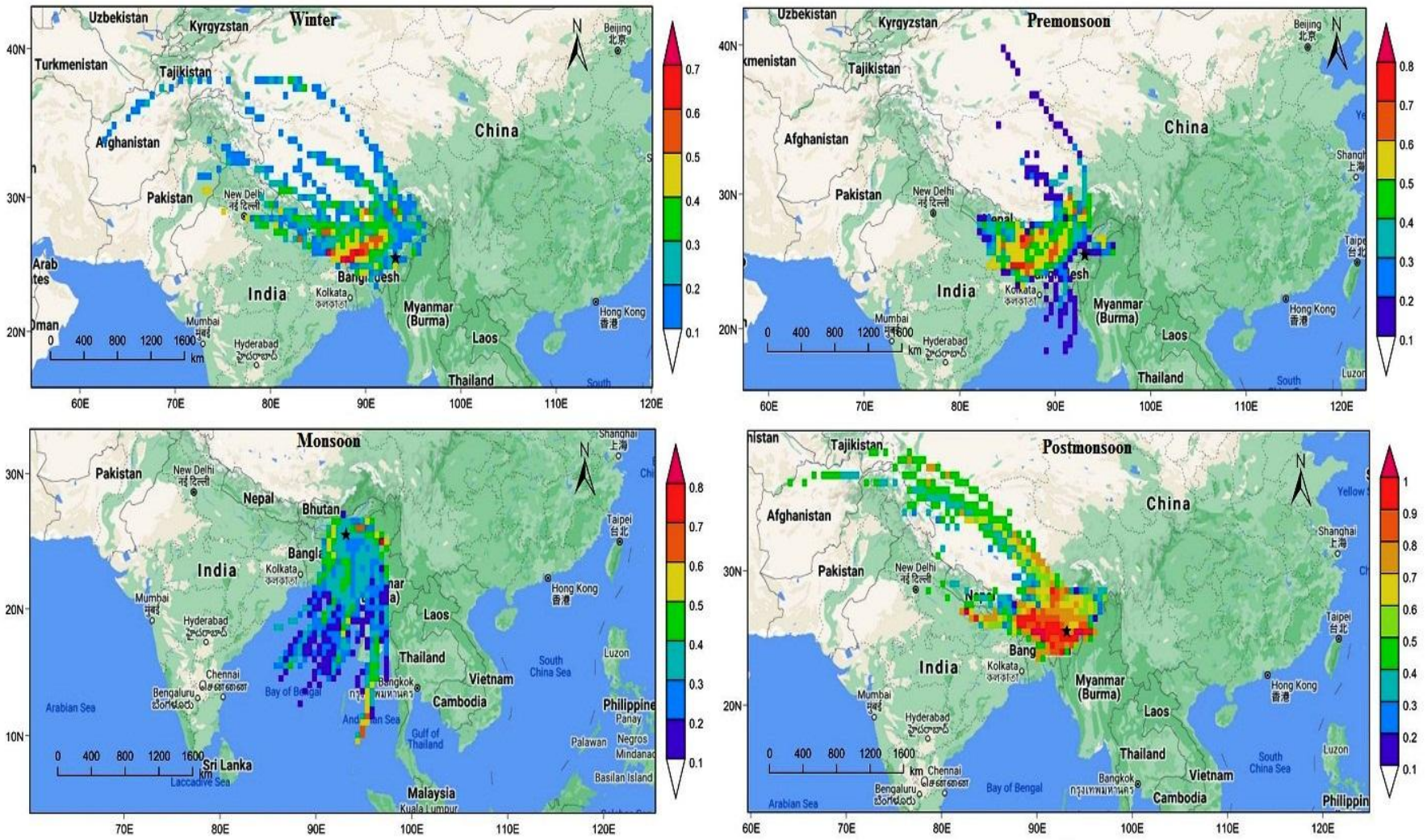

Fig 4.34(B). PSCF density maps of NO_2 concentration for Tezpur during the year 2015. The position of the cities is marked with a black star.

(C)

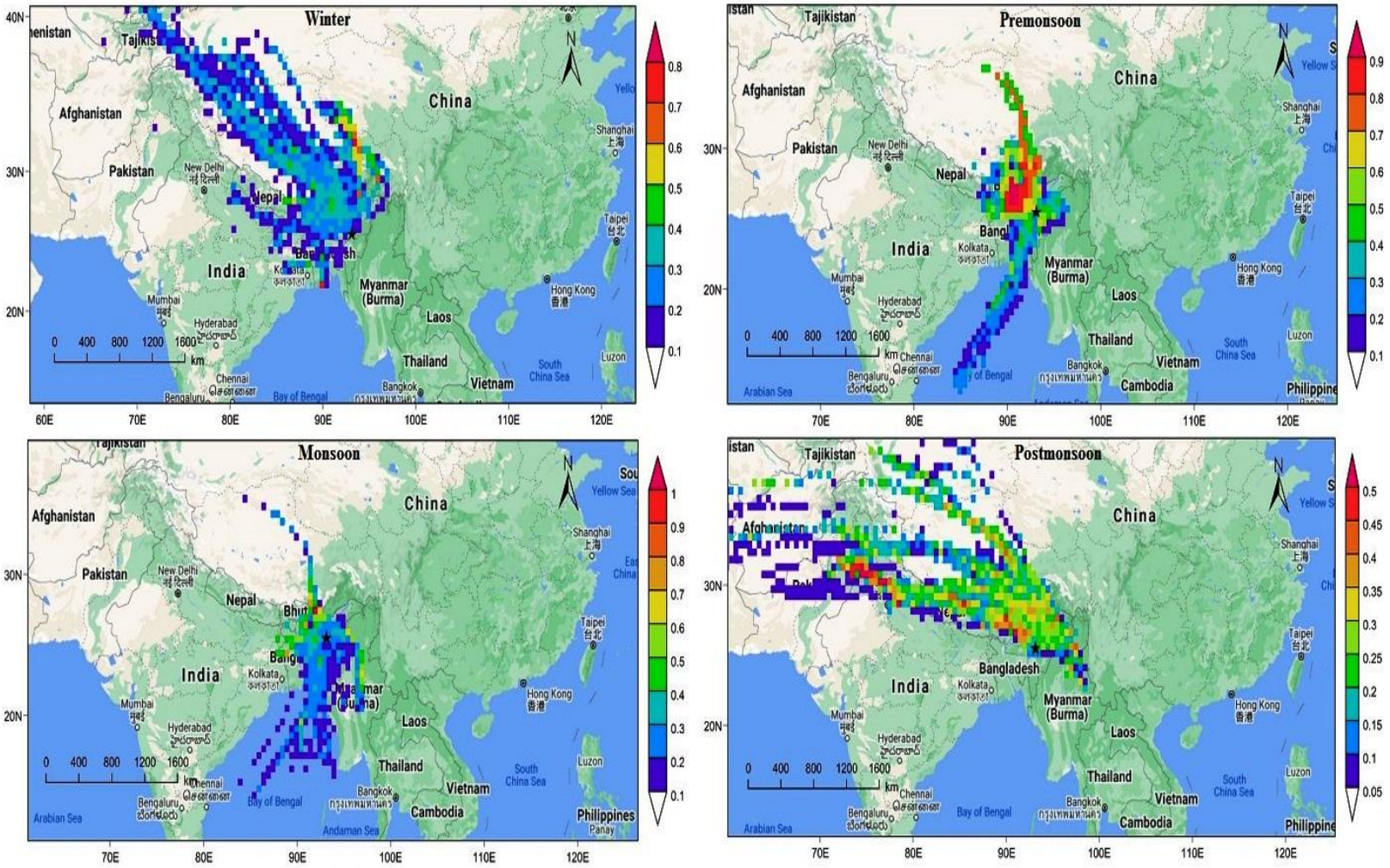

Fig 4.34(C). PSCF density maps of NO_2 concentration for Tezpur during the year 2016. The position of the cities is marked with a black star.

(D)

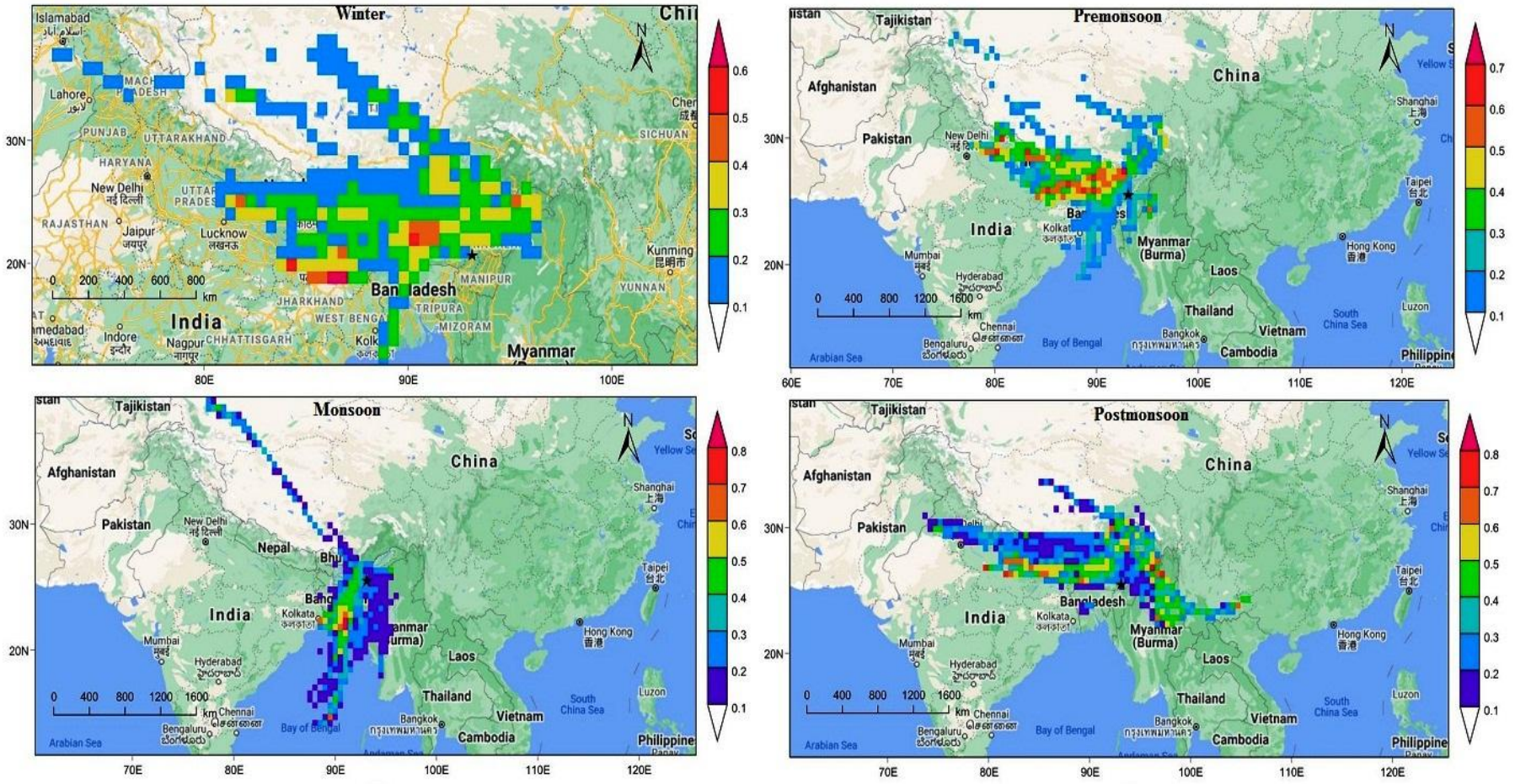

Fig 4.34(D). PSCF density maps of NO_2 concentration for Tezpur during the year 2017. The position of the cities is marked with a black star.

4.14.1: Concentrated weighted trajectories (CWT) of O_3

HYSPLIT airmass trajectories for four years (2014-2017) together reaching the site were weighted with the concentrations of O_3 and the CWTs were computed(Fig.4.35) and also separately for all the four years dividing in four seasons were shown in fig.4.35 (A),(B),(C) and (D) respectively. When the trajectories originated or passed over the IGP, the IndianHimalayan region including Nepal, Bangladesh, and the Bay of Bengal, the site experienced higher O_3 concentrations (shown as colors above yellow). Moderate concentrations of O_3 (color codes green to yellow) were observed when the trajectories originated or passed over Myanmar, the lower Brahmaputra Valley, the Shillong Plateau, and the western regions of China. These results suggest that the O_3concentrations are strongly affected when the trajectories originated or travelled over polluted regions transporting O_3precursors such as PAN to the area. In all the four years it was seen that highest concentrations of O_3 were originated from regions like Bangladesh, West Bengal, Guwahati etc and least concentrations of O_3 were originated from the areas like Myanmar, New Delhi, Pakistan, Tajikistan etc.

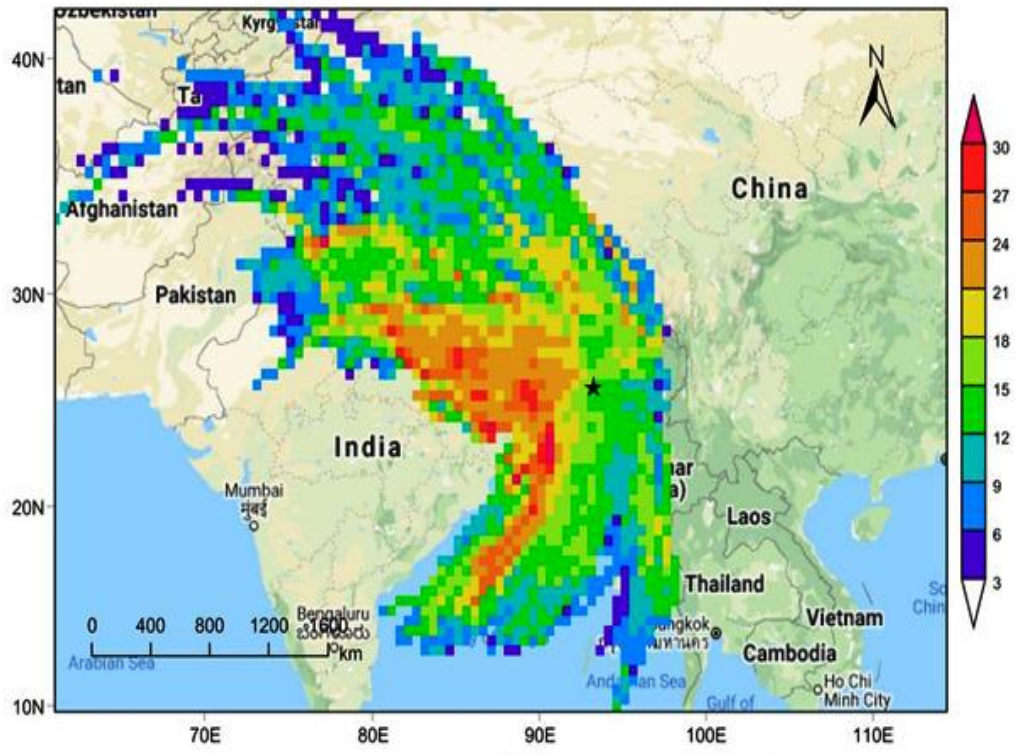

Fig 4.35. Concentration weighted trajectories (CWT) for four years (2014-2017) together were computed from three-days HYSPLIT back trajectories reaching the site every hour for O_3; Tezpur station is shown as the black star.

(A)

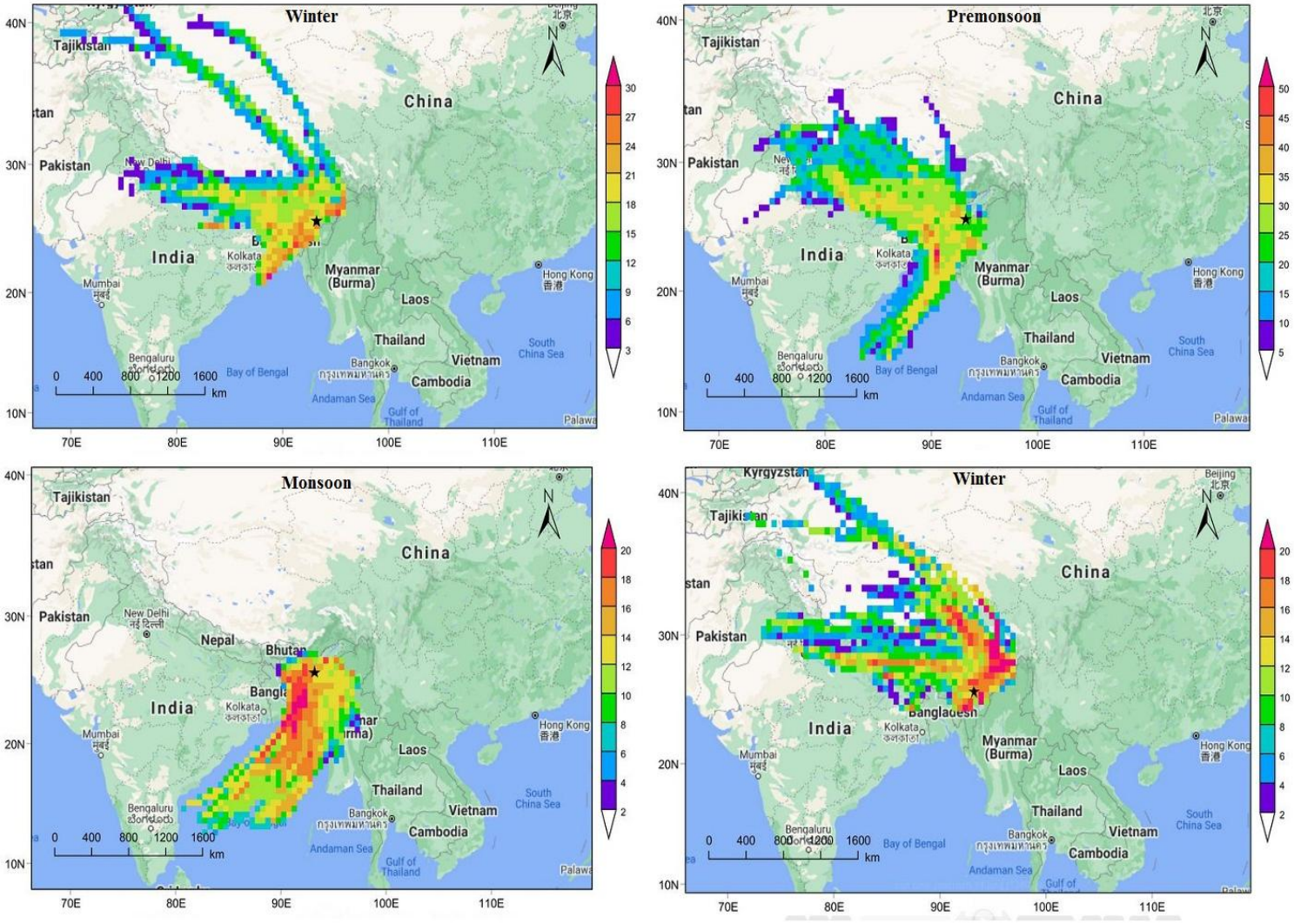

Fig 4.35 (A). Concentration weighted trajectories (CWT) computed from three-days HYSPLIT back trajectories reaching the site every hour for $O_3$for the year 2014; Tezpur station is shown as the black star.

(B)

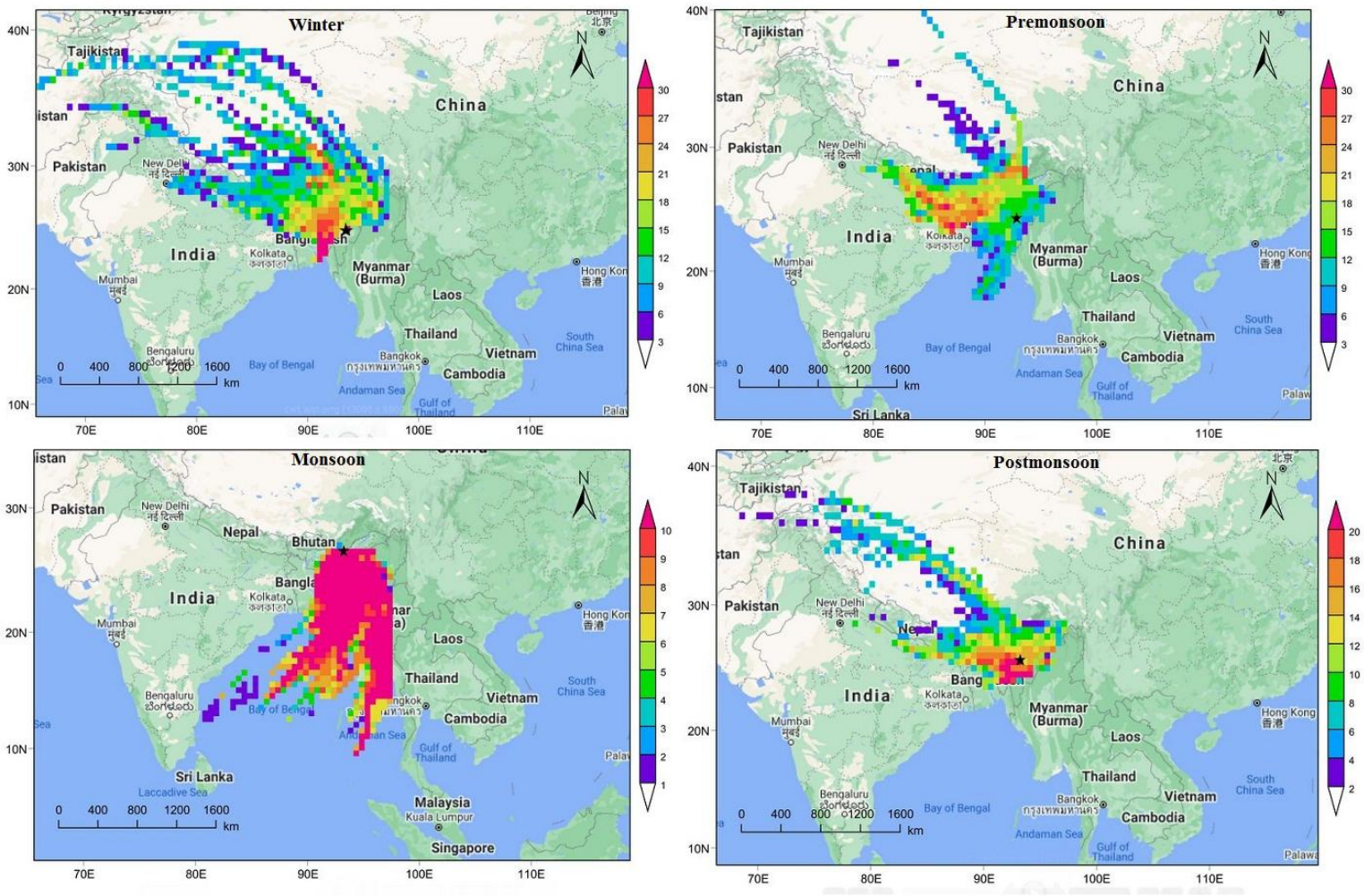

Fig 4.35 (B). Concentration weighted trajectories (CWT) computed from three-days HYSPLIT back trajectories reaching the site every hour for $O_3$for the year 2015; Tezpur station is shown as the black star.

(C)

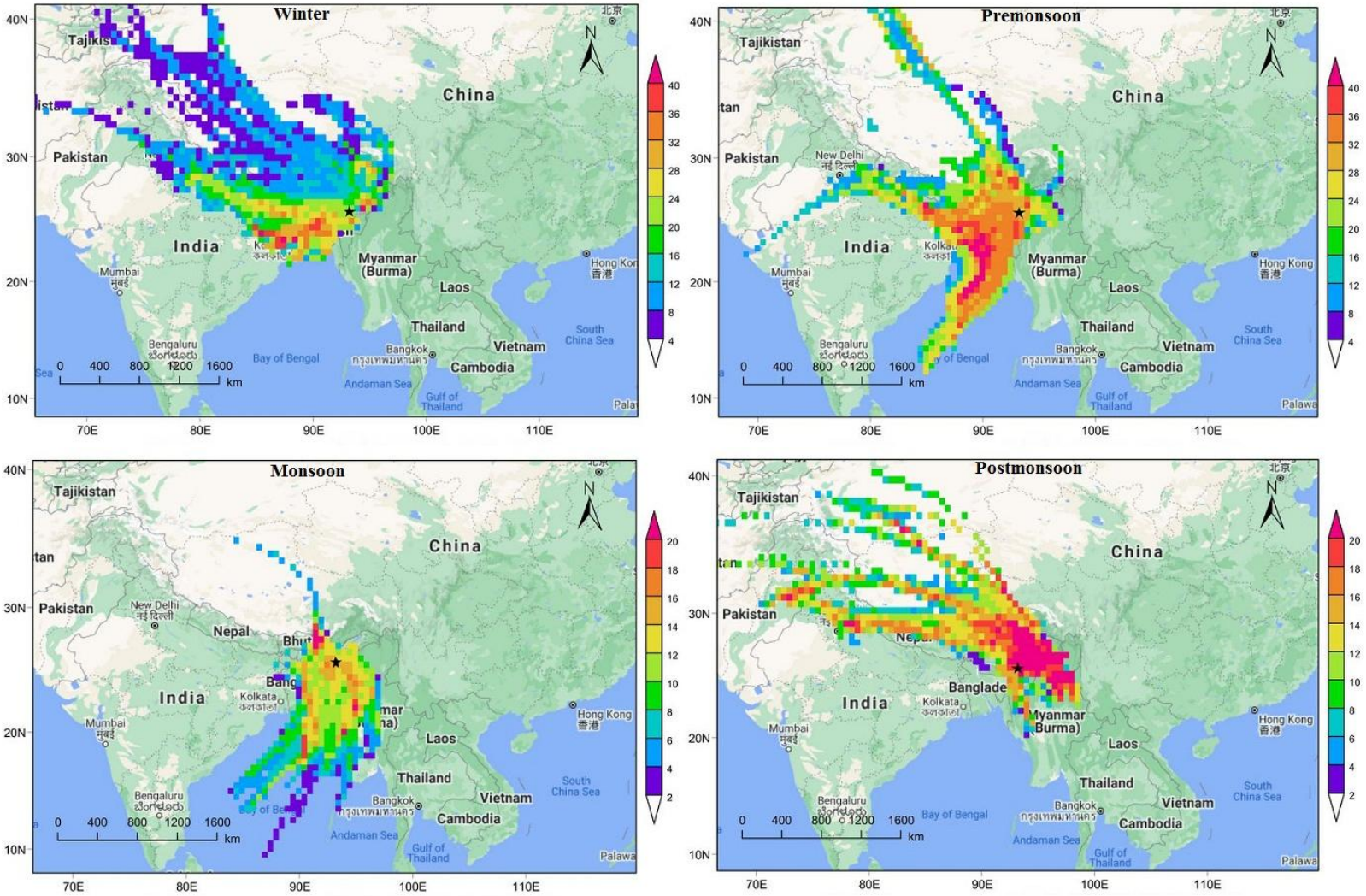

Fig 4.35(C). Concentration weighted trajectories (CWT) computed from three-days HYSPLIT back trajectories reaching the site every hour for $O_3$for the year 2016; Tezpur station is shown as the black star.

(D)

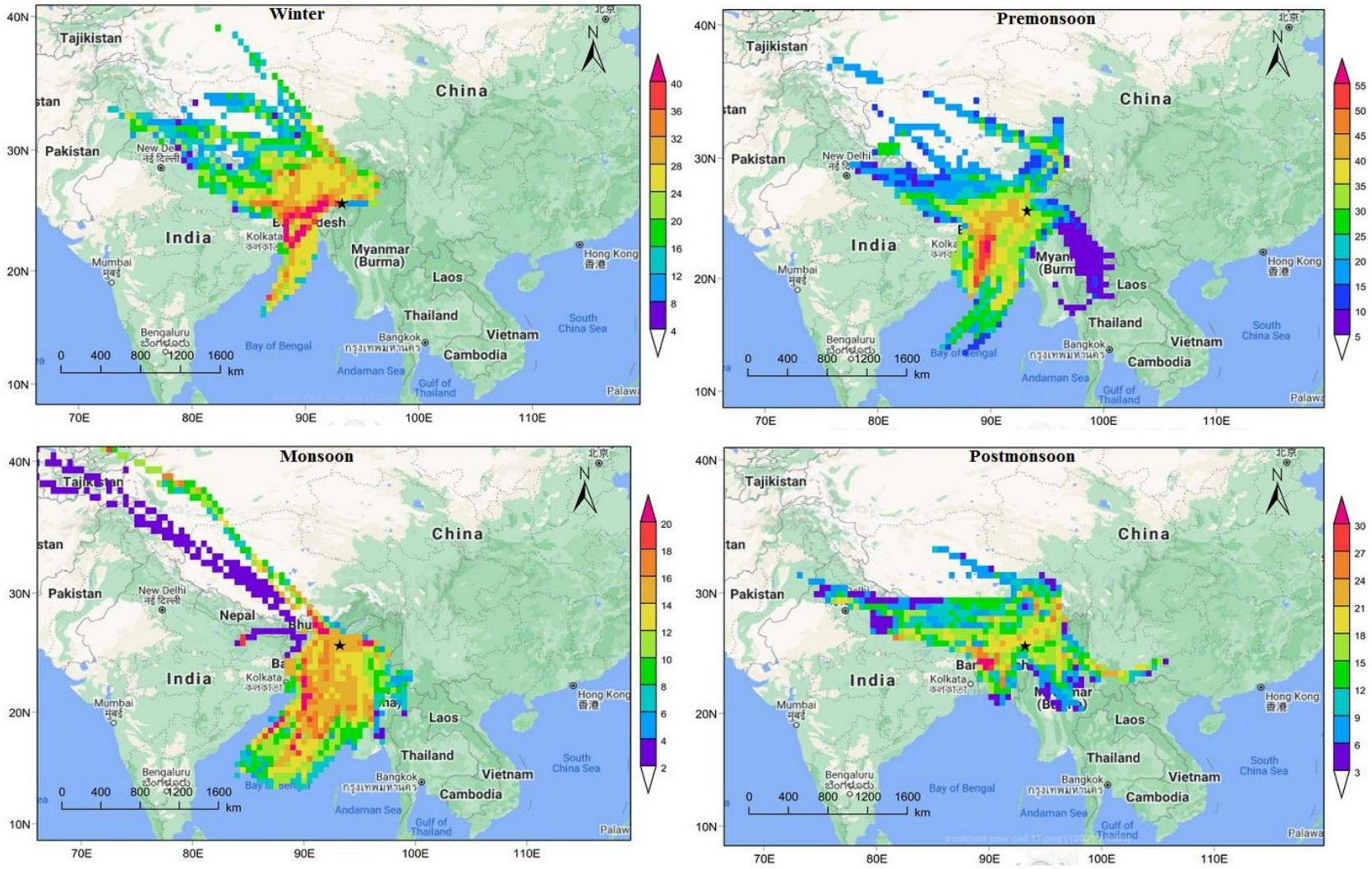

Fig 4.35(D). Concentration weighted trajectories (CWT) computed from three-days HYSPLIT back trajectories reaching the site every hour for $O_3$for the year 2017; Tezpur station is shown as the black star.

4.14.2: Concentrated weighted trajectories of NO_2

HYSPLIT airmass trajectories for four years (2014-2017) together reaching the site was weighted with the concentrations of NO_2 and the CWTs were computed (Fig. 4.36). High concentrations of NO_2 were observed when the trajectory passes over the areas like West Bengal and Jharkhand. Moderate concentration were observed when the trajectory of NO_2 passes over areas like Bangladesh, New Delhi, Patna, Lucknow and Nepal and lowest concentrations were observed when the trajectories originates from areas like Pakistan, Bhutan, Bay of Bengal and Myanmar. From the above results it was evident that highly polluted areas contribute to the transportation of high concentration of NO_2 to the receptor site.In all the four years it was seen that highest concentrations of NO_2 were originated from regions like Bangladesh, Patna, Jharkhand etc and least concentrations were originated from regions like Tajikistan, Dehradun, Bay of Bengal, Bhutan etc.

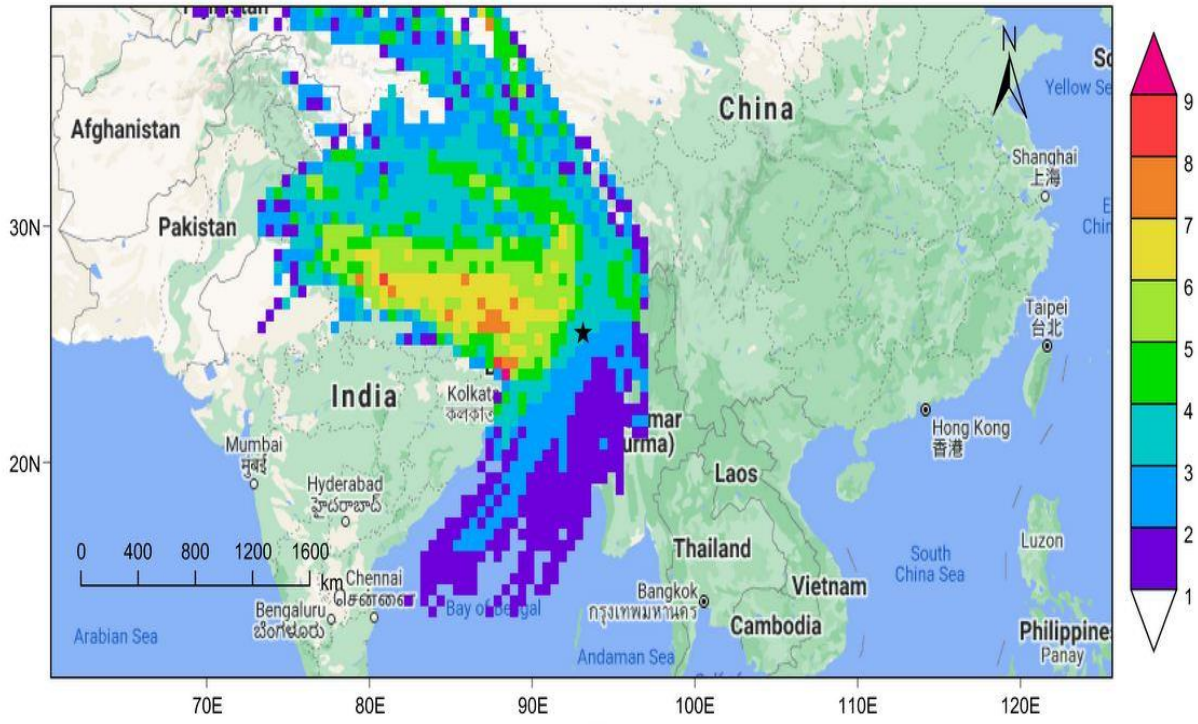

Fig 4.36. Concentration weighted trajectories (CWT) for four years (2014-2017) together were computed from three-days HYSPLIT back trajectories reaching the site every hour for NO_2; Tezpur station is shown as the black star.

(A)

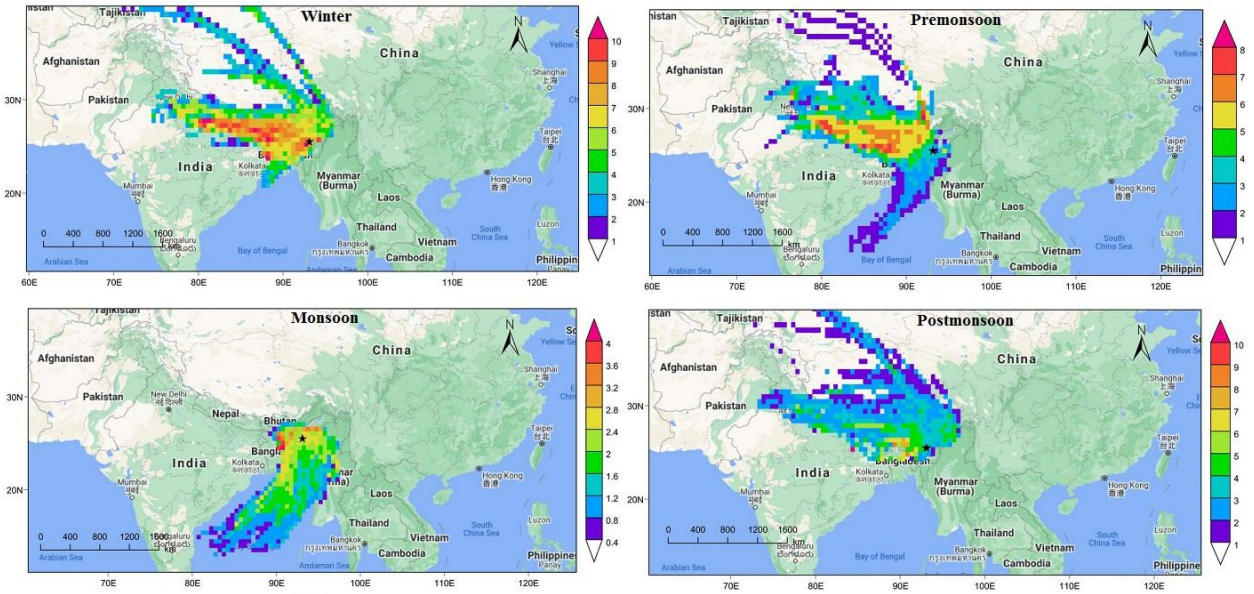

Fig 4.36(A). Concentration weighted trajectories (CWT) computed from three-days HYSPLIT back trajectories reaching the site every hour for $NO_2$for the year 2014; Tezpur station is shown as the black star.

(B)

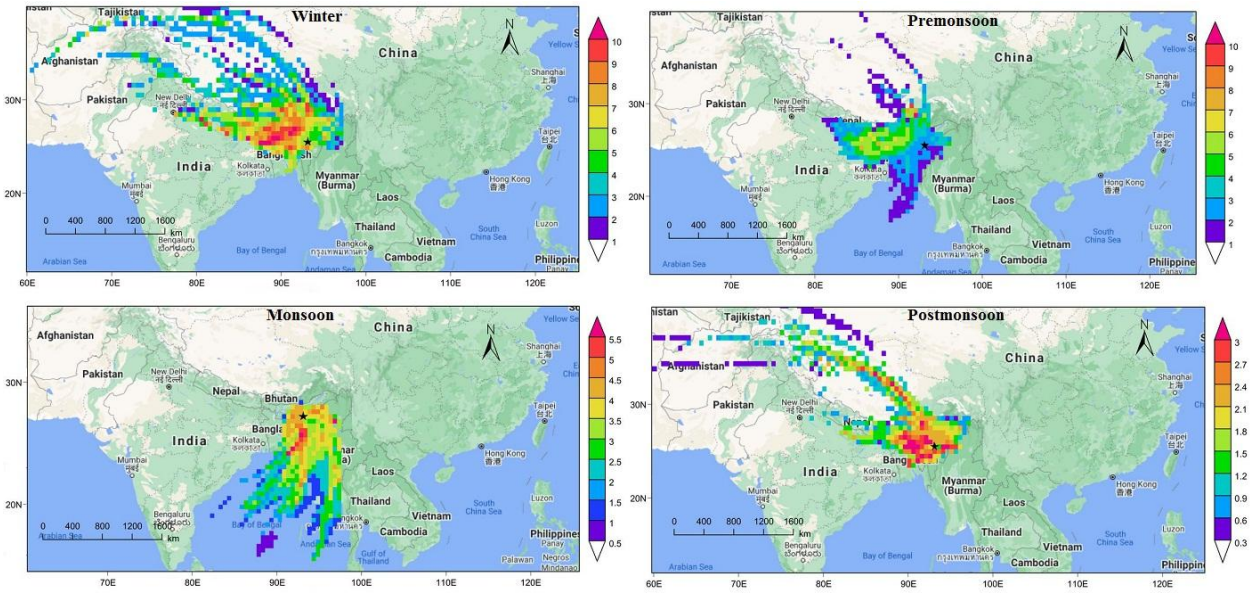

Fig 36(B). Concentration weighted trajectories (CWT) computed from three-days HYSPLIT back trajectories reaching the site every hour for $NO_2$for the year 2015; Tezpur station is shown as the black star.

(C)

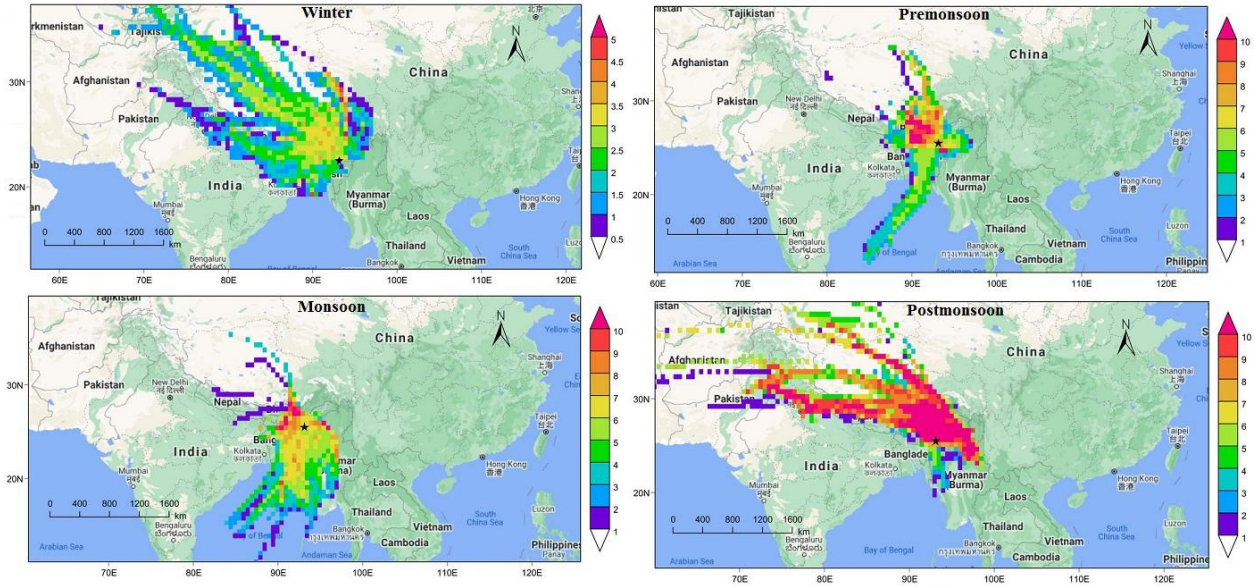

Fig 4.36(C). Concentration weighted trajectories (CWT) computed from three-days HYSPLIT back trajectories reaching the site every hour for $NO_2$for the year 2016; Tezpur station is shown as the black star.

(D)

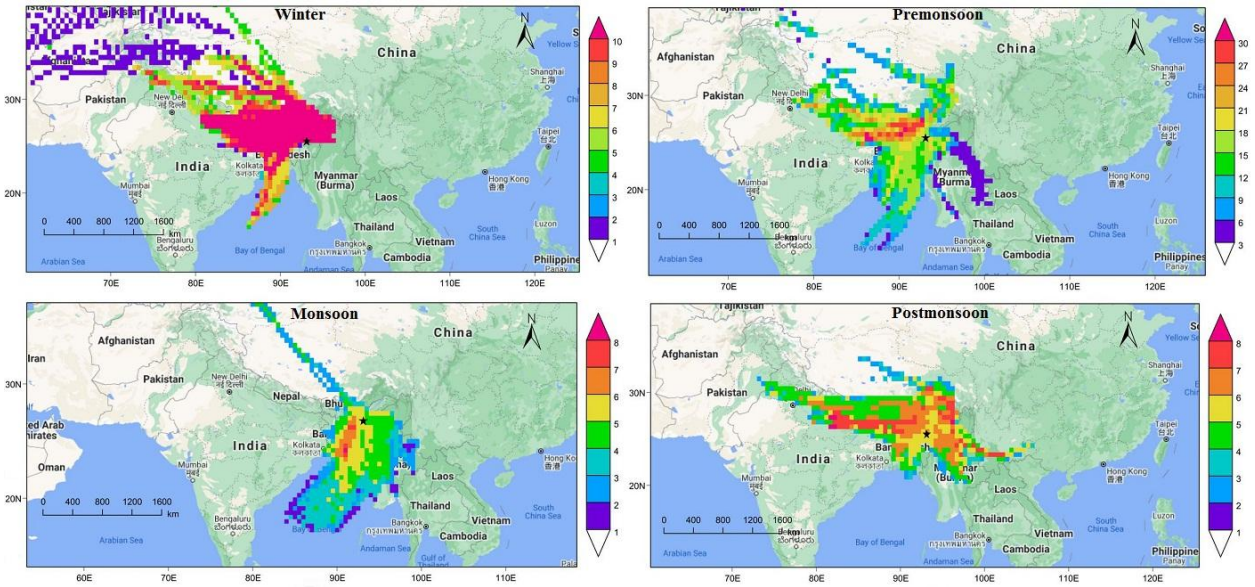

Fig 4.36(D). Concentration weighted trajectories (CWT) computed from three-days HYSPLIT back trajectories reaching the site every hour for $NO_2$for the year 2017; Tezpur station is shown as the black star.

4.15: References

1. Al-Jeelani, H. A. Diurnal and seasonal variations of surface ozone and its precursors in the atmosphere of Yanbu, Saudi Arabia. *Journal of Environmental Protection*, 5(5):408, 2014.
2. Atkinson, R. Atmospheric chemistry of VOCs and NOx. *Atmospheric environment*, 34:2063-2101, 2000.
3. Clapp, L. J., Jenkin, M. E. Analysis of the relationship between ambient levels of O_3, NO_2 and NO as a function of NOx in the UK. *Atmospheric Environment,* 35(36):6391-6405, 2001.
4. Sillman, S. The relation between ozone, NOx and hydrocarbons in urban and polluted rural environments. In Developments in Environmental Science, *Elsevier*, 339-385, 2002.
5. Jacob, D. J. Introduction to atmospheric chemistry. *Princeton University Press, NJ*, 1999.
6. Xue, L. K., Wang, T., Gao, J., Ding, A. J., Zhou, X. H., Blake, 454 D. R., ... Zhang, Q. Z. Ozone production in four major cities of China: sensitivity to ozone precursors and heterogeneous processes. *Atmospheric Chemistry and Physics Discuss,* 13: 27243-27285, 2013.
7. Sarangi, T., Naja, M., Ojha, N., Kumar, R., Lal, S., Venkataramani, S., ... Chandola, H. C. First simultaneous measurements of ozone, CO, and NOy at a high-altitude regional representative site in the central Himalayas. *Journal of Geophysical Research: Atmospheres,* 119(3):1592-1611, 2014.
8. Bhuyan, P. K., Bharali, C., Pathak, B., & Kalita, G. The role of precursor gases and meteorology on temporal evolution of O_3 at a tropical location in northeast India. *Environmental Science and Pollution Research*, *21*(10):6696-6713, 2014.
9. Yadav R., Sahu, L.K., Jaaffrey, S.N.A., Beig, G. Distributions of ozone and related trace gases at an urban site in western India. *Journal of Atmospheric Chemistry,* 71(2):125–144, 2014.
10. Lal S, Naja M, Subbaraya BH. Seasonal variation in the surface ozone and its precursors over an urban site in India. *Atmospheric Environment*, 34:2713–2724, 2000.

11. Debaje, S.B., Johnson, S.J., Ganesan, K., Jadhav, D.B. and Seetaramayya, S. Surface Ozone Measuerements at Tropical Rural Coastal Station Tranquebar, India. *Atmospheric Environment,* 37: 4911–4916, 2003.

12. Pancholi, P., Kumar, A., Bikundia, D. S., &Chourasiya, S. An observation of seasonal and diurnal behavior of O_3–NOx relationships and local/regional oxidant (OX= O3+ NO2) levels at a semi-arid urban site of Western India. *Sustainable Environment Research*, 28(2):79-89, 2018.

13. Beig, G., Gunthe, S., & Jadhav, D. B. Simultaneous measurements of ozone and its precursors on a diurnal scale at a semi urban site in India. *Journal of Atmospheric Chemistry*, *57*(3): 239-253, 2007.

14. Satsangi, G. S., Lakhani, A., Kulshrestha, P. R., & Taneja, A. Seasonal and diurnal variation of surface ozone and a preliminary analysis of exceedance of its critical levels at a semi-arid site in India. *Journal of Atmospheric Chemistry*, 47(3):271-286, 2004.

15. Reddy, B. S. K., Kumar, K. R., Balakrishnaiah, G., Gopal, K. R., Reddy, R. R., Sivakumar, V., ... & Lal, S. Analysis of diurnal and seasonal behavior of surface ozone and its precursors (NOx) at a semi-arid rural site in southern India. *Aerosol and Air Quality Research*, 12(6):1081-1094, 2012.

16. Udayasoorian, C., Jayabalakrishnan, R. M., Suguna, A. R., Venkataramani, S., & Lal, S. Diurnal and seasonal characteristics of ozone and NOx over a high altitude Western Ghats location in Southern India. *Advances in Applied Science Research*, 4(5):309-320, 2013.

17. Nishanth T, Praseed KM, Satheesh Kumar MK, Valsaraj KT. Analysis of Ground Level O_3 and Nox Measured at Kannur, India. *Journal of Earth Science and Climate Change,* 3:111, 2012.

18. Tabinda, A. B., Munir, S., Yasar, A., & Ilyas, A. Seasonal and temporal variations of criteria air pollutants and the influence of meteorological parameters on the concentration of pollutants in ambient air in Lahore,

Pakistan. *Pakistan Journal of Scientific & Industrial Research Series A: Physical Sciences*, *59*(1): 34-42, 2016.

19. Sikder, H. A., Nasiruddin, M., Suthawaree, J., Kato, S., &Kajii, Y. Long term observation of surface O_3 and its precursors in Dhaka, Bangladesh. *Atmospheric research*, 122: 378-390, 2013.
20. Pochanart P, Hirokawa J, Kajii Y, Akimoto H. Influence of regional-scale anthropogenic activity in northeast Asia on seasonal variations of surface ozone and carbon monoxide observed at Oki, Japan. *Journal of Geophysical Research*, 104(D3):3621–3631F, 1999.
21. Im, U., Incecik, S., Guler, M., Tek, A., Topcu, S., Unal, Y. S., ... &Tayanc, M. Analysis of surface ozone and nitrogen oxides at urban, semi-rural and rural sites in Istanbul, Turkey. *Science of the Total Environment*, *443*: 920-931, 2013.
22. Roberts-Semple, D., Song, F. and Gao, Y. Seasonal Characteristics of Ambient Nitrogen Oxides and Ground- Level Ozone in Metropolitan Northeastern New Jersey. *Atmopheric. Pollution Research,* 3: 247–257, 2012.
23. Zunckel, M., Venjonoka, K., Pienaar, J. J., Brunke, E. G., Pretorius, O., Koosialee, A., ... & Van Tienhoven, A. M. Surface ozone over southern Africa: synthesis of monitoring results during the Cross border Air Pollution Impact Assessment project. *Atmospheric Environment*, 38(36): 6139-6147, 2004.
24. Bonasoni, P., Laj, P., Marinoni, A., Sprenger, M., Angelini, F., Arduini, J., ... & Di Biagio, C. Atmospheric Brown Clouds in the Himalayas: first two years of continuous observations at the Nepal Climate Observatory-Pyramid (5079 m), 2010.
25. Filella, I., & Penuelas, J. Daily, weekly and seasonal relationships among VOCs, NOx and O_3 in a semi-urban area near Barcelona. *Journal of Atmospheric Chemistry*, 54(2): 189-201, 2006.
26. Khoder, M. I. (2009). Diurnal, seasonal and weekdays–weekends variations of ground level ozone concentrations in an urban area in greater Cairo. *Environmental Monitoring and Assessment*, 149(1-4): 349-362, 2009.

27. Kgabi, N. A., & Sehloho, R. M. Seasonal variations of tropospheric ozone concentrations. *Global Journal of Science Frontier Research Chemistry*, 12: 21-29, 2012.
28. Kuniyal, J. C., Choudhary, S., & Sharma, P. Five years surface ozone behaviour in a semi rural location at Mohal-Kullu in the north-western Himalaya, India, 2021.
29. Kanchana, A. L., Sagar, V. K., Pathakoti, M., Mahalakshmi, D. V., Mallikarjun, K., &Gharai, B. Ozone variability: Influence by its precursors and meteorological parameters-An investigation. Journal *of Atmospheric and Solar-Terrestrial Physics*, 211:105468, 2020.
30. Naja, M. and Lal, S. Surface Ozone and Precursor Gases at Gadanki (13.5°N, 79.2°E), a Tropical Rural Site in India. *Journal of Geophysical Research,* 107: 4197, 2002.
31. Alghamdi, M. A., Khoder, M., Harrison, R. M., Hyvärinen, A. P., Hussein, T., Al-Jeelani, H., ... &Lihavainen, H. Temporal variations of O_3 and NOx in the urban background atmosphere of the coastal city Jeddah, Saudi Arabia. *Atmospheric environment*, 94: 205-214, 2014.
32. Han, S., Bian, H., Feng, Y., Liu, A., Li, X., Zeng, F., & Zhang, X. Analysis of the Relationship between O_3, NO and NO_2 in Tianjin, China. *Aerosol Air Quality Research*, 11(2): 128-139, 2011.
33. Dumka, U. C., Gautam, A. S., Tiwari, S., Mahar, D. S., Attri, S. D., Chakrabarty, R. K., ... Hooda, R. Evaluation of urban ozone in the Brahmaputra River Valley. *Atmospheric Pollution Research*, 11(3): 610-618, 2020.
34. Crutzen, P. J. Tropospheric ozone: An overview. In Tropospheric ozone. *Springer, Dordrecht*, 3-32, 1988.
35. Gilge, S., Plass-Duelmer, C., Fricke, W., Kaiser, A., Ries, L., & Buchmann, B. Ozone, Carbon monoxide and Nitrogen oxides time series at four Alpine GAW mountain stations in Central Europe. *Atmospheric Chemistry & Physics Discussions,* 10(8), 2010.
36. Ojha N, Naja M, Singh KP, Sarangi T, Kumar R, Lal S, Lawrence MG, Butler TM, Chandola HC. Variabilities in ozone at a semiurban site in the Indo-Gangetic Plain region: association with the meteorology and regional processes. *Journal of Geophysical Research,* 117: D20301, 2012.

37. Tsai DH, Wang JL, Wang CH, Chan CC. A study of ground-level ozone pollution, ozone precursors and subtropical meteorological conditions in central Taiwan. *Journal of environmental monitoring*, 2007.
38. David LM, Nair PR. Diurnal and seasonal variability of surface ozone and NOx at a tropical coastal site: association with mesoscale and synoptic meteorological conditions. *Journal of Geophysical Research,* 116: D10303, 2011.
39. Tu J, Xia Z-G, Wang H, Li W. Temporal variations in surface ozone and its precursors and meteorological effects at an urban site in China. *Atmospheric Research,* 85:310–337, 2007.
40. Reddy, B.S.K., Kumar, K.R., Balakrishnaiah, G., Gopal, K.R., Reddy, R.R., Narasimhulu, K., Ahammed, Y.N., Reddy, L.S.S. and Lal, S. Observational Studies on the Variations in Surface Ozone Concentrations at Anantapur in Southern India. *Atmospheric Research*, 98: 125–139, 2010.
41. Reddy KK, Naja M, Ojha N, Mahesh P, Lal S. Influences of the boundary layer evolution on surface ozone variations at a tropical rural site in India. *Journal of Earth System Science,* 121(4):911–922, 2012.
42. Kalita G, Bhuyan P K. Spatial heterogeneity in tropospheric column ozone over the Indian subcontinent: long-term climatology and possible association with natural and anthropogenic activities. *Advances in Meteorology*, 2011.
43. Pathak B, Bhuyan PK, Biswas J, Takemura T. Long term climatology of particulate matter and associated microphysical and optical properties over Dibrugarh, North-East India and inter-comparison with SPRINTARS simulations. *Atmospheric Environment,* 2013.
44. Li, K., Chen, L., Ying, F., White, S. J., Jang, C., Wu, X., ... Cen, K. 2017. Meteorological and chemical impacts on ozone formation: A case study in Hangzhou, China. *Atmospheric research*, 196: 40-52, 2017.
45. Hassan, I. A., Basahi, J. M., Ismail, I. M., &Habeebullah, T. M. Spatial distribution and temporal variation in ambient ozone and its associated NOx in the atmosphere of Jeddah City, Saudi Arabia. *Aerosol Air Quality Research*, 13: 1712-1722.
46. Brown, S.S., Ryerson, T.B., Wollny, A.G., Brock, C.A., Peltier, R., Sullivan, A.P., Weber, R.J., Dube, W.P., Trainer, M., Meagher, J.F.,

Fehsenfeld, F.C. and Ravishankara, A.R. Variability in Nocturnal Nitrogen Oxide Processing and Its Role in Regional Air Quality. *Science*, 311: 67–70, 2006.

47. Sillman, S. Overview: Tropospheric ozone, smog and ozone-NOx-VOC sensitivity. *Treatise on Geochemistry*, 2003.
48. Pudasainee, D., Sapkotab, B., Shresthac, M., Kagac, A., Kondoc, A. and Inoue, Y. Ground Level Ozone Concentrations and Its Association with NOx and Meteorological Parameters in Kathmandu valley, Nepal. *Atmospheric Environment,* 40: 8081–8087, 2006.
49. Guttikunda, S.K. and Gurjar, B.R. Role of Meteorology in Seasonality of Air Pollution in Megacity Delhi, India. *Environmental Monitoring and Assessment,* 184: 3199–3211, 2011.
50. Khodeir, M.I. Diurnal, Seasonal and Weekdays- Weekends Variations of Ground Level Ozone Concentrations in an Urban Area in Greater Cairo. *Environmental Monitoring Assessment,* 149: 349–362, 2009.
51. Smith, L.A., Mukerjee, S., Chung, K.C.and Afghani, J. Spatial Analysis and Land Use Regression of VOCs and NO_2 in Dallas, Texas during Two Seasons. *Journal of Environmental Monitoring,* 13: 999–1007, 2011.
52. Shiu, C. J., Liu, S. C., Chang, C. C., Chen, J. P., Chou, C. C., Lin, C. Y., Young, C. Y., 2007.
53. Ooi, M. C. G., Chan, A., Ashfold, M. J., Oozeer, M. Y., Morris, K. I., Kong, S. S. K. The role of land use on the local climate and air quality during calm inter-monsoon in a tropical city. *Geoscience Frontiers*, 10(2): 405-415, 2019.
54. Ghude, S. D., Jain, S. L., Arya, B. C., Beig, G., Ahammed, Y. N., Kumar, A., Tyagi, B. Ozone in ambient air at a tropical megacity, Delhi: characteristics, trends and cumulative ozone exposure indices. *Journal of Atmospheric Chemistry,* 60: 237-252, 2008.
55. Tiwari, S., Dahiya, A., Kumar, N. Investigation into relationships among NO, NO_2, NOx, O_3, and CO at an urban background site in Delhi, India. *Atmospheric Research*, 157: 119-126, 2015.
56. Attri AK, Kumar U, Jain VK 2001. Formation of ozone by fireworks. *Nature*, 411:1015, 2001.

57. Victoria Advocate, 2005. Mexico City begins 2005 with air pollution ratings unsatisfactory. In Victoria Advocate, 2nd January, 2005.
58. Nishanth, T., Praseed, K. M., Rathnakaran, K., Satheesh Kumar, M. K., Krishna, R. R., & Valsaraj, K. T. Atmospheric pollution in a semi-urban, coastal region in India following festival seasons. *Atmospheric Environment*, 47: 295–306, 2012.
59. Ganguly, N. D. Surface ozone pollution during the festival of Diwali, New Delhi, India. *Earth Science India*, 2, 2009.
60. Verma, C., & Deshmukh, D. K. The ambient air and noise quality in India during diwali festival: A Review. *Recent Research in Science and Technology*, *6*(1): 2014.
61. Finlayson-Pitts, B.J., Pitts, J.N. Tropospheric air pollution: ozone, airborne toxics, polycyclic aromatic hydrocarbons and particles. *Science*, 276: 1045–1052, 1997.
62. Ambade, B. The air pollution during Diwali festival by the burning of fireworks in Jamshedpur city, India. *Urban climate*, 26: 149-160, 2018.
63. Sharma, A., Mandal, T. K., Sharma, S. K., Shukla, D. K., & Singh, S. Relationships of surface ozone with its precursors, particulate matter and meteorology over Delhi. *Journal of Atmospheric Chemistry*, 74(4): 451-474, 2017.
64. Nishanth, T., Ojha, N., Kumar, M. S., & Naja, M. Influence of solar eclipse of 15 January 2010 on surface ozone. *Atmospheric environment*, 45(9): 1752-1758, 2011.
65. Solomon P, Cowling E, Hidy G, Furiness C. Comparison of scientific findings from major ozone field studies in North America and Europe. *Atmospheric Environment,* 34:1885–1920, 2000.
66. Ordonez, C., Mathis, H., Furger, M., Henne, S., Hüglin, C., Staehelin, J., Prévôt, A. S. Changes of daily surface ozone maxima in Switzerland in all seasons from 1992 to 2002 and discussion of summer 2003. *Atmospheric Chemistry and Physics,* 5(5): 1187-1203, 2005.
67. Camalier, L., Cox, W., & Dolwick, P. The effects of meteorology on ozone in urban areas and their use in assessing ozone trends. *Atmospheric Environment*, 41: 7127-7137, 2007.

68. Wise, E. K., Comrie, A. C. Meteorologically adjusted urban air quality trends in the Southwestern United States. *Atmospheric Environment*, 39(16): 2969-2980, 2005.
69. Elminir, H. K. Dependence of urban air pollutants on meteorology. *Science of the Total Environment,* 350(1-3): 225-237, 2005.
70. Morris, R. E., Gery, M. W., Liu, M. K., Moore, G. E., Daley, C. Sensitivity of a regional oxidant model to variations in climate parameters. *Systems Applications, Inc., San Rafael, CA (USA),* 1989.
71. Aw, J., Kleeman, M. J. Evaluating the first-order 301 effect of intraannual temperature variability on urban air pollution. *Journal of Geophysical Research*: *Atmospheres*, 108(D12), 2003.
72. Sanchez-Ccoyllo, O. R.,Ynoue, R. Y., Martins, L. D.,de Fátima Andrade, M. Impacts of ozone precursor limitation and meteorological variables on ozone concentration in Sao Paulo, Brazil. *Atmospheric Environment,* 40: 552-562, 2006.
73. Steiner, A. L., Tonse, S., Cohen, R. C., Goldstein, A. H., Harley, R. A. Influence of future climate and emissions on regional air quality in California. *Journal of Geophysical Research: Atmospheres,* 111(D18), 2006.
74. Arundel, A. V., Sterling, E. M., Biggin, J. H., Sterling, T. D. Indirect health effects of relative humidity in indoor environments. *Environmental health perspectives,* 65: 351-361, 1986.
75. Korsog, P.E. and Wolff, G.T., 1991. An examination of urban ozone trends in the northeastern US (1973–1983) using a robust statistical method. *Atmospheric Environment. Part B. Urban Atmosphere*, 25(1): 47-57, 1991.
76. Seinfeld, J. H., Pandis, S. N. *Atmospheric Chemistry and Physics*, From air pollution to climate change. 2nd edition, John Wiley & Sons, Inc. New Jersey, 2006.
77. Leighton, P. Photochemistry of Air Pollution. *Academies press, New York*, 300, 1961.
78. Seinfeld, J. H., & Pandis, S. N. *Atmospheric Chemistry and Physics*, From air pollution to climate change. 3rd edition, John Wiley Sons, Inc. New Jersey, 2016.

79. Greiner, N.R. Hydroxyl-Radical Kinetics by Kinetic Spectroscopy. I. Reactions with H_2, CO, and CH_4 at 300° K. *The Journal of Chemical Physics,* 46(7): 2795-2799, 1967.

80. Stedman, D.H., Steffenson, D. and Niki, H. The reaction between active hydrogen and Cl2-evidence for the participation of vibrationally excited H2. *Chemical Physics Letters,* 7(2): 173-174, 1970.

81. Khalil, M. A. K., Butenhoff, C. L., & Harrison, R. M. Ozone balances in urban Saudi Arabia. *npj Climate and Atmospheric Science*, *1*(1): 1-9, 2018.

82. Deka, P., & Hoque, R. R. Chemical characterization of biomass fuel smoke particles of rural kitchens of South Asia. *Atmospheric Environment*, 108: 125-132, 2015.

83. Hoque, R. R., & Deka, P. Aerosol and CO emissions during meji burning. *Current Science(Bangalore)*, 98(10): 1270, 2010.

84. Deka, P., & Hoque, R. R. Incremental effect of festive biomass burning on wintertime PM10 in Brahmaputra Valley of Northeast India. *Atmospheric Research*, 143: 380-391, 2014.

85. Singh, H. B., Kanakidou, M., Crutzen, P. J., & Jacob, D. J. High concentrations and photochemical fate of oxygenated hydrocarbons in the global troposphere. *Nature*, 378(6552): 50-54, 1995.

86. Gan, J., Yates, S. R., Ohr, H. D., & Sims, J. J. Production of methyl bromide by terrestrial higher plants. *Geophysical Research Letters*, 25(19): 3595-3598, 1998.

87. Mead, M. I., White, I. R., Nickless, G., Wang, K. Y., & Shallcross, D. E. An estimation of the global emission of methyl bromide from rapeseed (Brassica napus) from 1961 to 2003. *Atmospheric Environment*, 42(2): 337-345, 2008.

88. Das K.K. Study on the production pattern and marketing of rapeseed and mustard cultivation in Assam with special reference to Nagaon district. Ph.D.Thesis, Nagaland University, Medziphema, 2015.
89. Horticulture Statistics Division. Horticulture Statistics Division Department of Agriculture. Cooperation & Farmers' Welfare Ministry of Agriculture and Farmers' Welfare Government of India, 2018.

90. Orlando, J. J., Tyndall, G. S., & Wallington, T. J. Atmospheric oxidation of CH3Br: Chemistry of the CH2BrO radical. *The Journal of Physical Chemistry*, 100(17): 7026-7033, 1996.

91. Altshuller, A. P. PANs in the atmosphere. *Air & Waste*, 43(9): 1221-1230, 1993.

92. Bhuyan, P., Barman, N., Bora, J., Daimari, R., Deka, P., & Hoque, R. R. Attributes of aerosol bound water soluble ions and carbon, and their relationships with AOD over the Brahmaputra Valley. *Atmospheric Environment*, 142: 194-209, 2016.

93. Deka, J., Baul, N., Bharali, P., Sarma, K. P., & Hoque, R. R. Soil PAHs against varied land use of a small city (Tezpur) of middle Brahmaputra Valley: seasonality, sources, and long-range transport. *Environmental monitoring and assessment*, 192: 1-14, 2020.

94. Ommi, A., Emami, F., Zíková, N., Hopke, P. K., & Begum, B. A. Trajectory-based models and remote sensing for biomass burning assessment in Bangladesh. *Aerosol and Air Quality Research*, 17(2): 465-475, 2017.

95. Rahman, M. M., Begum, B. A., Hopke, P. K., Nahar, K., & Thurston, G. D. Assessing the PM2. 5 impact of biomass combustion in megacity Dhaka, Bangladesh. *Environmental Pollution*, 264: 114798, 2020.

96. Hatzianastassiou N, Katsoulis BD, Antakis B. Extreme nitrogen oxide and ozone concentrations in Athens atmosphere in relation to meteorological conditions. *Environmental Monitoring and Assessment*, 128:447–64, 2007.

97. Dimitriou, K., & Kassomenos, P. Three year study of tropospheric ozone with back trajectories at a metropolitan and a medium scale urban area in Greece. *Science of The Total Environment*, 502: 493-501, 2015.

98. Mazzeo, N. A., Venegas, L. E., & Choren, H. Analysis of NO, NO_2, O_3 and NOx concentrations measured at a green area of Buenos Aires City during wintertime. *Atmospheric Environment*, *39*(17): 3055-3068, 2005.

99. Pollack, I. B., Ryerson, T. B., Trainer, M., Neuman, J. A., Roberts, J. M., & Parrish, D. D., 2013. Trends in ozone, its precursors, and related secondary oxidation products in Los Angeles California: A synthesis of measurements from 1960 to 2010. *Journal of Geophysical Research: Atmospheres*, 118(11):5893-5911.

100. Zhu, B., Akimoto, H., Wang, Z., Sudo, K., Tang, J., and Uno, I.: Why does surface ozone peak in summertime at Waliguan?, *Geophysical Research Letters,* 31, 2004.

101. Ma, J., Zheng, X., and Xu, X.: Comment on "Why does surface ozone peak in summertime at Waliguan?" by Bin Zhu et al. *Geophysical Research Letters,* 32: L01805, 2005.

102. Wang, T.,Wong, H. L. A., Tang, J., Ding, A.,Wu,W. S., and Zhang, X. C.: On the origin of surface ozone and reactive nitrogen observed at a remote mountain site in the northeastern Qinghai- Tibetan Plateau, western China. *Journal of Geophysical Research: Atmosphere*, 111: D08303, 2006b.

103. Xue, L. K.,Wang, T., Zhang, J. M., Zhang, X. C., Deliger, Poon, C. N., Ding, A. J., Zhou, X. H., Wu, W. S., Tang, J., Zhang, Q. Z., and Wang, W. X.: Source of surface ozone and reactive nitrogen speciation at Mount Waliguan in western China: New insights from the 2006 summer study. *Journal of Geophysical Research,* 116: D07306, 2011.

104. Xu, W. Y., Xu, X. B., Lin, M. Y., Lin, W. L., Tarasick, D., Tang, J., ... & Zheng, X. D. Long-term trends of surface ozone and its influencing factors at the Mt Waliguan GAW station, China-Part 2: the roles of anthropogenic emissions and climate variability, 2018.

105. Tsitouridou, R.; Papazova, P.; Simeonova, P.; Simeonov, V. Chemical and statistical interpretation of sized aerosol particles collected at an

urban site in Thessaloniki, Greece. *Journal of Environmental Science and Health*, 48: 1815–1828, 2013.

106. Donnelly, A. A., Broderick, B. M., & Misstear, B. D. The effect of long-range air mass transport pathways on PM10 and NO_2 concentrations at urban and rural background sites in Ireland: Quantification using clustering techniques. *Journal of Environmental Science and Health, Part A*, 50(7): 647-658, 2015.

107. Zien, A. W., Richter, A., Hilboll, A., Blechschmidt, A. M., & Burrows, J. P. Systematic analysis of tropospheric NO_2 long-range transport events detected in GOME-2 satellite data. *Atmospheric Chemistry and Physics*, 14(14): 7367-7396, 2014.